

# Constraints and Engineering Standards Index

## For

**Project Title: Terrestrial Radioisotope Thermoelectric Generator For Power Distribution in Remote Regions**

Team Members: Ethan Owenby, Ian Aranda, Israel Marin, and Patricio Bunt

CONSTRAINT	PAGE	PAGE	PAGE	PAGE
Economic	60	61		
Environmental	48			
Social	8			
Political	-			
Ethical	8			
Health and Safety	51			
Manufacturability	62			

ENGINEERING STANDARD	PAGE	PAGE	PAGE	PAGE
IAEA	52			

**Team 4**

**Ethan Owenby**

**Ian Aranda**

**Israel Marin**

**Patricio Bunt**

**Texas A&M University Nuclear Engineering: Senior Design**

**Project Report**

**Advisor: Dr. Ford**

**Signature:**

---

## ***Table of Contents***

<b>Acronym List</b>	<b>5</b>
<b>Executive Summary</b>	<b>6</b>
<b>1. Introduction</b>	<b>8</b>
1.1. Design Objectives	10
<b>2. Material Selection Analysis</b>	<b>11</b>
2.1. Overview	11
2.2. Radioisotope Selection for Heat Source	11
2.3. Heat Source Specifications	14
2.4. Thermocouple Material Selection	16
2.5. Surrounding Material Selection	18
2.6. Future Considerations for Improvement	19
<b>3. Mechanical Design - First Prototype</b>	<b>20</b>
3.1. Non-Modular Fuel	20
3.2. Ceramic Cage	21
3.3. Thermoelectric Generators	22
3.4. Heat Sink & Shielding	24
3.5. Thermal Study 1 Results	26
<b>4. Mechanical Design - Final Prototype</b>	<b>30</b>
4.1. Modular Fuel	30
4.2. Ceramic Cage Revisited	33
4.3. Thermoelectric Generators	34
4.4. Shielding and Heat Sinks	35
4.5. Support Structure and Infrastructure	37
4.6. Thermal Study 2 Results	39
4.7. Future Work	40
<b>5. Thermoelectric Analysis</b>	<b>41</b>
5.1. Overview	41
5.2. Utilizing Seebeck Effect to Produce Power	41
5.3. Thermoelectric Generator Module	42
5.4. Optimizing Load Resistance	44
5.5. Thermoelectric Conversion Results	46
5.6. Performance of System in Different Environments	48

5.7. Transient Analysis	48
<b>6. Radiation Shielding and Safety Analysis</b>	<b>50</b>
6.1. Overview	50
6.2. Background Information on Possible Radiation Types	50
6.3. Radioactive Qualities of the Fuel Source	51
6.4 Utilizing Attenuation and Activity to Calculate Dose Rate	54
6.5 Overall Safety Analysis	59
<b>7. Economic Analysis</b>	<b>60</b>
7.1. Overview	60
7.2. Total Cost Estimate of Design	60
7.3. Electricity Rates	60
7.4. How Can the Design be Improved Economically?	61
<b>8. Conclusion</b>	<b>62</b>
<b>9. Acknowledgements</b>	<b>63</b>
<b>10. References</b>	<b>64</b>
<b>Appendices</b>	<b>66</b>
Appendix A. Time Discretization of Heat Source Decay Python Script	66
Appendix B. Thermoelectric Analysis Python Script	67
Appendix C. Heat Calculator according to Pellet Dimensions	69
<b>Author Contributions</b>	<b>84</b>

## *Acronym List*

<b>BOL</b>	Beginning of life
<b>EOL</b>	End of life
<b>RTG</b>	Radioisotope Thermoelectric Generator
<b>MCNP</b>	Monte Carlo N-Particle Transport Code
<b>LWR</b>	Light Water Reactor
<b>SMR</b>	Small Modular Reactor
<b>kWe</b>	Kilowatts electric
<b>kWth</b>	Kilowatts thermal
<b>SiGe</b>	Silicon Germanium
<b>FOM</b>	Figure of Merit
<b>INL</b>	Idaho National Laboratory
<b>GPHS-RTG</b>	General Purpose Heat Source Radioisotope Thermoelectric Generator
<b>TEG</b>	Thermoelectric Generator
<b>Ci</b>	Curie
<b>keV</b>	Kiloelectron Volt
<b>MeV</b>	Megaelectron Volt
<b>mSv</b>	Millisievert
<b>Rad</b>	Radiation Absorbed Dose
<b>SrTiO<sub>3</sub></b>	Strontium Titanate

## ***Executive Summary***

Resilient forms of energy capable of functioning independent of human intervention for decades at a time are rather useful tools, particularly for terrestrial applications. Such a device can be conceived in the form of a RTG, some forms of which can last upwards of 40 years at functional power levels. This form of energy can be applied to various scenarios requiring exceptionally resilient and human-independent power, such as autonomous satellites, remote lighthouses and buoys, remote scientific outposts, deep-water data collection devices, and many other applications that are located in remote environments.

The main objective for this project is to design a high-powered terrestrial RTG that can be implemented for a variety of applications in remote areas. For this design, the specific goals include producing power on a scale of 1 kWe, maintaining a thermoelectric efficiency greater than 7%, and providing a system that is economically feasible for customers.

The design of this terrestrial RTG can be split up into five different technical areas: material analysis, mechanical design, thermoelectric analysis, shielding design, and economic analysis. Before any work can be done, a decision making process is to be established in order to determine which type of materials need to be used for the design to achieve the set goals. In terms of fuel, this is done by first choosing many preliminary candidates and then analyzing them against set criteria, each having its own weight factor based on the set goals. Once a fuel source is selected, then comes the process of developing a framework for how to actually go about creating such a device. Research into thermocouples and the Seebeck effect, which is the physical phenomenon that converts the thermal energy from the radioactive decay of the fuel source into an electrical current, had to be done in order to fully grasp the project's background and know the next steps that must be taken. Next, a prototype 3D SolidWorks design of the RTG is created in order to run a series of thermal studies where certain geometric and material parameters are optimized to ensure the best performance. This mechanical design section is the most intensive and is crucial for the other three technical areas. The thermoelectric analysis takes the output from the SolidWorks thermal study, and quantifies how the system is converting the energy created from the radioisotope into electrical power. Both the mechanical design and thermoelectric analysis areas work hand in hand in order to achieve the design goals. Quantities such as power output and efficiency will be the main focus of this section and ultimately the results that determine the feasibility of the design. Next, a shielding and radiation safety analysis will be performed on the final design by comparing different shielding designs, and ensuring the RTG is following regulatory standards set by the nuclear engineering community. Finally a rough cost estimate will be made for customers to know how much it would take to develop, manufacture, and implement this design in the real world.

After going through the entire design process, the RTG design was able to meet the objective goals of producing power on a 1 kWe scale while maintaining a thermoelectric efficiency around 10 %. It was determined that the design has the best performance in colder climates and would greatly benefit remote communities in Alaska and Northern Canada. This is mainly due to the fact that the current design relies on natural convection to dissipate heat. By placing the RTG into a naturally cold environment, the ambient environment will in turn draw more heat from the heatsinks, creating a larger temperature differential between both extremities of the thermocouples, in turn generating more electrical power output. In addition, the design of the RTG is modular and allows for multiple units to be implemented by simply wiring multiple devices together in series and linearly increasing the power output in order to achieve whatever end goal is needed. The upfront economic cost to implement such a design is not favorable. This is due to the fact that no preset manufacturing methods are currently available, as each part of the RTG's design is completely proprietary.

## ***1. Introduction***

The need for modular power producing devices has become more prevalent in the nuclear industry as are many roadblocks for constructing a traditional LWR. These include a large upfront capital investment, inflexible location possibilities, and no scalability [1]. Modular power producing devices address all of these issues and provide a more appealing product for customers. As the demand for emission free energy sources increases, systems such as RTGs and SMRs become vital in combating this challenge.

One of the greatest challenges that people tend to forget is providing energy to areas that are desolate and experience harsh environmental conditions. Currently, remote communities in North America that are not connected to an electric grid or natural gas infrastructure produce their own energy by burning diesel fuel [2]. Not only is this very unhealthy for the surrounding environment, but the logistics and cost to transport the diesel fuel to these areas is inefficient and costly [3]. As these areas and communities begin to become more developed, the demand for energy has increased which only places more strain on the guarantee of receiving diesel from outside sources. In addition, the price and availability of diesel is constantly fluctuating due to the political climate, which leaves these communities with a fluid price to obtain their energy needs. These communities can greatly benefit financially and environmentally from a clean energy source that provides a baseload of power for long periods of time without refueling. This is where the motivation for the design project was born.

RTGs have typically been utilized within a variety of space applications such as providing power to spacecraft and propulsion. By taking advantage of a decaying radioisotope, RTGs are able to produce power over long periods of time while being lightweight and compact [4]. Those systems that are out in the field currently produce power on the scale of a 100 W which is not close to being sufficient to power a community. This led the team to investigate the feasibility to design a terrestrial RTG that produces significantly more power which could then be used in cases such as remote areas. In addition, it was determined that a modular system would be necessary to account for the ever changing energy needs. Through this unique design, it opens the possibilities for these communities to become self-reliant for their energy needs, and pave the way for the next generation of modular power systems.

A combination of design and analysis techniques will be used throughout the design process which are made possible through engineering tools such as Python, SolidWorks, and MCNP. A more detailed discussion is available in the preceding sections for the different technical areas, and all supplemental codes can be found in the appendix.

The aim for this project is to design a unique RTG that is specifically suited to serve in environments that experience harsh weather conditions. The uniqueness of this design is

dependent on producing power on a scale that has not been deployed in the field while allowing for modular capabilities. In addition, certain features from space applied RTGs will be improved upon for terrestrial use. Ultimately, this design will showcase that RTGs are plausible solutions for terrestrial energy solutions and should not only be limited to space.

## ***1.1. Design Objectives***

Several design objectives were established at the beginning of this project, and were used as a guideline throughout the process. These objectives were created to demonstrate the implementation of unique features and capabilities that have not yet been physically applied in the nuclear field. Below are the main objectives listed for a successful design project, and were used as a starting benchmark of feasibility.

1. Design a modular RTG that is terrestrial based and can be operated in remote and harsh environments for many years. Specific applications include powering cellular towers, airport run-way lights, and military bases just to name a few.
2. Optimize and improve upon power output and efficiency that RTG's in the field currently have. Specifically produce power on a scale of 1 kWe with a thermoelectric conversion efficiency of 7% or greater.
3. Design a system that is economically and logically feasible to implement without an on-site operator.

The motivation of these objectives stem from the idea that RTGs have typically been used in the field for space applications with small power producing output. With these set objectives, a clear goal has been set to improve upon and push the limits for RTGs in an area that has not been addressed.

## **2. Material Selection Analysis**

### **2.1. Overview**

In this section, a variety of decisions will be analytically made regarding which type of materials to use for the RTG design. The main components of the system that required in-depth material analysis to achieve the design goals included the heat source, thermocouples, and any surrounding material that is near the heat source. The material selection for all three of these components play a pivotal role in how the RTG will function, and determine whether it can feasibly achieve the predefined objective goals. Throughout this analysis, a series of comparisons will be made for each component of potential materials for the design. These materials that have been determined as plausible choices were established during the inception of the project, and are shown to describe the unique needs and goals of the design.

### **2.2. Radioisotope Selection for Heat Source**

A radioisotope has the capability to be used as a heat source through its continuous radioactive decay which produces heat energy with every emission. This heat is then transferred throughout the entire system and eventually is converted into electrical energy. Before any progress can be made in the design process, the most important step is determining which radioisotope should be used as the primary heat source. Based upon this decision, the following technical areas will construct their design and analysis around the selected radioisotope. First a set of material properties for an ideal heat source were established to determine a group of potential radioisotopes to be used for the design. Below in Table 1 is a list of all the radioisotopes that were considered for the final design and their given properties that were deemed the most important to meet the design goals.

**Table 1.** RTG fuel candidates with their given properties.

Fuel Isotope	Specific Power (W/g)	Half-Life (Years)	Cost (\$/g)
Sr-90	0.45	28.8	~\$1,800
Pu-238	0.56	87.7	~\$4,000
Po-210	141	0.38	~\$8,800
Am-241	0.11	432.2	~\$1,500

All four of the radioisotopes in Table 1 have excellent thermal and structural characteristics where no one isotope has any significant advantage over the other. This is why the properties that are a part of the decision making process include specific power, half-life, and cost. These three properties directly affect the overall design goals the most, and in order to provide an unbiased decision amongst the team, a decision making model was developed. This decision making model is able to quantify which isotope is best to use based on the material properties through a given ‘weight factor’ that was determined by the team. Below in Table 2 are the given weight factors for each property used throughout the decision making process.

**Table 2.** Decision Making Model with each property’s weight factor.

Property	Weight Factor	Unit
Specific Power	0.35	W/g
Half-Life	0.3	Years
Material Cost	0.2	\$/g
Accessibility	0.15	Prior Research

Notice that in addition to the other three properties mentioned, there is one labeled ‘Accessibility’. Accessibility can be defined as the ability to get your hands on the material due to the abundance or degree of difficulty to chemically separate a given isotope. Since there is no real quantity that can measure this parameter, a dimensionless value in between 1 and 10 will be given for each isotope. This value will be based upon research done on each isotope and the process it would take to obtain such material. For instance, Pu-238 will be given a low score for ‘Accessibility’ since it can only be obtained through reprocessing nuclear waste and the security permission required to handle it [5].

The following tables are the results from the decision making process from which the most ideal radioisotope to use for the heat source was determined to be Sr-90. Each isotope was scored on a scale of 1 to 10 where each property was given a ‘Score’ and then multiplied by the weight factor. After summing each property’s value, an overall utility score is given which was the sole factor that the decision was made from.

**Table 3.** Decision making model for Sr-90.

Objective	Weight Factor	Parameter	Magnitude	Score	Overall Value
Specific Power	0.35	W/g	0.45	7	2.45
Half-Life	0.3	Years	28.8	7	2.1
Material Cost	0.2	\$/g	1,800	9	1.8
Accessibility	0.15	Prior Research	...	7	1.05
<b>Total Overall Utility Score: 7.4</b>					

**Table 4.** Decision making model for Pu-238.

Objective	Weight Factor	Parameter	Magnitude	Score	Overall Value
Specific Power	0.35	W/g	0.56	8	2.8
Half-Life	0.3	Years	87.7	9	2.7
Material Cost	0.2	\$/g	4,000	5	1.0
Accessibility	0.15	Prior Research	...	3	0.45
<b>Total Overall Utility Score: 6.95</b>					

**Table 5.** Decision making model for Po-210.

Objective	Weight Factor	Parameter	Magnitude	Score	Overall Value
Specific Power	0.35	W/g	141	10	3.5
Half-Life	0.3	Years	0.38	1	0.3
Material Cost	0.2	\$/g	8,800	2	0.4
Accessibility	0.15	Prior Research	...	9	1.35
<b>Total Overall Utility Score: 5.55</b>					

**Table 6.** Decision making model for Am-241.

Objective	Weight Factor	Parameter	Magnitude	Score	Overall Value
Specific Power	0.35	W/g	0.11	3	1.05
Half-Life	0.3	Years	432.2	10	3.0
Material Cost	0.2	\$/g	1,500	10	2.0
Accessibility	0.15	Prior Research	...	1	0.15
<b>Total Overall Utility Score: 6.2</b>					

It is interesting to note how Pu-238 was not the radioisotope with the highest utility score. Glancing over the material properties quickly, it may seem that Pu-238 fits the design goals best, however, the ability to attain the material is incredibly difficult in the current day and age. This can change as the United States begins to move towards reprocessing spent nuclear fuel, and having a storage of Pu-238 readily available for clean energy solutions. Frankly, the design of this RTG must proceed with the current state of policies in mind and build around this. Sr-90 will be the heat source for this RTG, and will serve as the backbone for this design moving forward.

### 2.3. Heat Source Specifications

It is unrealistic to have a heat source that is a pure radioisotope. The heat source must be composed of the radioisotope in combination with some metal. Once again, a simplistic approach was taken for this decision and a material that has been proven in the field before was chosen. Strontium Titanate has been used as the fuel source in previous applications of RTGs where there is plenty of research and analysis available [8]. Below are the properties of Strontium Titanate that are used throughout the analysis in the preceding sections.

**Table 7.** Properties of Strontium Titanate [9].

Property	Value
Density [g/cc]	5.12
Thermal Conductivity [W/m-K]	12

Specific Heat [J/kg-K]	537.1
Melting Point [K]	2353

In addition, a python script was written to estimate how much Sr-90 is present in the fuel source as a function of the RTGs operation time. Furthermore, the script can compute the amount of heat produced by the source as the specific power and mass are known. This script time discretized the exponential decay equation over a 10-year period at 1 day intervals. Below in Figure 1 and Figure 2 are the results from the script and will be eventually used for a transient analysis on the thermoelectric side.

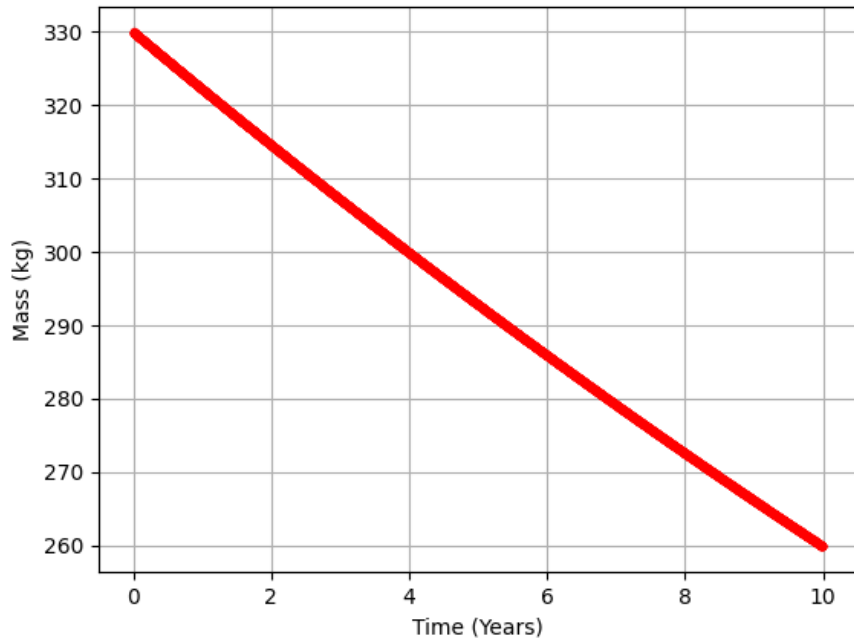


**Figure 1.** Mass of Strontium Titanate fuel as a function of time.

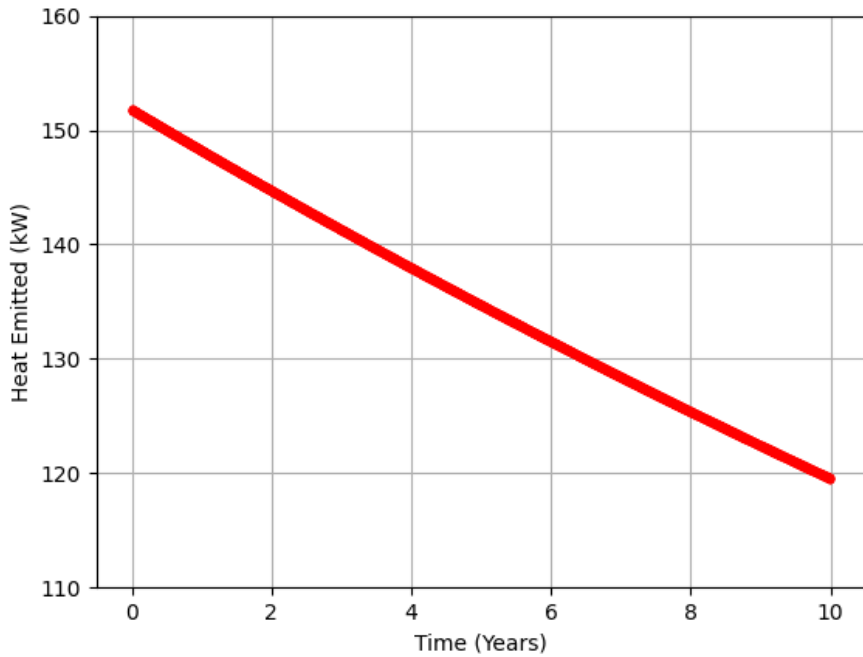


**Figure 2.** Heat emitted of Strontium Titanate fuel as a function of time.

## 2.4. Thermocouple Material Selection

The next material component that must be chosen are the two dissimilar metals in which the thermocouple itself is made out of. For this design, previously used materials were studied and a decision was made based upon the respective thermal and electrical properties. An ideal thermocouple must have properties that have high electrical resistivity and low thermal conductance. This allows for a temperature gradient to be created across the thermocouple, and provides the electrical current created through the Seebeck effect to move freely through the system. Since materials are still being researched and developed for thermoelectric generation, it was decided to simplify the decision and choose a material that has been proven to work in the field which is n and p-Type SiGe.

**Table 8.** Thermoelectric properties for n-Type SiGe at a temperature of 1000 K [6].

Property	SiGe
Thermal Conductivity [W/m*K]	3.93

Electrical Resistivity [ $10^{-5}$ R-m]	2.11
Seebeck Coefficient [ $\mu\text{V/K}$ ]	-258
Melting Point [K]	1500

**Table 9.** Thermoelectric properties for p-Type SiGe at a temperature of 1000 K [6].

Property	SiGe
Thermal Conductivity [W/m*K]	4.07
Electrical Resistivity [ $10^{-5}$ R-m]	2.68
Seebeck Coefficient [ $\mu\text{V/K}$ ]	-228
Melting Point [K]	1500

Based upon the given thermoelectric properties of the two different types of SiGe, a FOM can be used to quantify how efficient thermal energy is converted into electrical power. This FOM is labeled as the ‘ZT’ and is important for the thermoelectric analysis which is discussed in a later section.

$$ZT = \frac{S^2 \sigma}{\lambda} T \quad \text{Eq. 1}$$

Where:

S = Seebeck Coefficient [ $\mu\text{V/K}$ ]

$\sigma$  = Electrical Conductivity [S/cm]

$\lambda$  = Thermal Conductivity [W/mK]

T = Temperature [K]

Since it is dependent on the thermocouple temperature, this FOM changes depending on certain operating conditions. To provide a full-scope of analysis for the thermoelectric side, the ZT FOM was plotted for temperature ranging from 300 K to 1300 K.

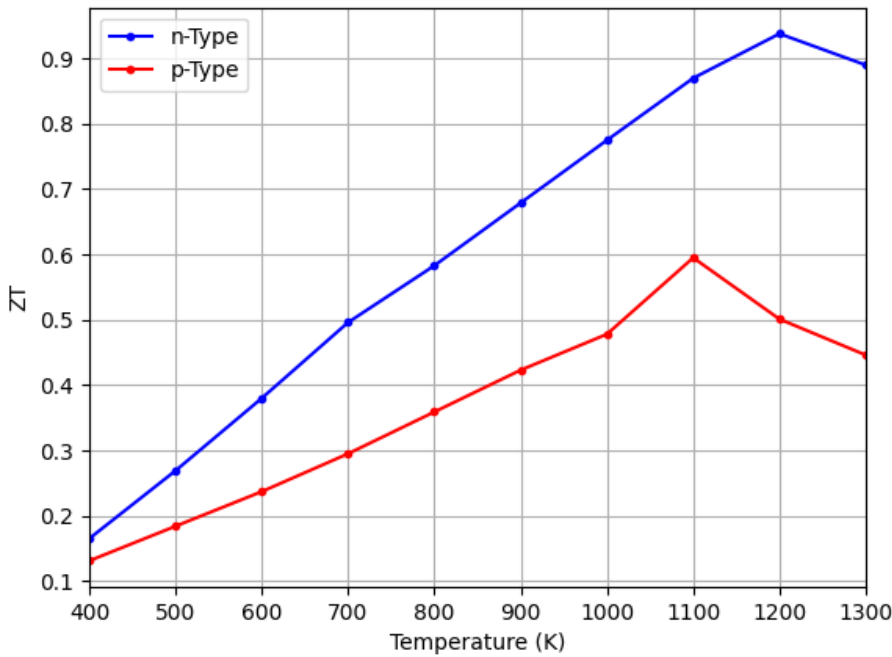


**Figure 3.** ZT FOM as a function of thermocouple temperature.

## 2.5. Surrounding Material Selection

In order to house the fuel source, a ceramic frame is placed on each of the 6 sides of the fuel assembly. The optimal material for these frames must have a very low thermal expansion, as well as good electrical insulation. These properties are both crucial to the design, as any thermal expansion that occurs will affect the contact interface between the heat source and the thermocouples. This will impact overall efficiency by reducing the temperature difference within the thermocouples, in turn reducing the power output. The reasoning behind requiring the material to be a good electrical insulator is to ensure that the array of thermocouples are not short circuited. For these reasons, Aluminum Oxide was selected as the frame material. As can be seen in Table 10, Aluminum Oxide's material properties prove it to be optimal for this purpose.

**Table 10.** Material properties for Aluminum Oxide [13].

Property	Cordierite Ceramic
Thermal Expansion [ $\mu\text{m}/\text{m}^*\text{K}$ ]	8.1
Electrical Resistivity [ $\text{ohms}^*\text{cm}$ ]	$1 \times 10^{14} - 1 \times 10^{15}$

Melting Point [K]	2345.15
-------------------	---------

A separate but crucial element in the design is the method by which heat is removed from the system and a “cold” side is generated. This is achieved by using large heat sinks placed on each of the six outer faces of the cube. These heatsinks will be made using aluminum. The reasoning behind using aluminum vs a separate material with a higher thermal conductivity such as copper or silver, is primarily due to the cost and amount that will be required. Due to the fact that the dissipation of the heat is reliant on natural convection, the limiting factor is non-dependant on this material. A material with a higher thermal conductivity would bring marginal benefit while bringing significant price increase. This can be seen below in Table 11. This same reasoning is applied to the wiring. The entire circuit is to be wired together using copper wire, even though there are many other more efficient ways to transfer electrical energy such as through gold. It is simply not economically justifiable.

**Table 11.** Thermal Expansion Coefficients and cost of Aluminum, Copper, and Silver [14][15][16][17][18][19].

Material	Thermal Conductivity [W/m*K]	Cost [\$ USD/Kg]
Aluminum	210	3.26
Copper	385	10.38
Silver	419	823.38

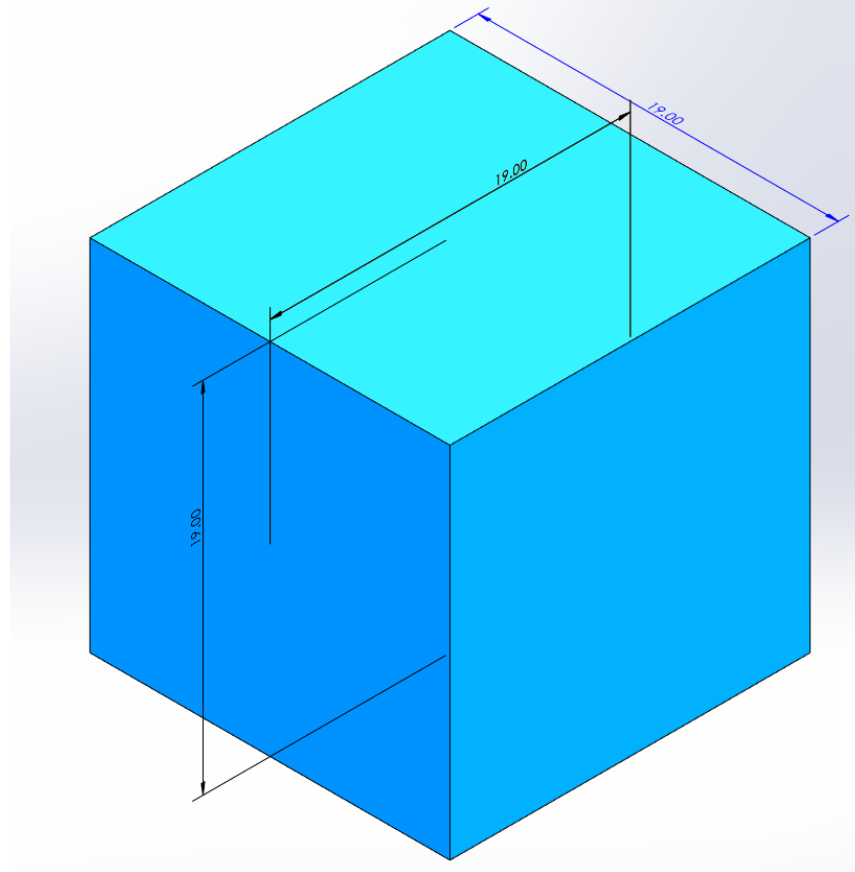
## 2.6. Future Considerations for Improvement

The material side for any design in the nuclear industry is usually the bottleneck compared to the rest of the technical areas. Nuclear applications tend to operate at very extreme conditions that commonly used materials are not suitable to handle such systems. This RTG design is no different and is bottlenecked by the lack of materials that are plausible to be used in the system. For instance, there were several materials that could have performed better in place of the current dissimilar metals in the thermocouples, but there was a lack of research and information on such materials. Material classes such as skutterudites, clathrates, and Half-Heuslers show promising results, but are less commercially established and are in the preliminary stage of research [7]. With the material engineering field rapidly progressing, the hope is that in the future there will be more suitable materials for this RTGs certain application.

### **3. Mechanical Design - First Prototype**

#### **3.1. Non-Modular Fuel**

**Figure 4:** Strontium Titanate Fuel, dimensions are in cm.



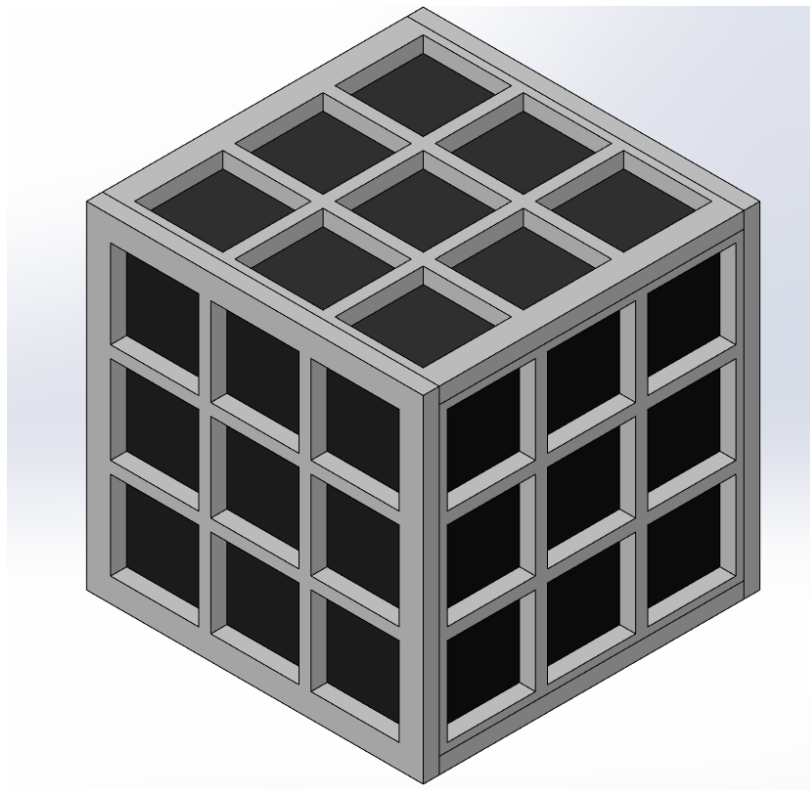
Initial designs were carried out using the code referenced in Appendix C, which used data from ORNL to calculate the ideal volume for the source to generate around 1kWe at an estimated 8% transfer efficiency from thermal energy to electric [21]. This 19 by 19 by 19 centimeter volume of Strontium Titanate as a heat source produces 16898.89 We, which was deemed plenty to transfer into the goal of 1kWe. This is assuming around 15000 Wth of parasitic heat loss, something that is typical for thermoelectric generators.

For the source shape, it was determined that an ideal shape would be a sphere. However, this volume would be extremely difficult to manufacture, particularly with a source that produces its own heat. Additionally, the manufacturing of curved surfaces for the TEG pieces would further complicate the design. This led to the determination that, although slightly less ideal for heat transfer, a cube is the ideal shape for the source in this design, particularly with respect to feasibility. The assumption here was that all surface areas of the cube could be covered with TEG, and any additional space would have a thermal insulator to minimize heat losses.

### 3.2. Ceramic Cage

The next step in the design process was to find a way to transfer as much heat as possible into the hot shoe of the TEG. This meant there would need to be some form of thermal insulation around the hot shoe and as much of the source as possible. An ideal solution, that also aided in manufacturability, was a modular ceramic cage with space for the TEGs to be placed directly into contact with the source. Figure 5 is the final CAD drawing of the ceramic cage surrounding the source.

**Figure 5:** Original Ceramic cage



### 3.3. Thermoelectric Generators

The thermoelectric generators, or TEGs, were placed in the open spots within the ceramic cage. With a total of 54 TEGs, the heat transfer was maximized for the source cube. These TEGs were designed in tandem with existing systems seen within the industry, such as those used by NASA [4]. For the design, it was clear that the portion in contact with the fuel source needed maximal heat transfer properties while also serving as an electrical insulator. This is to prevent any electrical conduction or shorts between thermoelectric generators in contact with the source, and this part is generally referred to as the “hot shoe”. The next stage is a high melting temperature metal that can also conduct electricity between the n-type and p-type legs of the thermoelectric SiGe material. To solve this need, Molybdenum was an ideal material as it is very good at transferring heat and electricity without melting. Finally, the thermoelectric material itself is bonded to the molybdenum hot shoe following the procedures outlined by RCA [20]. The copper contact pads are then bolted into the aluminum oxide ceramic, which is also bolted into the molybdenum hot shoe. This process creates a single assembly that can easily be inserted into the thermoelectric system.

**Figure 6:** Thermoelectric Generators in an array surrounding the source.

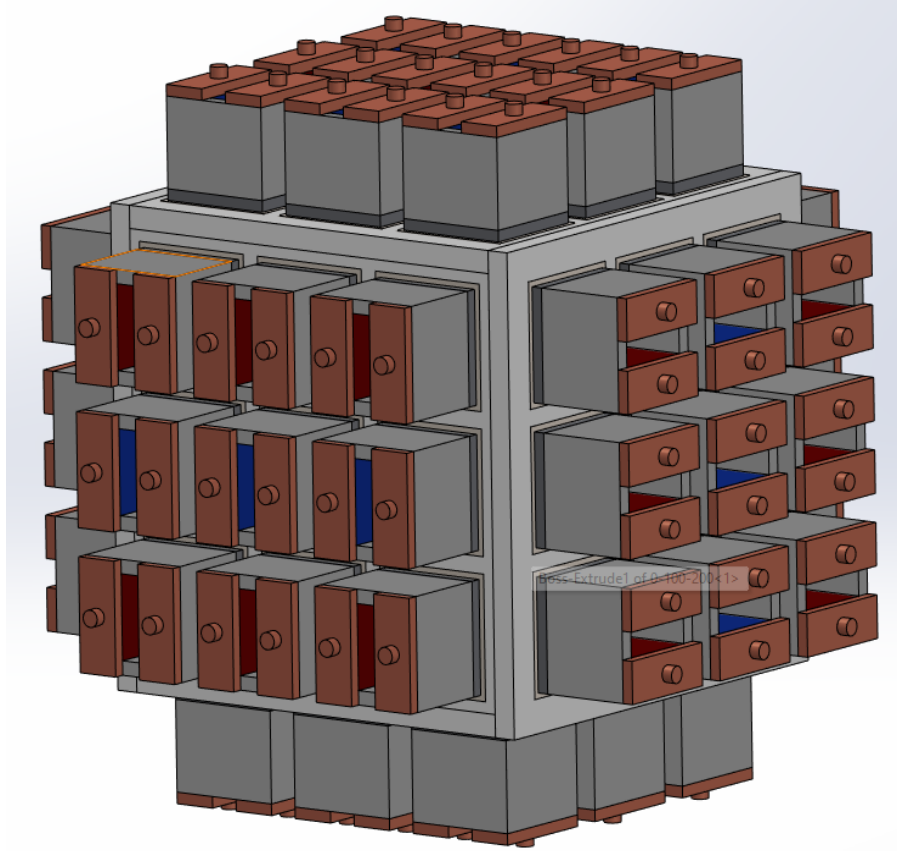


**Figure 7:** Isometric view of the Thermoelectric Generator.

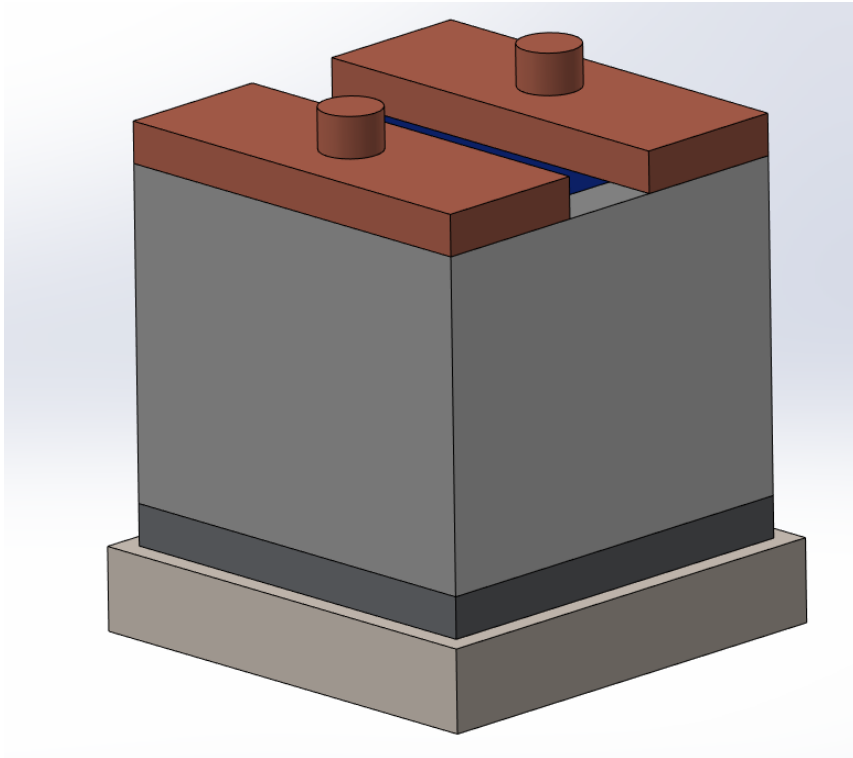


**Figure 8:** Split View of a Thermoelectric Generator with material outlines.

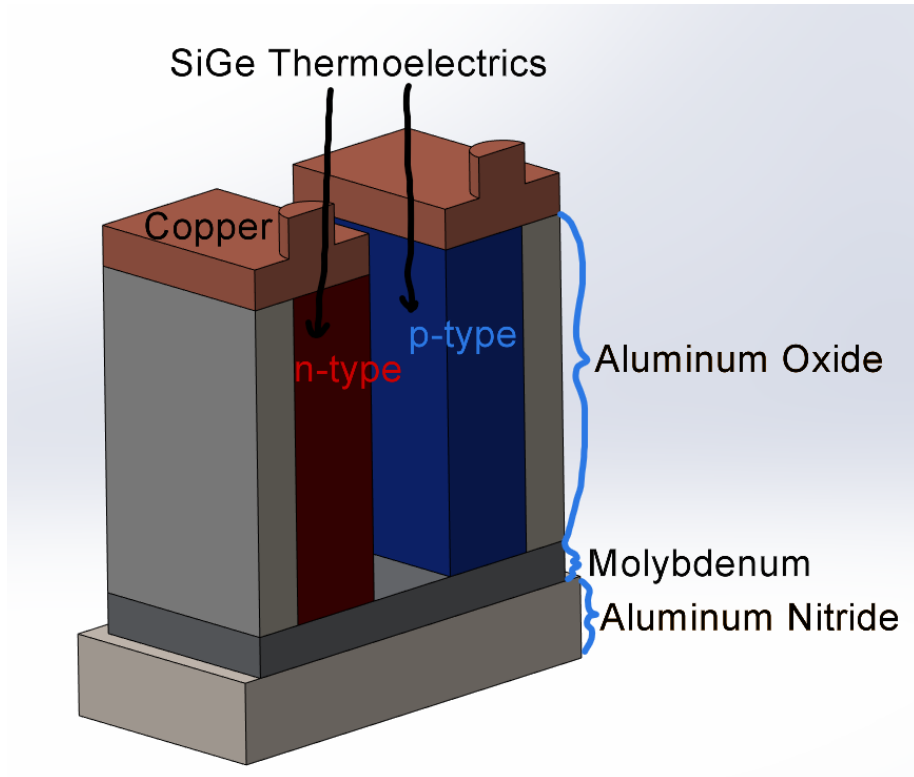
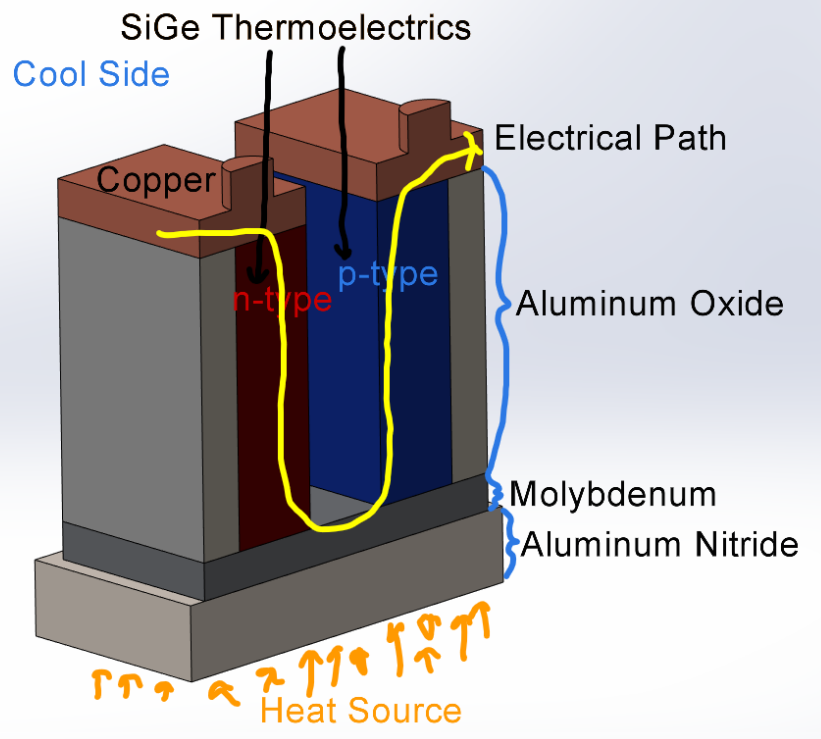


**Figure 9:** Split View with Electrical path overlay



### 3.4. Heat Sink & Shielding

The final step in completing the design was to come up with a method cooling the thermoelectrics. It is clear that to maximize the efficiency of this system the cooling method must be passive. In order to find a solution that fits that criteria, it was determined that natural convection to large heat sinks was the ideal choice to cool the system. These heat sinks were designed in such a way that they could be easily manufactured using simple steel presses and molten aluminum to maximize cost effectiveness. An electrical insulator was again needed between the heat sink and the copper wiring of the thermocouples to prevent shorts, and so an Aluminum Nitride sheet was mounted above the thermocouple array on each face. Mounted to the Aluminum Nitride sheet is the aluminum heat sink, which is a series of fins that allow air to flow within the gaps, creating a form of weak convective cooling. Although a larger finned heat sink may provide a slight improvement to the temperature differential within the TEG, there is also a possibility of increasing the parasitic heat losses within the system, so the current dimensions were kept.

**Figure 10:** Full RTG Assembly along with split view.

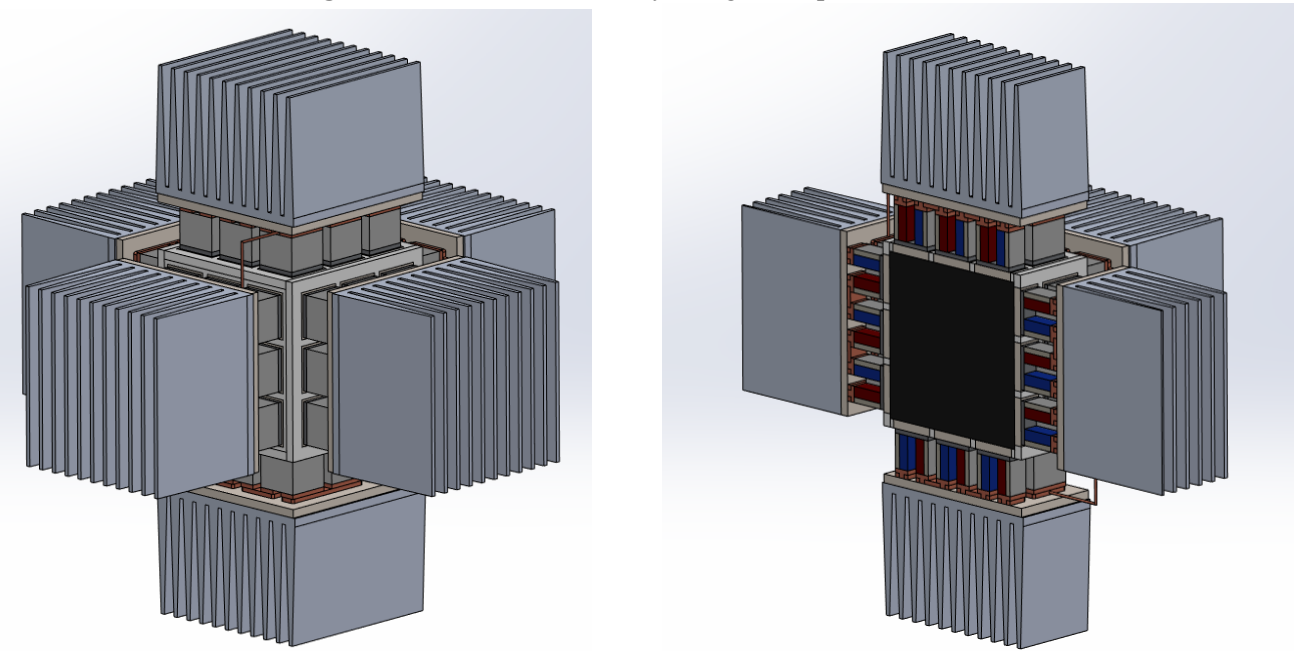
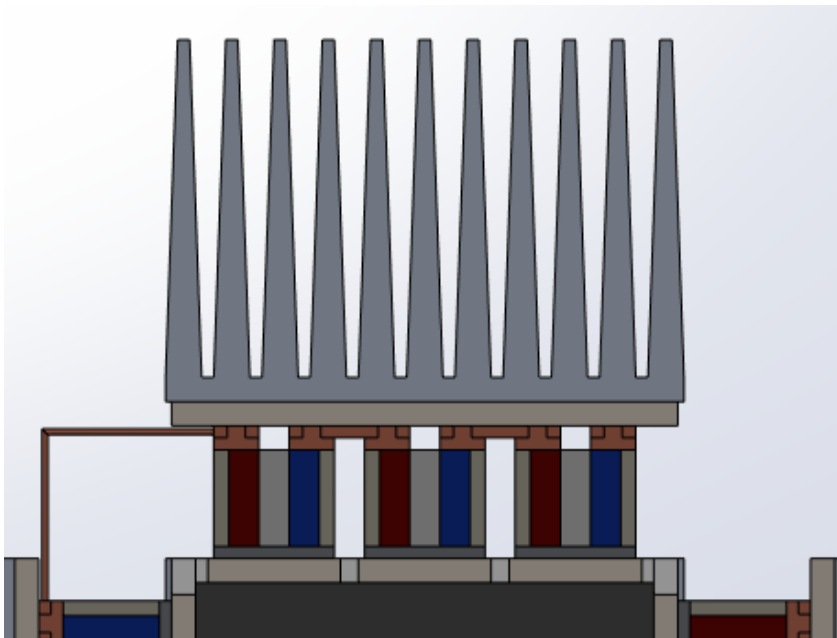


**Figure 11:** Heat sink in contact with the TEG array.



### 3.5. Thermal Study 1 Results

Transient thermodynamic analysis is an extremely lengthy and difficult process, therefore utilizing an existing program to calculate and fully model the thermodynamics of the assembly greatly simplifies the design process. This tool is called a Solidworks Thermal Study, and it was used to model the entire assembly. The process involves declaring the thermal power in watts for a body within the system, in this case 16878 W<sub>th</sub>, and the cooling methods which are natural convection coefficients of between 8-25 W/m<sup>2</sup>K at 300 K. Using these values a dT of 1329K was recorded, which corresponds to 1350W<sub>e</sub>. These values allowed for successful attainment of the power goals for this system, however, there are a number of issues that became clear with the design by this system.

**Figure 12:** Full assembly with a temperature overlay and convection markers.

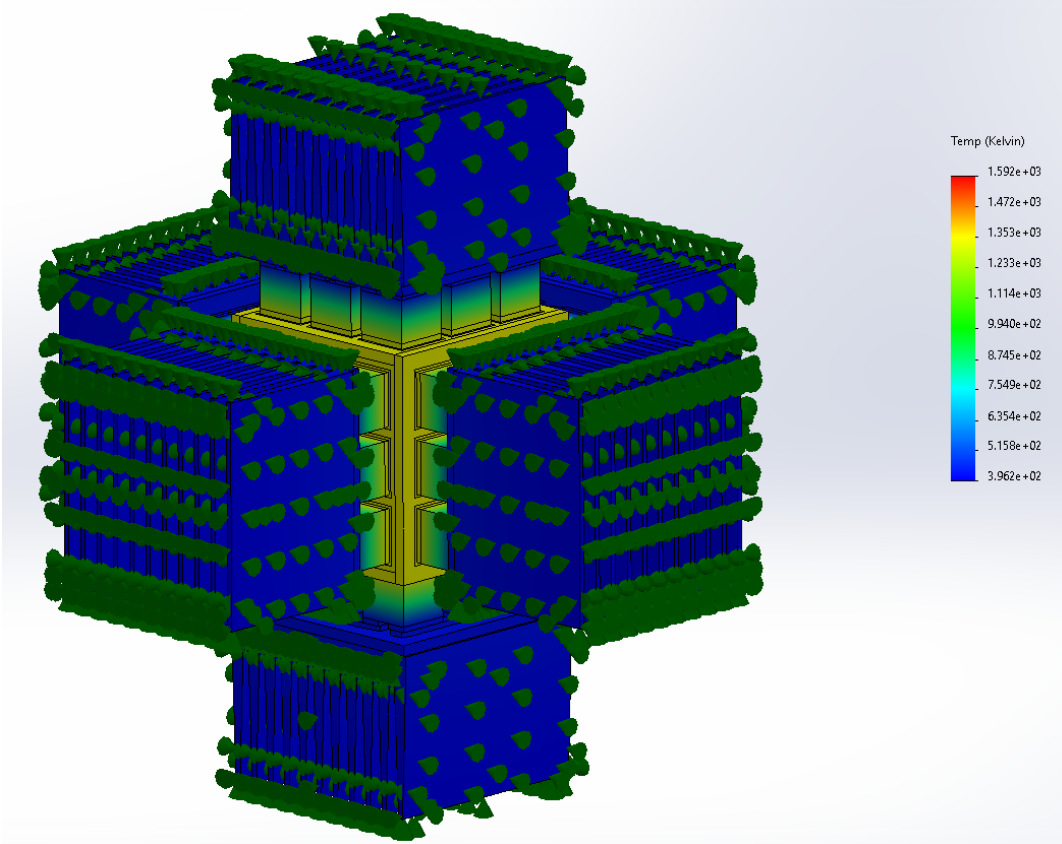
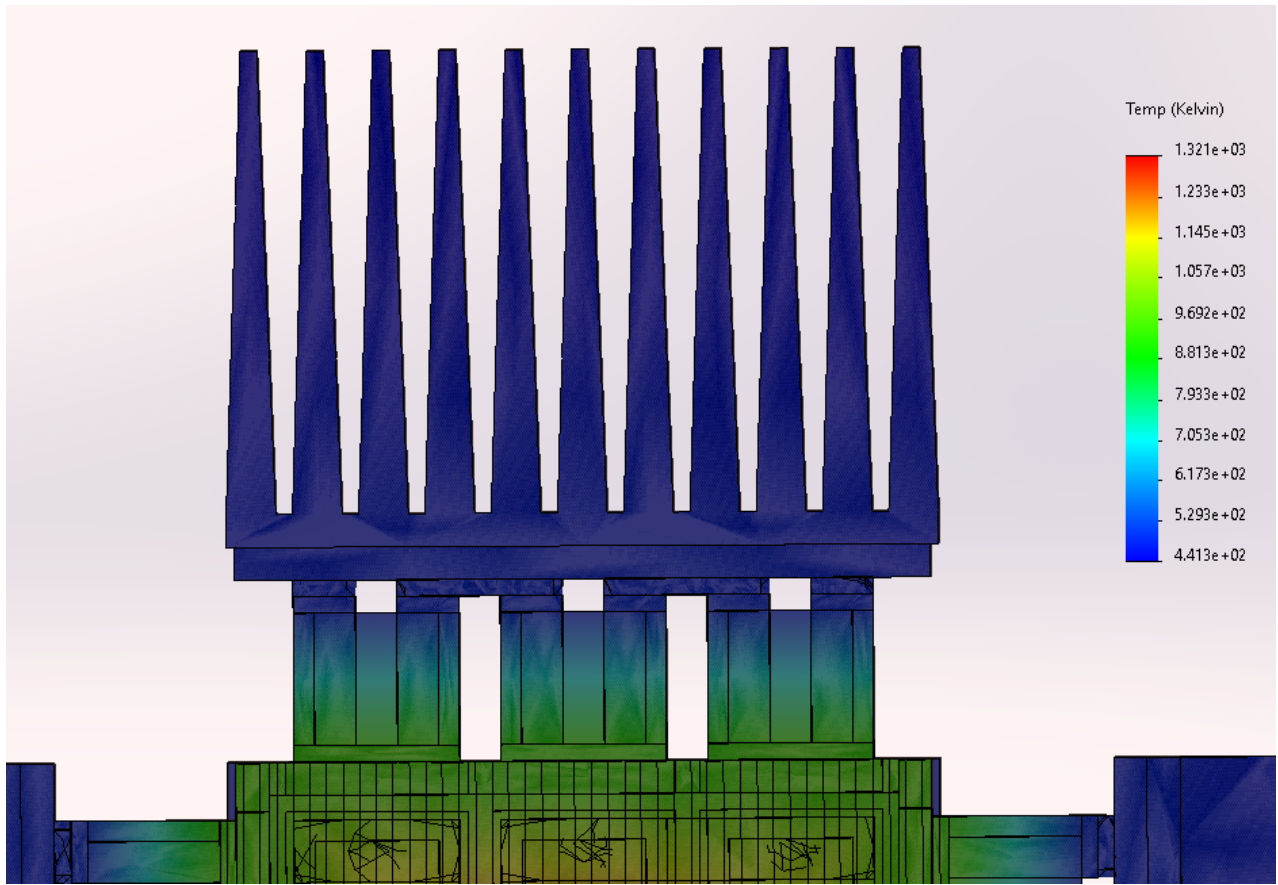


**Figure 13:** Split view of the heat sink and TEGs displaying the change in temperature.



The first glaring issue was temperatures greater than 2200 K at the core of the fuel, temperatures that exist with a large measure of the heat being lost to both parasitic heat and the materials and systems within the device. While the melting point of our Strontium Titanate source material is 2350 K, higher than the temperatures recorded within the hottest points of the source, that value will be quickly passed before assembly. This is because the source generates its own heat and without a massive heat sink into which it can dump its heat, it would melt rather quickly. Additionally, the source would need to be stored somewhere after its manufacture and prior to assembly within the system, and would therefore need special contaminants that allow it to dump its heat without melting down. These systems could be simple in design, a large aluminum oxide cube of about 1 m with a split assembly into which the source could be placed would more than suffice. Another solution would be to create a modular fuel system made up of smaller fuel pellets that are assembled into a large source upon system assembly. This idea is discussed in a section of this report titled “modular fuel”.

**Figure 14:** Split of isolated source with a temperature overlay.

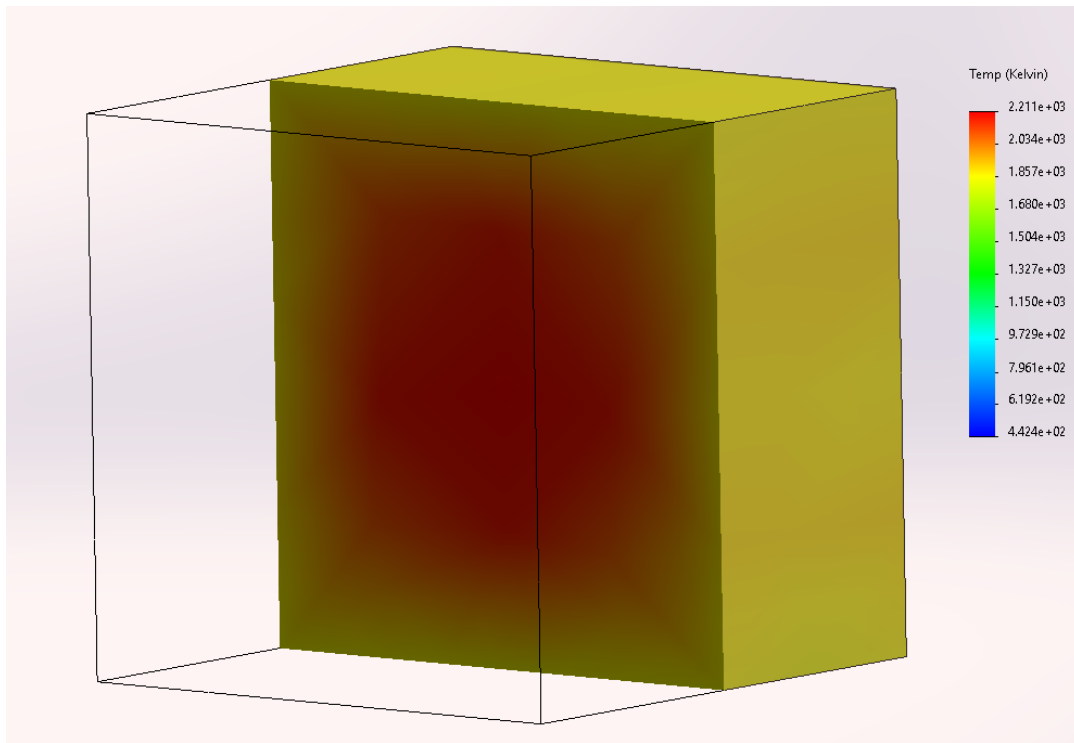


**Figure 15:** Split view of isolated TEG subassembly with a temperature overlay.

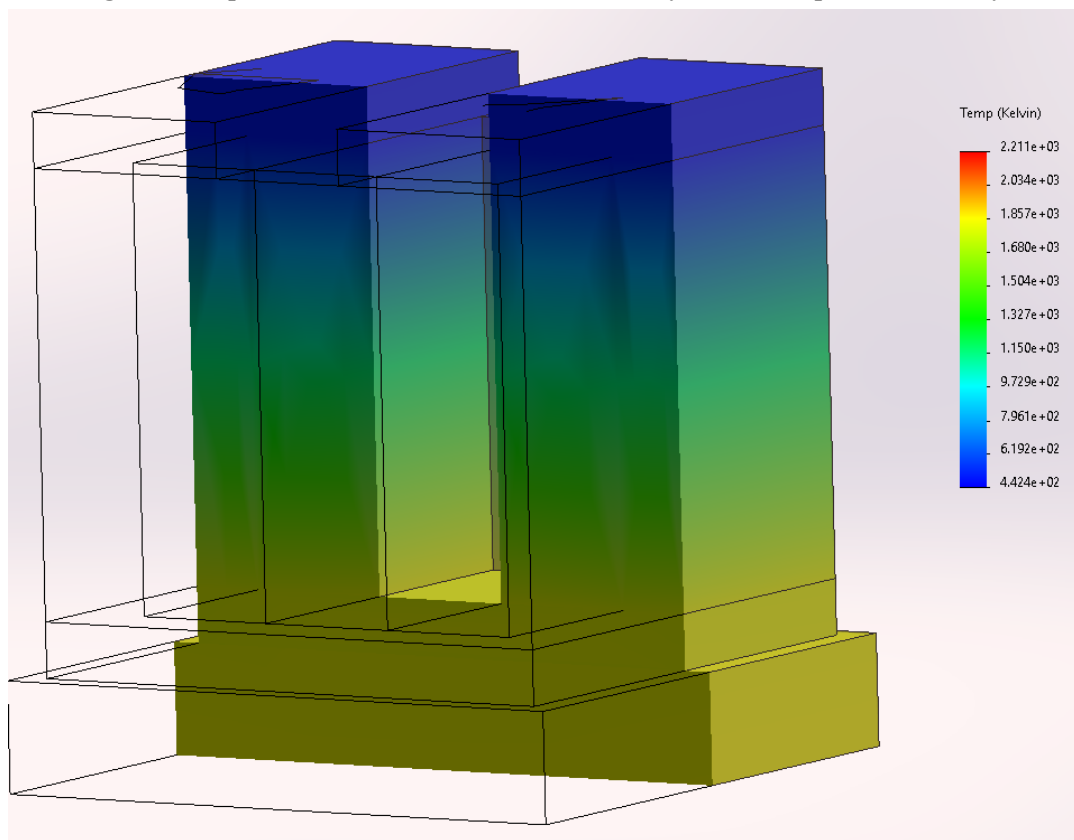
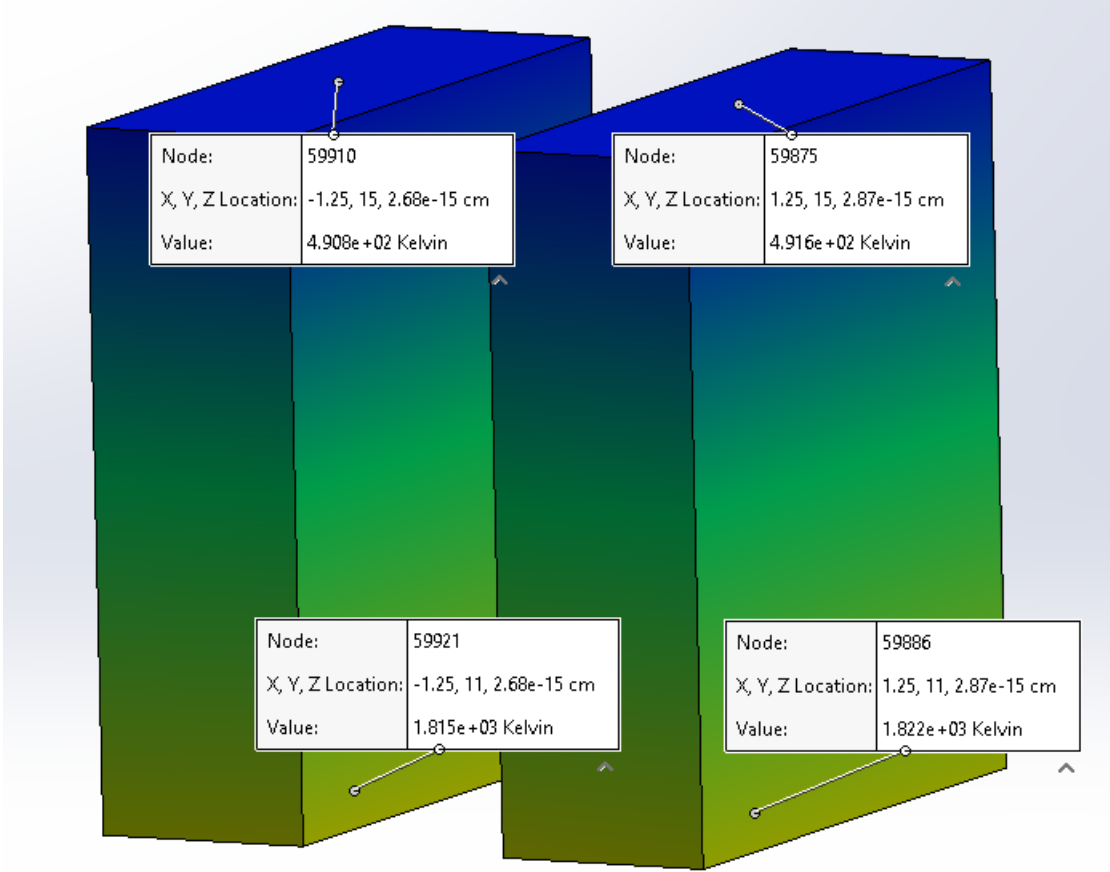


**Figure 16:** Image of isolated TEG only SiGe material w/ Temperature Sensor



Another issue that stands out is the lack of a supporting structure within the system. As it stands, there was no support structure/shielding placed along the edges of the ceramic structure. This is because it would essentially serve as a large parasitic heat sink into which usable heat, although not following the path of least resistance towards the TEG, would still be lost at a degree that could greatly affect the efficiency of the system.. A possible solution to this issue would be to create a large vacuum around the areas of the design currently exposed, sealed in by welds at the base of each heat sink. A valve would be present within the system to allow all air to be pulled from the system. Because this vacuum pulls any additional medium through which the components can lose heat beyond conduction, the current thermodynamic model can be considered an accurate one.

Finally, and most glaringly, is the issue of material failures at the current temperatures. The melting point of SiGe, even in the most ideal of circumstances, is 1500K. Knowing this, and the model running temperatures closer to 1800K, it is clear that our current system is dealing with melting within our most important material. A number of solutions exist for this issue, such as adding precise amounts of poor heat transfer mediums into which enough heat can be conducted to get the SiGe thermoelectrics to an ideal temperature without melting them. The primary issue with this solution is the computational burden of getting the proper amount of material to act as an ideal heat sink without taking too much heat and decreasing the efficiency of the system. Another option is to create a slight air gap between the TEG hot shoe and the source. This would

serve the double purpose of acting as an electrical insulator for the TEG, removing the need for an electrically insulating hot shoe and allowing for a material to be used better for heat transfer. In considering this solution, there is a significant issue with both properly modeling the dynamics of the system with calculations, and therefore determining the ideal distance for the TEG was impractical for our purposes. It was finally decided that the ideal solution would be to decrease the heat power marginally using a modular fuel system and in turn increase the parasitic heat losses within the system.

## **4. Mechanical Design - Final Prototype**

### **4.1. Modular Fuel**

As previously mentioned, the need for a modular fuel system was made clear to solve both the manufacturability issues for the source as well as the overheating issues. This system was therefore pursued, and the code in Appendix C was used to calculate the exact number of fuel pins and their dimensions for an 8% efficient system. This led to a 2.5 cm cube design that was placed in an array of 7 by 7 by 7 pellets as seen in Figure 18. It was then determined that an ideal housing material for the sources would be graphite, as it is a good heat transfer medium with a high melting point. Graphite is also significant for its low atomic number, 12, as this minimizes the bremsstrahlung energy that is produced when the beta emissions from the source interact with the housing. For assembly of the fuel system, a series of layered sheets that use inlaid pins to align them was created. The layers were then stacked 7 layers high to create an even spacing between the fuel pins, as seen in Figure 20. These layers should form a similar heat source as the one in the previous design, with a noticeable difference in parasitic heat loss within the graphite.

**Figure 17:** Single fuel pellet, dimensions are in mm.

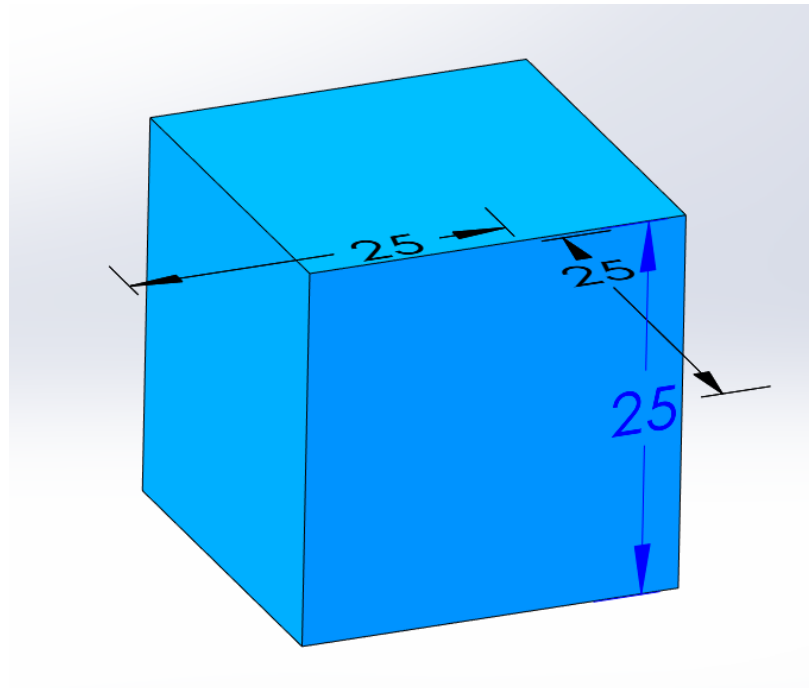


**Figure 18:** Source pellet array

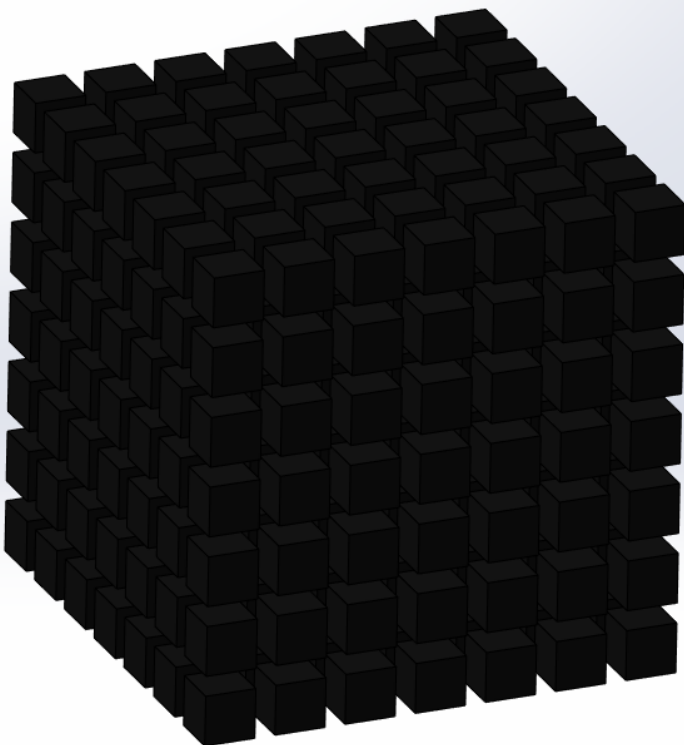


**Figure 19:** A single layer of the fuel system with fuel pins present

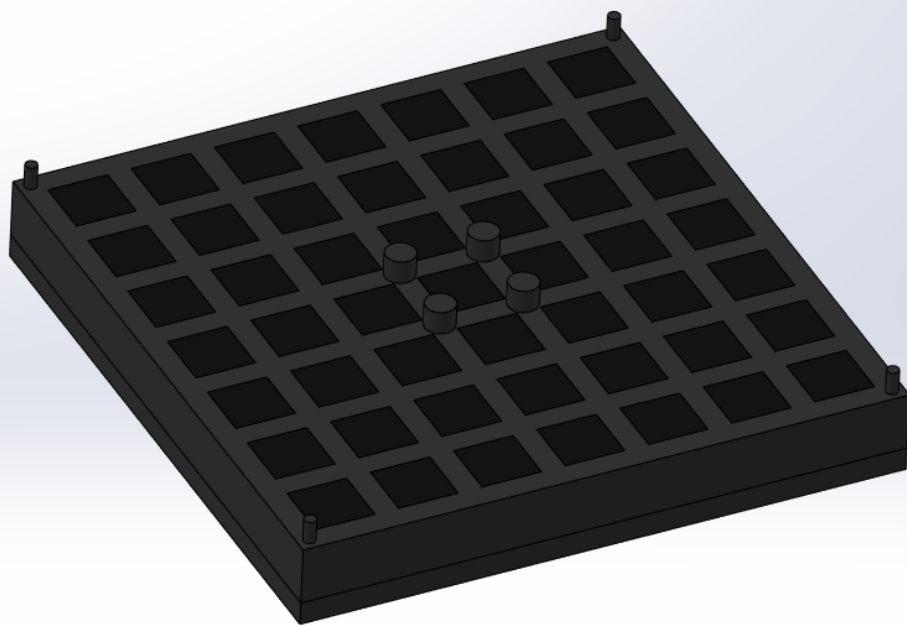
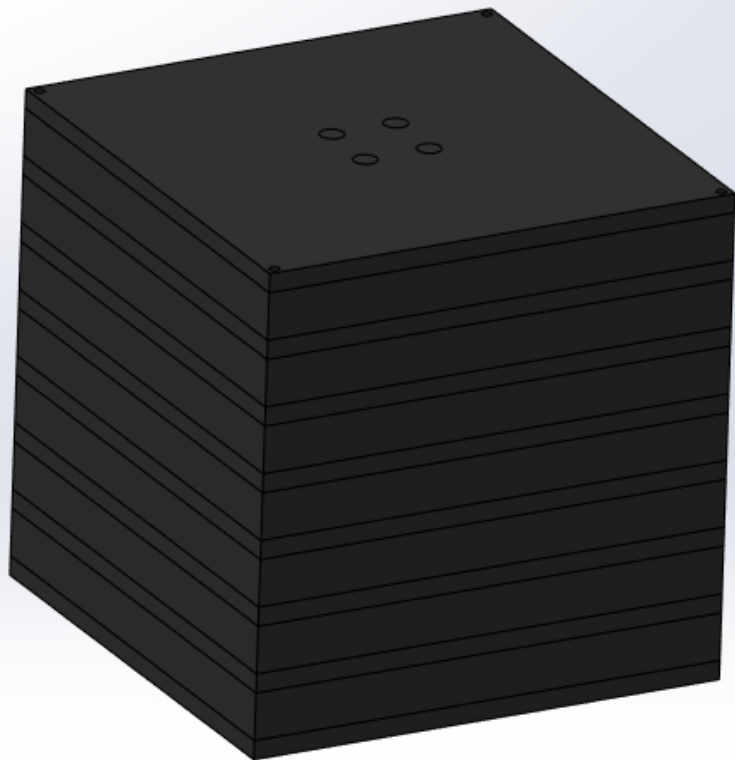


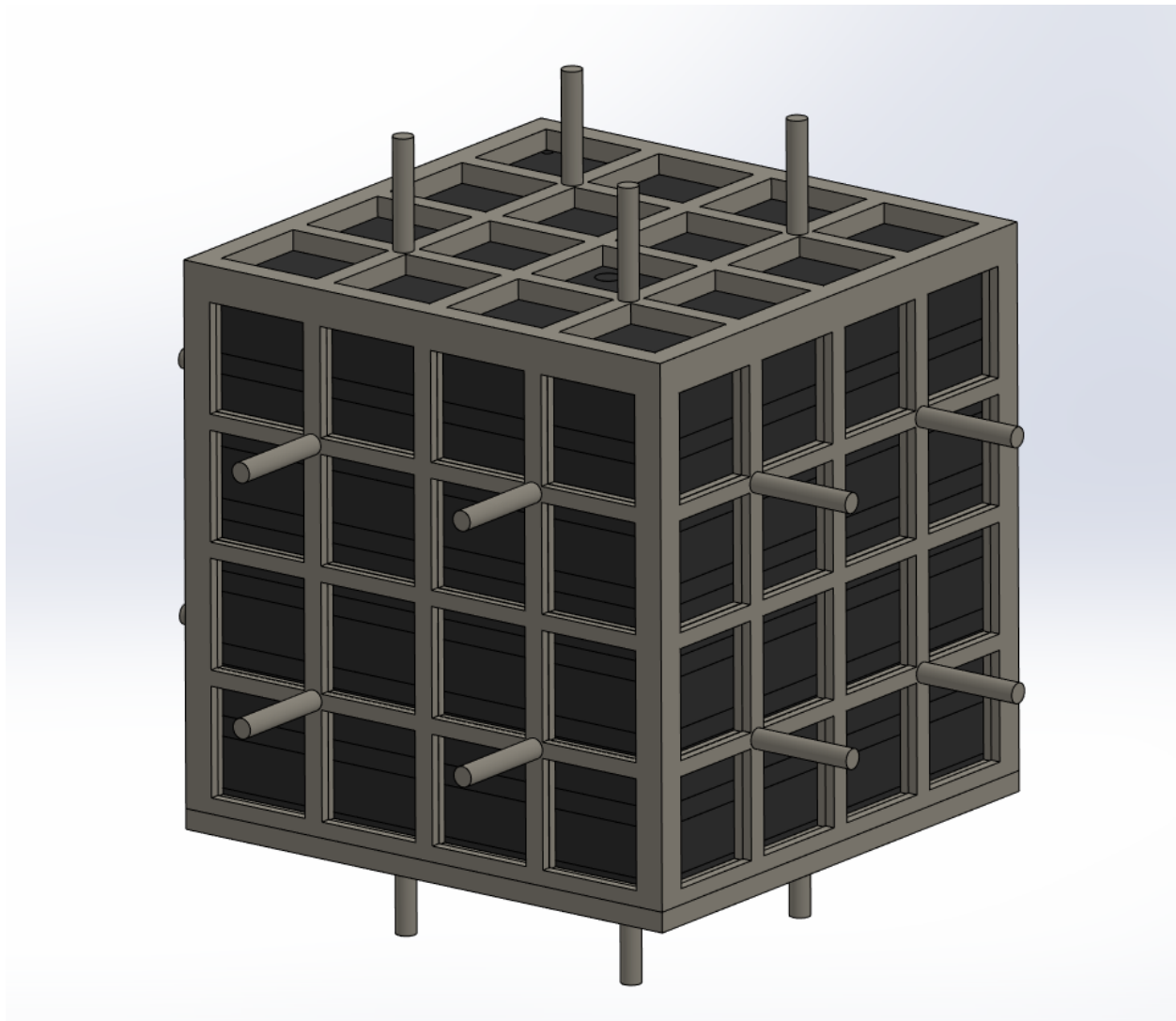
**Figure 20:** Fully assembled fuel source system with graphite structure.



## 4.2. Ceramic Cage Revisited

Given the redesign of the heat source into a now larger and pieced design, a more structured ceramic cage was needed. The new ceramic cage was designed as a two-part assembly, into which the assembled layers of fuel pins with the graphite supports can be placed. The two parts slide into one another to form the cohesive cage, forming a much stronger cage with a simpler manufacturing process. There are also standoffs built into the ceramic cage on each face, each with a 1 cm diameter, in order to provide a method onto which the aluminum nitride sheet can be fastened to the ceramic cage, sealing in the TEG array and its wiring.

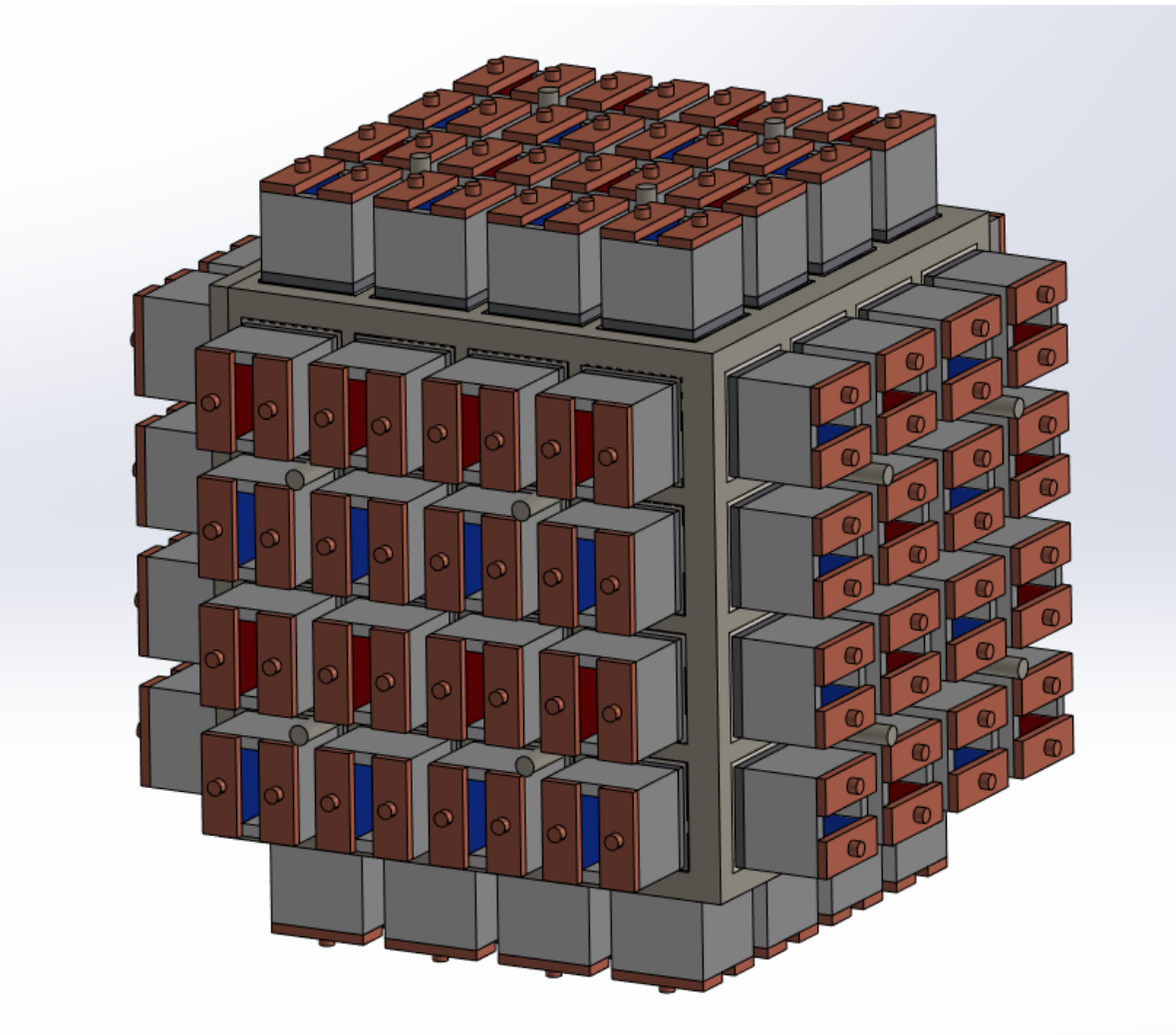
**Figure 21:** Image of Ceramic Cage and fuel



### 4.3. Thermoelectric Generators

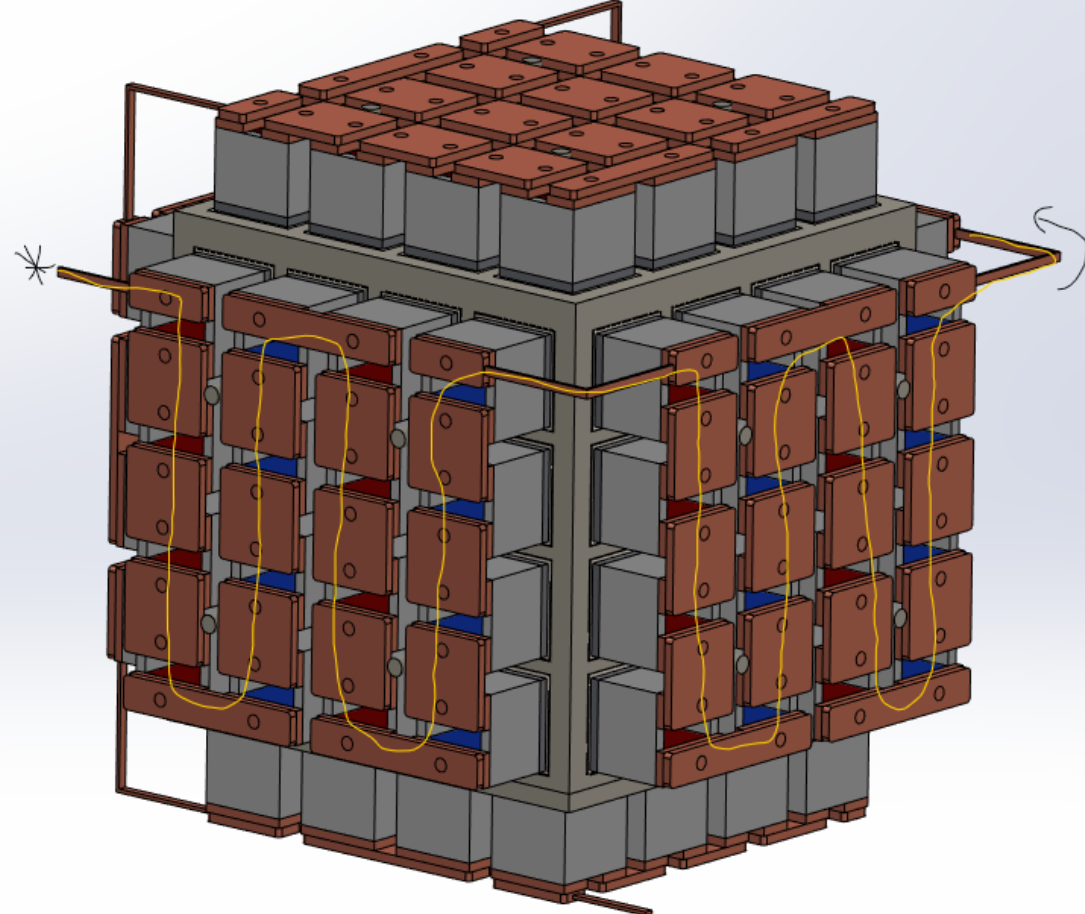
As the design has now increased in size, there is an additional surface area onto which more thermoelectric generators can be placed. In the final design, there were now 96 total TEGs, with 16 on each face of the cube. Theoretically, this should further improve the efficiency of the device at transferring the source heat into electricity.

**Figure 22:** Image of TEG array from Isometric Perspective



Another significant part of the design is wiring the array of TEGs in series. Thermoelectric generators function quite similarly to batteries within a circuit, meaning that wiring them in series is required to maximize the power within the system. Understanding this, and the solid-state nature of the p and n type legs of the thermocouples, an array path was developed for the TEGs across the entire system. This system used copper connecting plates, mostly to maximize current flow as well as heat transfer to the thermoelectric systems, while preventing shorts by being held in place by pins. A simple view into two sides of this complicated electrical system is shown in Figure 23.

**Figure 23:** Thermoelectric Generator array with copper plates wiring the system in series.



#### 4.4. Shielding and Heat Sinks

A primary need for the system at this stage is support structures to ensure structural integrity and manufacturability. For this problem, a large set of aluminum oxide ceramic blocks were designed to fit together around the other systems and hold them together. Large bolts will hold the blocks together and create an extremely sturdy structure into which the system is built. This structure can be seen independent of the electrical and cooling systems in Figure 25, and as a part of the whole assembly in Figure 26.

**Figure 24:** Split view of heat sinks

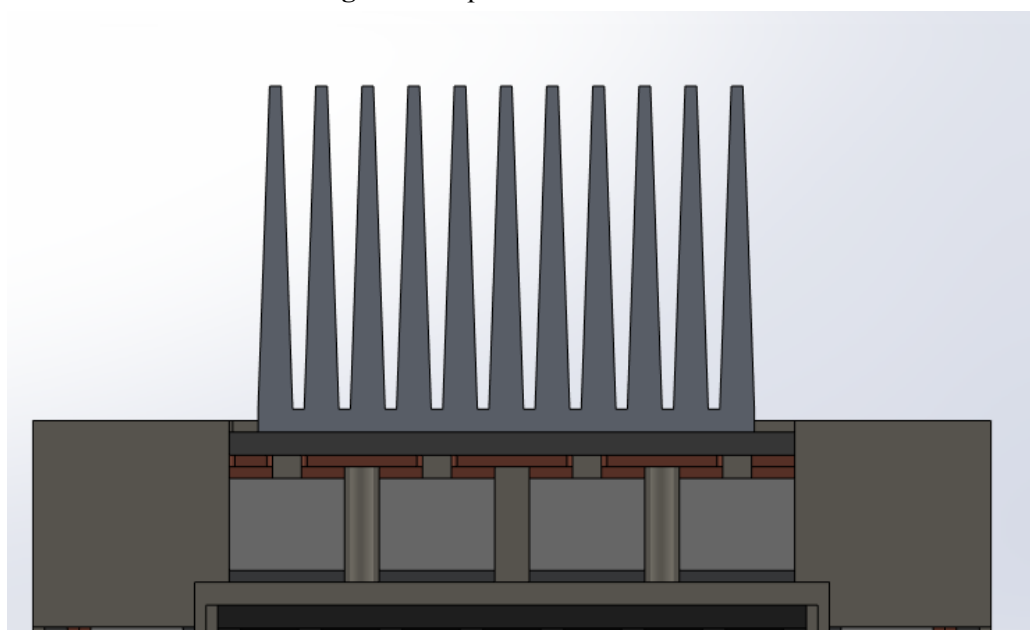


**Figure 25:** Isometric view of the support structures alone within the assembly

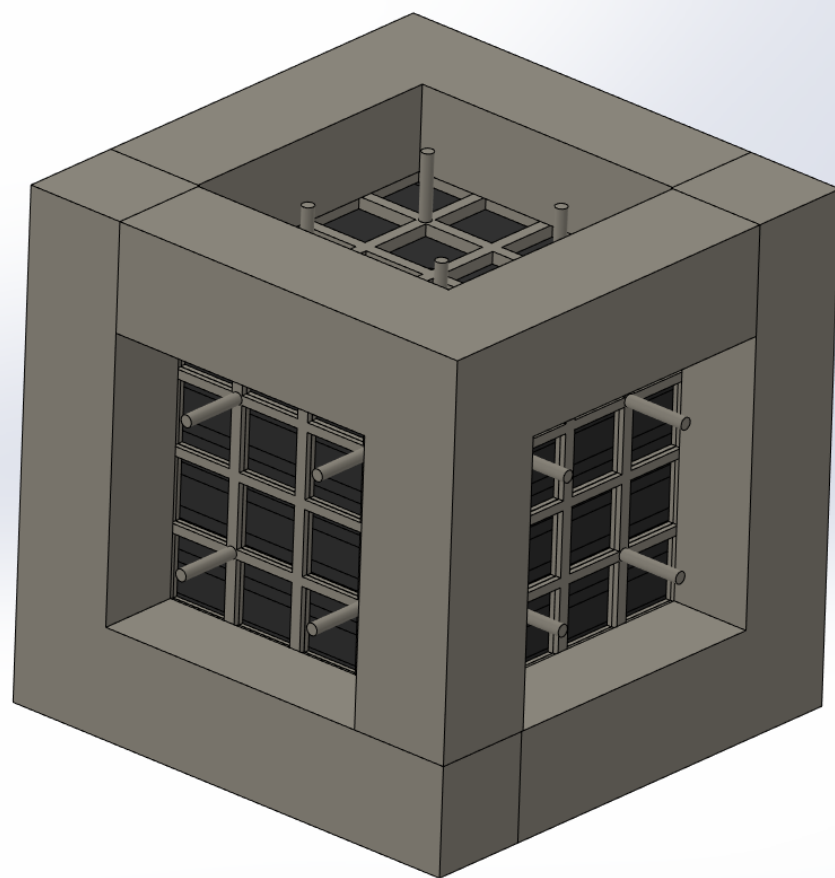
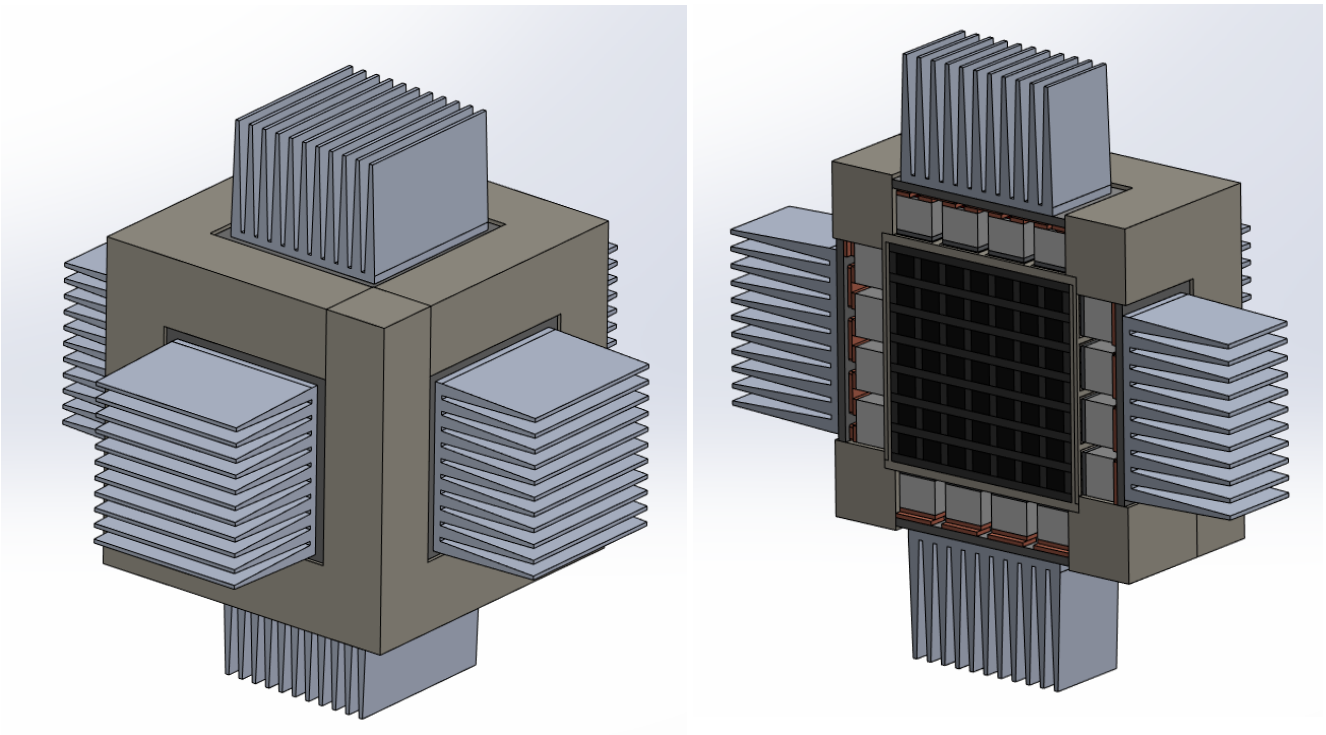


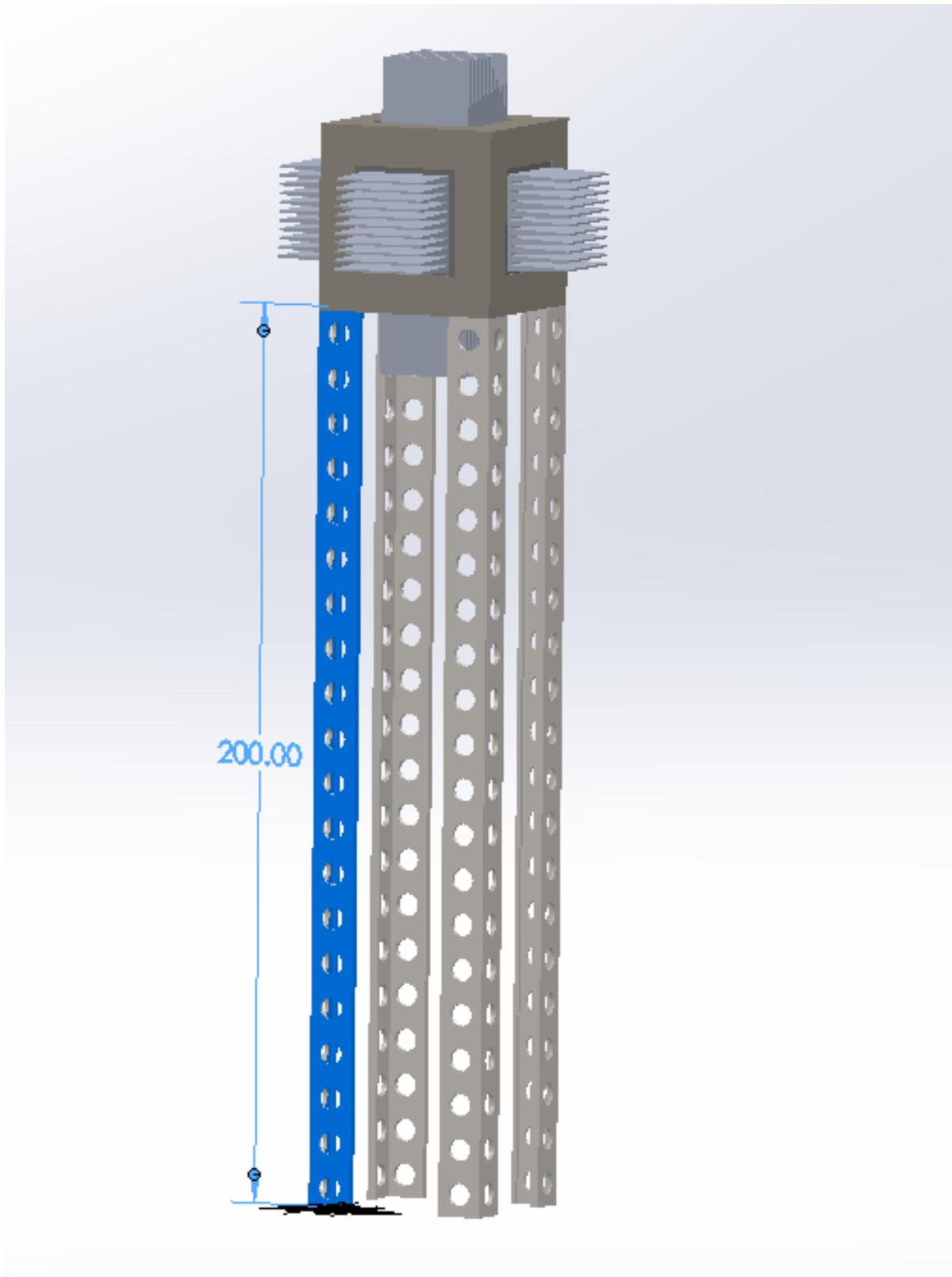
**Figure 26:** Final assembly for the modular fuel system prototype alongside split view.



#### 4.5. Support Structure and Infrastructure

The only remaining work for this design is to place it within a supporting structure in the real world. A simple solution to this task is to simply stand the system a few meters in the air on steel supports, welding a steel cage around the system. This would allow for maximum convective cooling, a simple way to keep bystanders from interacting with the radioactive device, and an additional heat sink into which cooling can occur. The only drawback is that it would require a heavy duty crane to suspend the device upwards into the steel cage, although this is typical for long-term infrastructure projects in other areas.

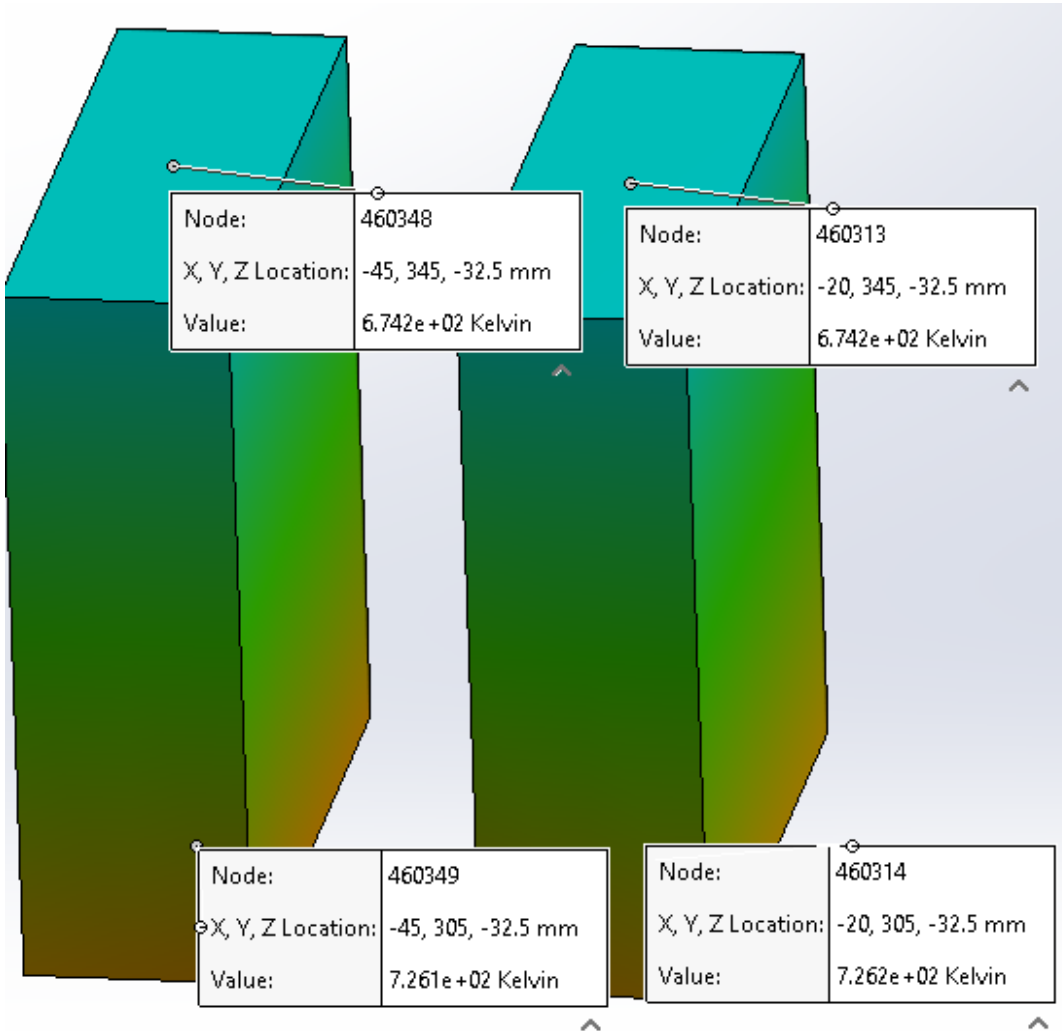
**Figure 27:** Full assembly suspended and mounted upon the support structure. Dimensions are in cm.



## 4.6. Thermal Study 2 Results

Despite repeated efforts and tests, the Solidworks model including the modular fuel appears to be too complex to provide effective data. The code posted in Appendix X using data from Reference X was used to calculate the exact number of fuel pellets, with specified dimensions, needed to produce 1kWe at a theoretical 8% efficiency. The code determined that, with fuel pellets of a 2.5cm by 2.5cm by 2.5 cm cube, the required number of pellets would be 324.707. It was then calculated that, for an even distribution of pellets within a fuel cell, the array would need to be 7 pellets by 7 pellets, in 7 layers. This meant 343 pellets producing heat power at 38.5 W thermal each, or approximately 13205.5 W thermal total. Using the graphite shell system, which is a good mode of heat transfer, there should be minimal heat loss from this heat power and results should be similar to that from the first prototype. However, this did not hold true, in fact there was a significant and notable difference between the two. After multiple iterations in an attempt to accrue accurate data from this model, the final dT measured was approximately 50 degrees Kelvin, as shown in Figure 28.

**Figure 28:** Final dT measured on the modular fuel prototype design thermoelectric material.



Another possible explanation for the vast temperature difference for the modular fuel is the large increase in the probability of parasitic heat loss. It is clear from the data that there is a large amount of parasitic heat loss within a cube system, mostly due to the nature of large void spaces at the edges of the cube that serve only as a heat sink and pulls heat away from the thermoelectrics. A solution to this problem, and a possible optimization for this system going forward, could be a vacuum sealed steel cage in place of the existing aluminum oxide support structure. This would prevent the edges of the heat source from dumping excess heat into the support structures through conduction and convection and force the heat to conduct through the thermoelectrics.

## 4.7. Future Work

All data and work up to this point has shown that this is a feasible solution for remote, long-term power. That being said, there are glaring issues with the final prototype, namely that the current Solidworks Thermal Analysis is only predicting around 12 We of total power. While this is grossly inaccurate and due to the computational weight of modeling a massive assembly in this way, there are also some optimization efforts within the design that could further improve the system and its efficiencies. The first opportunity for improvement is a true transient thermal analysis code in python, one that can give precise and consistent results for the final power output of the system without unexpected errors for overly large assemblies.

Another notable opportunity is the implementation of a vacuum around the heat source. Such a method would force the majority of heat to dissipate through conduction into the thermoelectrics along the faces of the cube, as the absence of a heat transfer medium in air would give the heat only one path. Implementing this system would be very simple and easy, even from a manufacturing standpoint, as the steel box could simply be welded to the heat sinks to create such a system. This would also simplify the manufacturing process greatly, as the existing ceramic supports are relatively complicated and thick geometries that could create excessive costs.

## **5. Thermoelectric Analysis**

### **5.1. Overview**

The thermodynamic analysis utilizes a combination of the two previous design disciplines to produce results that estimate how energy is converted throughout the system. This section will begin with a brief discussion on the theory of power production in RTGs and why thermal analysis of the system plays a pivotal role in estimating quantities of interest. Having learned the theory behind power output, the scope for optimization was narrowed down to a few key elements that overall greatly affect the final analysis. Moving on to the true analysis of the system, multiple SolidWork studies were run to solve for the temperature throughout the entire RTG. These simulations include the RTG operating in different environments and at various points in its lifetime. With these SolidWork simulations, a python script was created to quantify the conversion of heat to electrical energy. Through this analysis, a thorough understanding of the exact manner by which the RTG operates was understood allowing further proof of and trust in the feasibility of the design.

### **5.2. Utilizing Seebeck Effect to Produce Power**

The driving mechanism behind a RTG is the ability to convert heat energy into electrical energy without using a turbine. This may seem impossible, however, a physical phenomenon called the Seebeck effect makes this possible. This phenomenon occurs when two dissimilar metals experience a temperature differential across both ends and produces a current that passes through the metals. Taking advantage of the continuously decaying heat source and the unique thermoelectric properties of the semiconductors, the design focuses on maximizing this gradient to produce the most power efficiently.

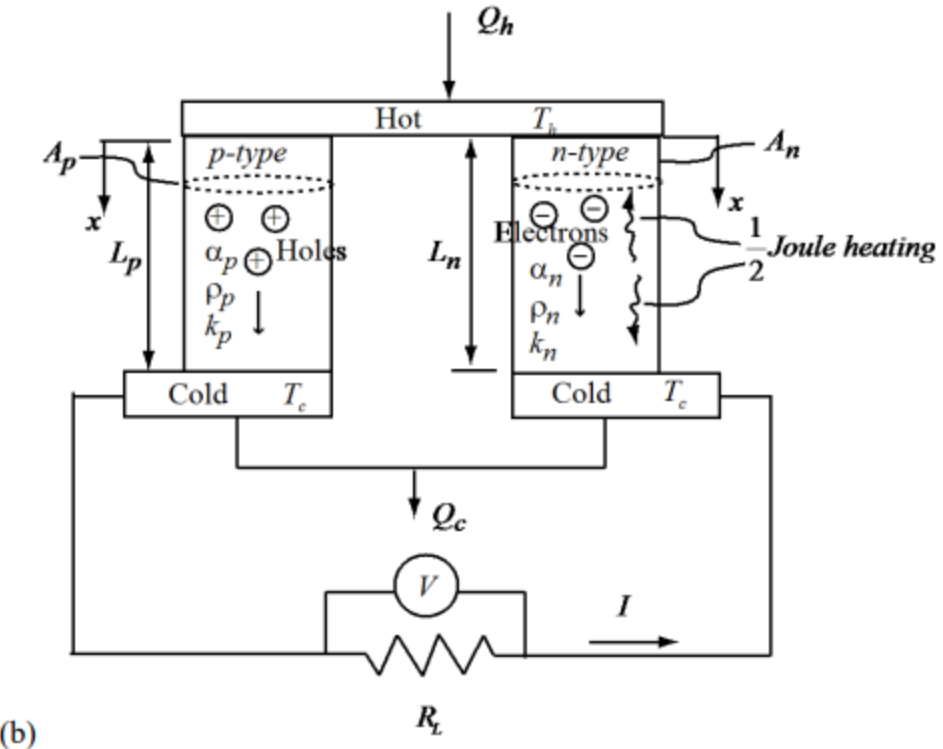


**Figure 29.** Basic 1D - schematic of a thermocouple. [X]

In Figure 29, it can be seen that with this current, a potential voltage difference is created through the implementation of a load resistor and the internal resistance of the materials themselves. For the system, there will be several of these thermocouples connected in series with the environment's electric grid. One of the quantities whose optimization is prioritized is the load resistor as it affects all of the electrical quantities of the circuit which determine the power output of the system.

### 5.3. Thermoelectric Generator Module

After running the various thermal studies in SolidWorks, the temperature gradients for each scenario were inputted within a python script that the team created to quantify the electrical energy produced by the RTG. The script utilizes a steady-state one dimensional thermoelectric generator module (visually shown in Figure 30) and computes values for the current, voltage, electrical power output, and efficiency. All of these quantities are as a result of the Seebeck effect taking place consistently throughout the system.

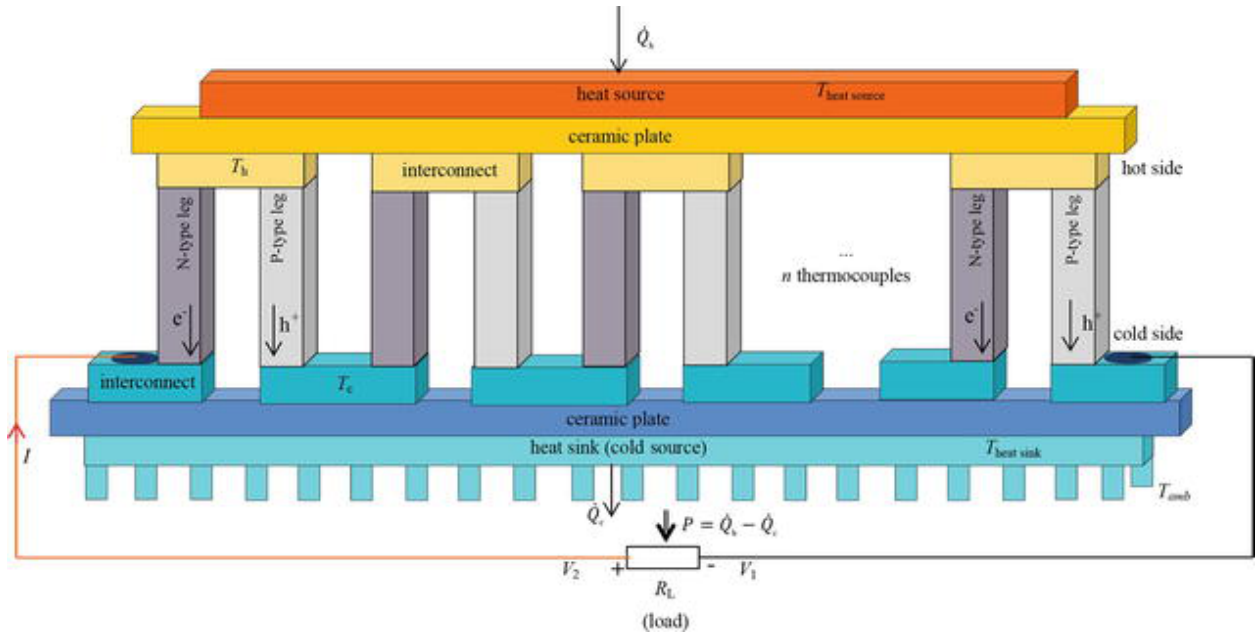


**Figure 30.** Visual of the steady-state 1D thermoelectric generator module used in the python script. [X]

Given the temperature differential across all of the thermocouples and the known material properties, the equation listed below produces the desired values of the circuit.

$$I = \frac{\alpha(T_h - T_c)}{R_L + R} \quad \text{Eq. 1}$$

$$V = \frac{n\alpha(T_h - T_c)}{\frac{R_L}{R} + 1} \left( \frac{R_L}{R} \right) \quad \text{Eq. 2}$$

$$P_{elec} = \frac{n\alpha^2(T_h - T_c)^2}{R} \frac{\frac{R_L}{R}}{(1 + \frac{R_L}{R})^2} \quad \text{Eq. 3}$$

$$\eta_{th} = \frac{P_{elec}}{Q_s} \quad \text{Eq. 4}$$

Where:

$I$  = current produced (A)  
 $V$  = voltage difference across module (V)  
 $P_{elec}$  = electrical power output (W)  
 $\eta_{th}$  = thermoelectric efficiency  
 $T_h$  = hot side of thermocouple (K)  
 $T_c$  = cold side of thermocouple (K)  
 $R_L$  = load resistance ( $\Omega$ )  
 $R$  = internal resistance ( $\Omega$ )  
 $\alpha$  = Seebeck Coefficient  
 $n$  = number of thermocouples  
 $Q_s$  = Heat energy produced by source (W)

## 5.4. Optimizing Load Resistance

Before any results can be displayed, a load resistor value must be determined to place within the circuit. This is to ensure that there is some kind of voltage difference across the thermoelectric module. When dealing with semiconductors which have a small electrical resistivity, it is crucial to ensure that there is additional resistance to prevent a short circuit. A study was performed where the power and efficiency of the system was calculated with respect to a changing load resistor value. The temperature differential across the thermocouple needed for this analysis was set to an arbitrary value since it only affects the magnitude, not the behavior of the system. For the sake of simplicity, the load resistor was quantified in terms of the internal resistance in Figures 31 which is displayed below.

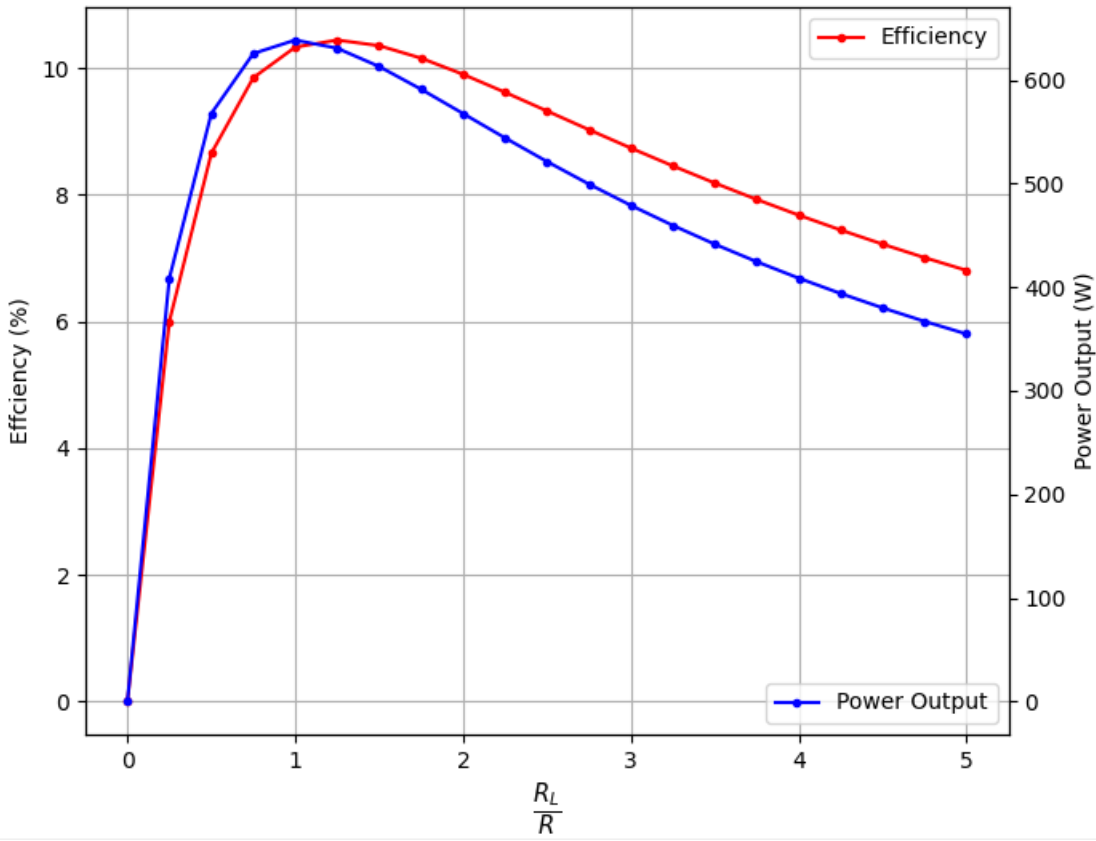


**Figure 31.** Electrical power output and efficiency as a function of the load resistance of the RTG design.

Based on Figure 31, the behavior of both the efficiency and power output as a function of the load resistance is relatively the same. The optimal load resistance value for both quantities differs slightly when it is equal to the internal resistance of the RTG module. With the assumption that all material properties used were at a constant temperature of 1000 K, the internal resistance of the module is 0.0041  $\Omega$ . To utilize a load resistor with this small of a resistance is risky, and a physical test would be needed to ensure the circuit will not short out. Performing this test requires knowledge of what to use as the current and voltage, and creating a simple circuit. This leads to the analysis of how the current and voltage are also affected by the load resistor. Below in Figure 32 is each quantity normalized by its maximum value.

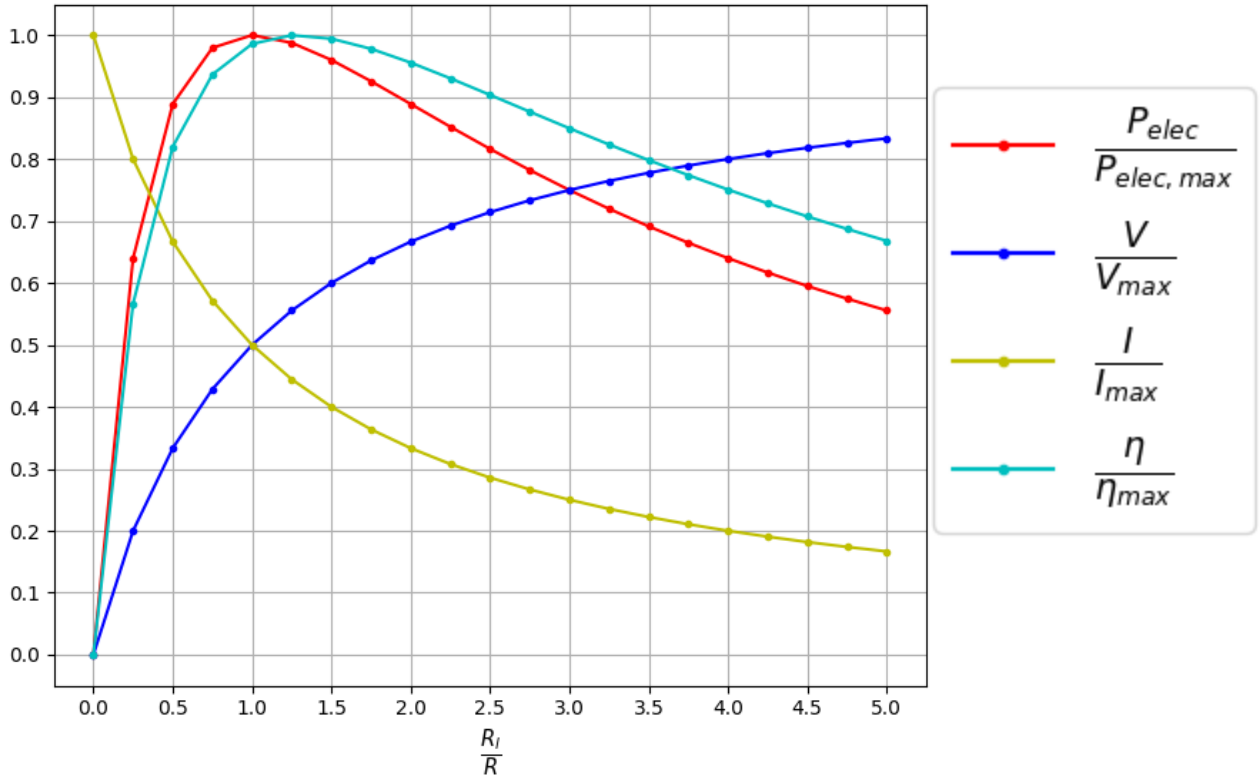


**Figure 32.** Normalized circuit parameters as a function of the load resistor.

Based upon Figure 32, it was decided that a load resistor of  $0.01 \Omega$  will be used throughout the thermoelectric analysis. Although this is not the most optimal value to produce the most power efficiently, it is slightly conservative to account for the possibilities of the circuit shorting out. Furthermore, there is approximately a 10% decrease in performance within the system which is not significant. One important feature the load resistor allows the RTG to have is the ability to alter power output based upon the application required. For this project, it was established that this system will be designed for a range of applications that require both small and large power consumption. Through this optimization analysis, it was unknowingly revealed that the system could utilize the load resistor as a control mechanism for the power output.

## 5.5. Thermoelectric Conversion Results

Utilizing the thermoelectric generator model script, a series of quantities of interest will be generated showcasing how the system converts the energy generated by the heat source into usable electrical energy. The following results are based from a

SolidWork simulation where the average temperature differential across the thermocouple is taken from the SolidWorks simulation and used for the python script.

**Table 12.** Preliminary Thermoelectric Results when RTG is at BOL.

Calculated Parameters for Maximum Power Output (BOL)	
Heat Emitted by Source (W)	16878
$\Delta T$ across Thermocouple (K)	1329
Electrical Power Output (W)	1350
Efficiency (%)	13.84
Voltage (V)	17.25
Current (A)	78.2
Load Resistance ( )	0.0049

**Table 13.** Preliminary Thermoelectric Results when RTG is at EOL.

Calculated Parameters for Maximum Power Output (EOL)	
Heat Emitted by Source (W)	16878
$\Delta T$ across Thermocouple (K)	1048
Electrical Power Output (W)	840
Efficiency (%)	11.52
Voltage (V)	13.61
Current (A)	61.66
Load Resistance ( )	0.0049

In order to ensure the design objective is met, two preliminary thermoelectric results are displayed above for the beginning and end of operation for the RTG. The EOL is calculated after 10 years which shows how much of a power drop off occurs during

operation. Despite this problem, the goal of maintaining an electrical power output on a scale of 1 kWe while keeping a thermoelectric efficiency above 8% is still met.

## 5.6. Performance of System in Different Environments

Since this design will be placed in areas that are rigid and inaccessible, it is important to understand how it behaves in contrasting environments. For this study, the performance of the design was tested at three different ambient temperatures: room temperature (80 F), -20 F, and 110 F. The SolidWorks thermal simulation was run for all three scenarios maintaining a constant convection coefficient of 25 W/m<sup>2</sup>K. For all three scenarios, the thermoelectric performance was analyzed when the source was at BOL. Needless to say there was no difference in performance between the varying ambient temperatures, thus it is useless to show tabular results. All three produced results that were the same as Table 14. The temperature gradient across the thermocouple remained the same for each scenario, however, the hot and cold sides temperatures changed depending on the environment. In table 14, the temperatures for each side of the thermocouple are shown for the varying environments. There is considerable change between the three ambient temperature cases, and shows that the design will function better in cold environments due to smaller possibility of material failure.

**Table 14.** Temperature of each side of thermocouple for different environments.

Ambient Temperature (F)	Hot Side (K)	Cold Side (K)
-20	1764	435
80	1820	491
110	1837	508

## 5.7. Transient Analysis

Finally, the last piece of analysis done was understanding how the design will perform throughout its operational lifespan. Since the heat source is continuously decaying and losing power, performance will slowly degrade over time. Utilizing the script from Appendix A, the heat produced by the Strontium source was calculated at one day intervals which is shown in Figure 33. The SolidWorks simulation was run at these varying heat source energies, and the resulting temperature difference across the thermocouples is shown below.

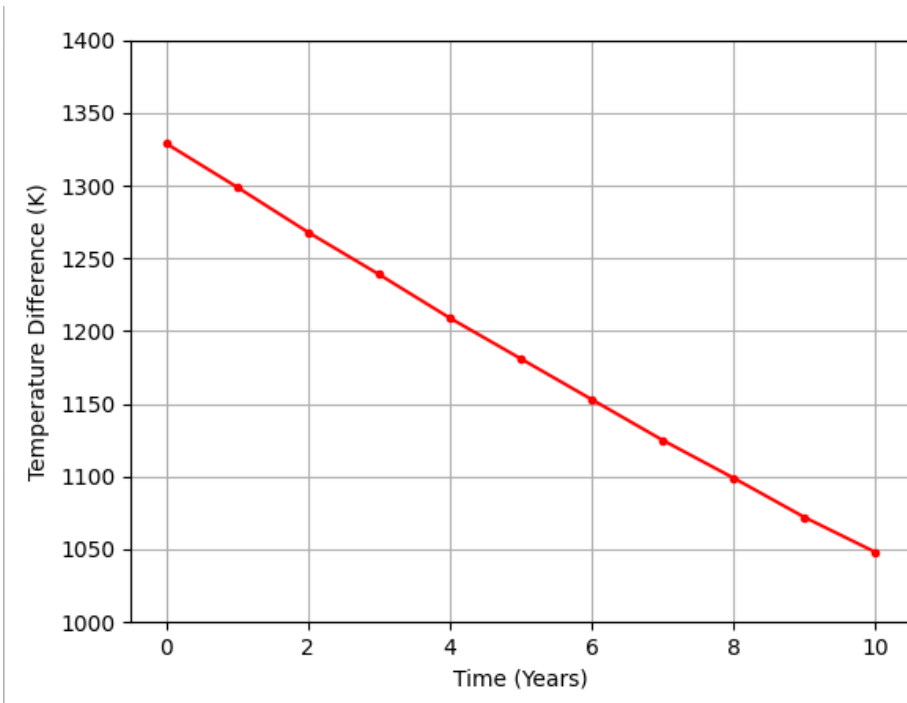


**Figure 33.** Temperature difference across thermocouple as a function of time.

Based on these varying temperature differences computed in SolidWorks, the thermoelectric analysis script was then used again to calculate the power output as a function of time.

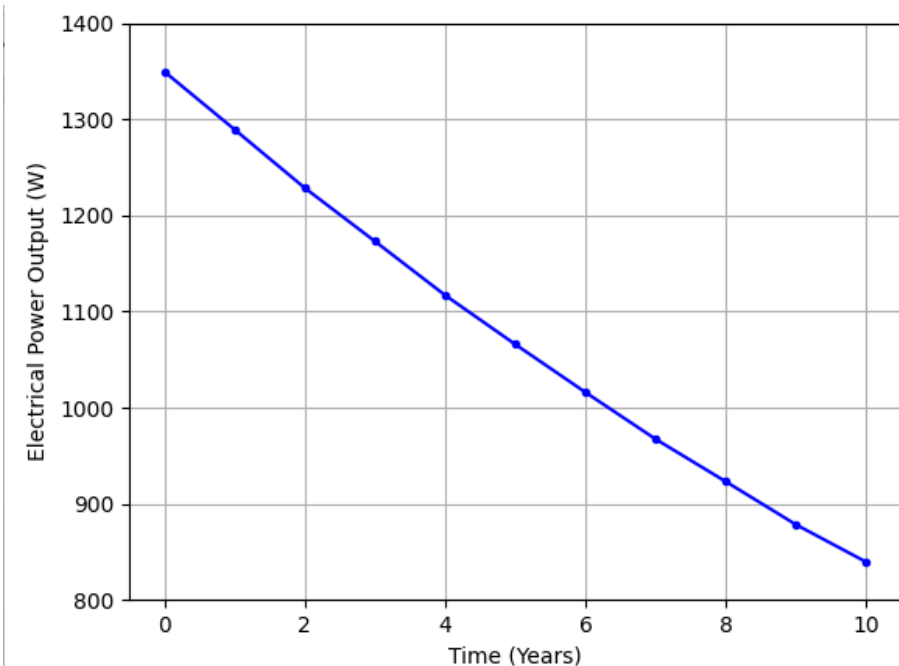


**Figure 34.** Power output as a function of time.

## **6. Radiation Shielding and Safety Analysis**

### **6.1. Overview**

The radiation shielding and safety analysis employs a combination of simple excel and python calculations while using proper activity, attenuation, and dose rate calculations. This section first briefly discusses the nature of radioactive isotopes such as half life values and the types of radiation that exist from both the isotope chosen and the other isotopes that were considered. This will also partly discuss the pros and cons of the four original isotopes that were considered for the source. After this, the original activity and dose rate calculations will also be discussed because they were done as preliminary calculations prior to using more thorough excel calculations. It is important to note that this includes the dose rate for the betas that people could be exposed to as well as the secondary bremsstrahlung which is far more dangerous. However, the bremsstrahlung being produced wasn't necessarily as big a hazard because of reasons that will be discussed in this section.

### **6.2. Background Information on Possible Radiation Types**

Prior to doing any sort of radiation calculations, it was necessary to identify all the isotopes that would be considered for the fuel source. The main concerns when first deciding on potential radioisotopes was their heat generation, half life values, and the type of radiation they emit.. After researching numerous radionuclides, four main options were chosen. These four isotopes were Plutonium-238, Polonium-210, Strontium-90, and Americium-241.

**Table 35.** Preliminary General Data of 4 Radionuclide Candidates

Radioisotope	Half Life (years)	Emitter	Q-Value (keV)
Plutonium-238	87.7	Alpha	5593.2
Polonium-210	0.378	Alpha	5407.46
Strontium-90	28.79	Beta	546.0
Americium-241	432.2	Alpha	5637.81

As shown, the isotope candidates were all relatively safe radiation emitters that hardly require little to no shielding in their decay state. All of these nuclei are radioactive, so they will naturally decompose by emitting the particles mentioned above and in doing so, become a different nucleus altogether. This occurs because in all other types of changes, only the electrons change. All nuclei with more than 83 protons are radioactive, and elements with 83 and less protons have both stable and unstable isotopes such as

strontium-90. In natural radioactive decay, three common emissions occur, these common emissions are alpha and beta particles, then the more severe, gamma rays.

Decay Type	Radiation Emitted	Generic Equation	Model
Alpha decay	${}_{2}^{4}\alpha$	${}_{Z}^{A}X \longrightarrow {}_{Z-2}^{A-4}X' + {}_{2}^{4}\alpha$	<p>Parent                          Daughter                          Alpha Particle</p>
Beta decay	${}_{-1}^{0}\beta$	${}_{Z}^{A}X \longrightarrow {}_{Z+1}^{A}X' + {}_{-1}^{0}\beta$	<p>Parent                          Daughter                          Beta Particle</p>
Gamma emission	${}_{0}^{0}\gamma$	${}_{Z}^{A}X^* \xrightarrow{\text{Relaxation}} {}_{Z}^{A}X' + {}_{0}^{0}\gamma$	<p>Parent (excited nuclear state)                          Daughter                          Gamma ray</p>

**Figure 36.** Types of radioactive decay emissions.

### 6.3. Radioactive Qualities of the Fuel Source

Another key aspect of maintaining absolute radiation safety is the dose limit humans and the environment can be exposed to. Humans are naturally exposed to background radiation from other sources as they about their day. The main objective is to identify the maximum amount of radiation an individual can receive before it starts to affect their health. The image below from the NRC shows some of the values that humans may or may not receive depending on their activities and workplace. Furthermore there are also values that humans should not exceed within a given span of time.

## Dose Limits



For occupational exposure of workers over the age of eighteen years\*:

**20** mSv effective dose per year - averaged over five years (100 mSv in 5 years) **and**

**50** mSv in any single year (in some countries the dose limit is 20mSv per year)

**20** mSv equivalent dose per year to the lens of the eye averaged over five years (100 mSv in 5 years) **and**

**50** mSv in any single year

**500** mSv equivalent dose per year to the extremities (hands and feet) or to the skin



For occupational exposure of apprentices or students of 16 to 18 years of age who are being trained for employment involving radiation or use sources in the course of their studies\*:

**6** mSv effective dose per year

**20** mSv equivalent dose per year to the lens of the eye

**150** mSv equivalent dose per year to the extremities (hands and feet) or to the skin

\* Additional restrictions apply to occupational exposure for a female worker who is pregnant or is breast-feeding.

**Figure 37.** General Values for Human Radiation Dose Limits

After taking all of this information into consideration, as well as all the information in the material analysis portion of this report, the fuel source was determined to be Strontium-90, more specifically Strontium Titanate. However, upon choosing said fuel source, a great amount of information needed to be ascertained in order to properly protect from its potentially dangerous radioactivity.

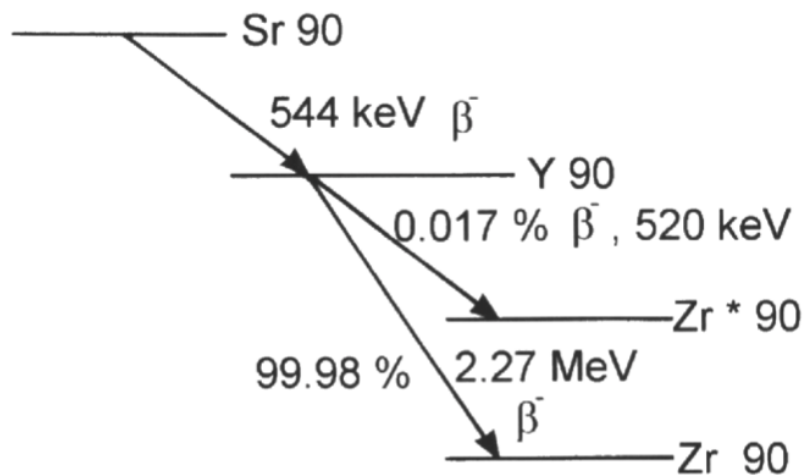


**Figure 38.** Decay Chain of Strontium-90

Upon first inspection of Strontium-90, it seemed like an ideal fuel source. The isotope has a long half life of about 30 years, and it could be much cheaper and easier to

procure than any of the other isotopes since it is produced as spent fuel from most western reactors. This is also coupled with the fact that the isotope has an ideal specific heat and melting point for a device like this. However, a number of issues began to arise when looking at its decay chain above. Even though Strontium-90 is only a beta emitter, it still needs to be properly shielded. One of the main issues however is the possible secondary bremsstrahlung that can occur as a result of the beta particle interacting with different materials. It was crucial to properly provide shielding for such an interaction as the gamma rays it produces can be extremely harmful to living tissue. A high atomic number in the material used was undesirable as it can increase the chances and damage of the gamma rays from secondary bremsstrahlung. Furthermore, not just any low “Z” value material can be used to prevent this as doing so would cause a number of issues for the RTG. A prominent issue that persevered was choosing a material that could properly attenuate these gamma rays as well as having a high melting point so as not to cause any kind of melting which could result in material failure across the entire device.

Another prominent issue was Strontium-90’s decay chain. Strontium-90 decays into Yttrium-90. This particular isotope will become more prominent as the Strontium-90 slowly decays into this product. The issue with Yttrium-90 is that it has a much higher energy value when compared to its parent isotope. Furthermore, it also emits beta particles much like Strontium-90. This causes the secondary bremsstrahlung radiation to potentially become much more potent to living tissue. Due to this, since Strontium-90 would exist in the device for a lengthy period of time, radiation shields needed to be strong enough to protect from its daughter product. By properly making a shield that protected from Yttrium-90’s radiation, Strontium-90 would also be properly shielded.

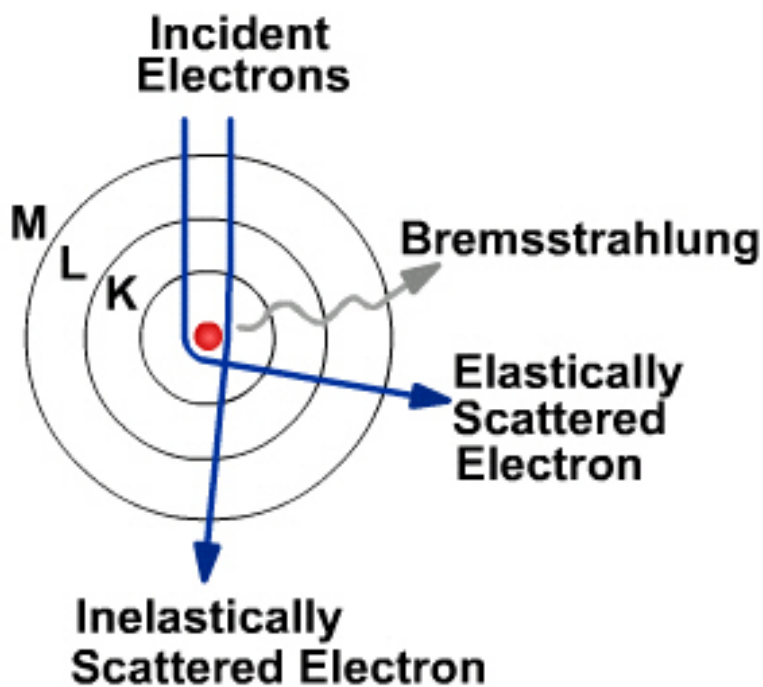


**Figure 39.** Diagram of potential Bremsstrahlung Occurring.

#### 6.4. Utilizing Attenuation and Activity to Calculate Dose Rate

$$\rho = \frac{m}{V} \quad \text{Eq. 5}$$

$$M = \frac{m}{\text{Mole}} \quad \text{Eq. 6}$$

$$N = \text{Mole} * \text{Avogadros' Number} \quad \text{Eq. 7}$$

Where:

$\rho$  = Density ( $g/cm^3$ )

$m$  = Mass ( $g$ )

$V$  = Volume ( $cm^3$ )

$M$  = Molar Mass ( $g/mol$ )

Mole = Amount of a substance ( $mol$ )

$$Avogadro's\ Number = 6.022 * 10^{23}$$

$$N = Number\ of\ Atoms$$

The equations above were a necessary calculation in order to determine several values that were needed for further calculations. The amount of nuclei and mass were necessary values to later determine the initial activity of the source, as well as the dose rate.

$$A = A_0 e^{-\lambda t} \quad \text{Eq. 8}$$

$$A_0 = \lambda N_0 \quad \text{Eq. 9}$$

Where:

$$A = Activity\ (Ci)$$

$$A_0 = Initial\ Activity\ (Ci)$$

$$\lambda = Decay\ Constant\ (s^{-1})$$

$$t = Time\ (years)$$

$$N_0 = Initial\ Number\ on\ Nuclei$$

After properly recovering the necessary values needed to calculate the activity was calculated. The calculated activity of a  $19 \times 19 \times 19$  centimeter cube of Strontium-90 was determined to be  $25.22 \times 10^5 Ci$  of beta particles. This equation was also used to calculate the activity of the source over a longer period of time. This was done because the device would ideally operate for a long period of time, and the fuel source's activity needed to be monitored for the thermoelectric analysis.

$$f = \frac{E_\beta Z}{3000} \quad \text{Eq. 10}$$

Where:

$$f = Fraction\ Beta\ Energy\ Released\ as\ Bremsstrahlung$$

$$Z = Atomic\ Number\ of\ the\ Target$$

$$E_\beta = Maximum\ Beta\ Energy\ of\ Radionuclide$$

The equation above allows a calculation of how severe the secondary bremsstrahlung can be depending on the energy level of the radionuclide as it emits betas. However, for this device simply attenuating for the gamma rays of Strontium-90 is not enough. As mentioned prior, its daughter product after it decays also emits betas but at a much higher energy level. After taking a number of factors into account such as what material will be used in the device to block the beta particles, it was determined that a safe energy level to attenuate these gammas would be between 2 MeV and 3 MeV. Below is a small list of a few of the materials that potentially would be used in the device.

Values	SrTiO <sub>3</sub>	Aluminum	Cordierite	Aluminum Nitride	Tungsten	Copper	Molybdenum	SiGe (72% Si)
Thermal Conductivity [W/m*K]	12	210	1.3-1.7	60-177	1.73	386	138	6.952
Specific Heat [J/kg*K]	537.109	870	800-850	780-820	133	390	25	503.245
Density [g/cm <sup>3</sup> ]	5.12	2.6989	2.0-2.3	2.92-3.33	19.3	5.96	10.22	3.2679
Melting Point [K]	2353.15	933.52	1733.15	2670-2780	3683.15	1358.5	2896.15	1499.13 K
Attenuation Coefficient @ (2MeV photon) [cm <sup>2</sup> /g]	0.042047517	0.04324	0.0439894	0.043670575	0.0433	0.04205	0.04163	0.048168
Attenuation Coefficient @ (3MeV photon) [cm <sup>2</sup> /g]	0.035614544	0.03541	0.036074424	0.035539856	0.04075	0.03599	0.03675	0.0363488

**Figure 40.** Material Data and Mass Attenuation at 2 MeV and 3 MeV

$$I = I_0 e^{-\mu x} \quad \text{Eq. 11}$$

$$\mu = m_\mu \times \rho \quad \text{Eq. 12}$$

Where:

$I$  = Shielded Dose Rate (rad/hr)

$I$  = Unshielded Dose Rate (rad/hr)

$\mu$  = Linear Attenuation Coefficient ( $cm^{-1}$ )

$m_\mu$  = mass attenuation coefficient ( $cm^2/g$ )

$\rho$  = Density of Shielding Material ( $g/cm^3$ )

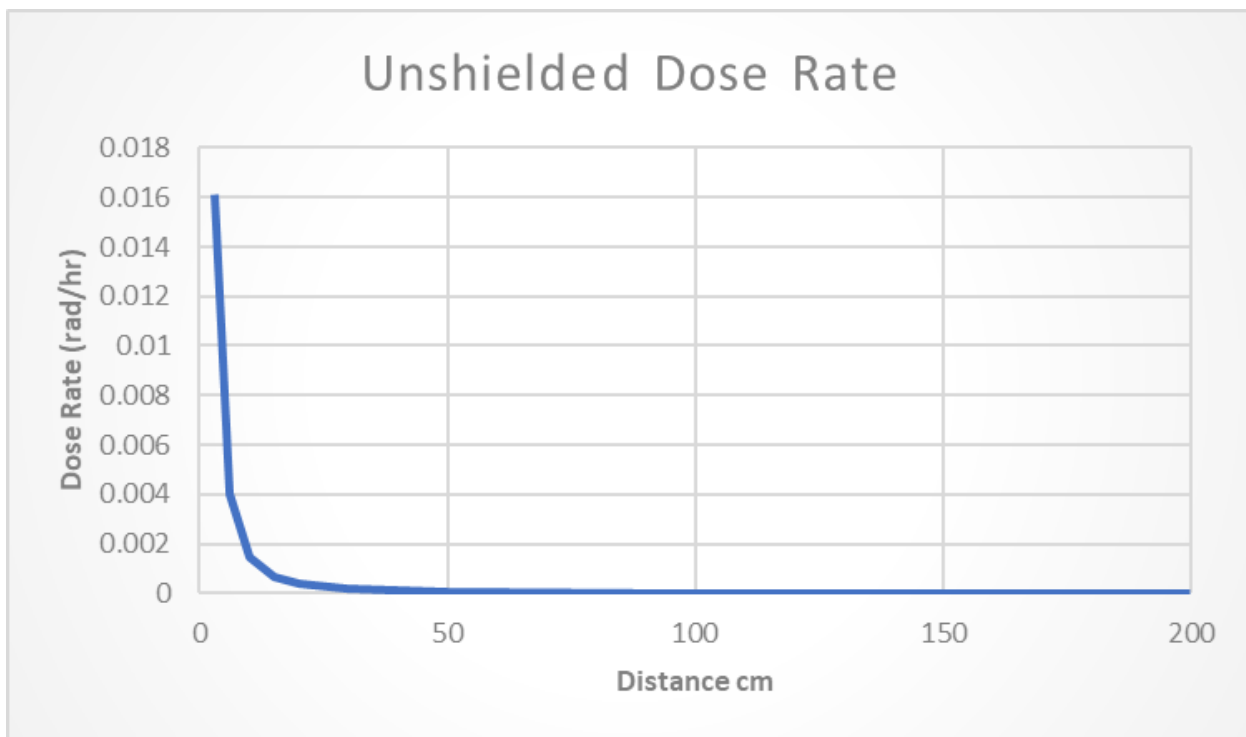


**Figure 41.** Unshielded Dose Rate of Yttrium-90

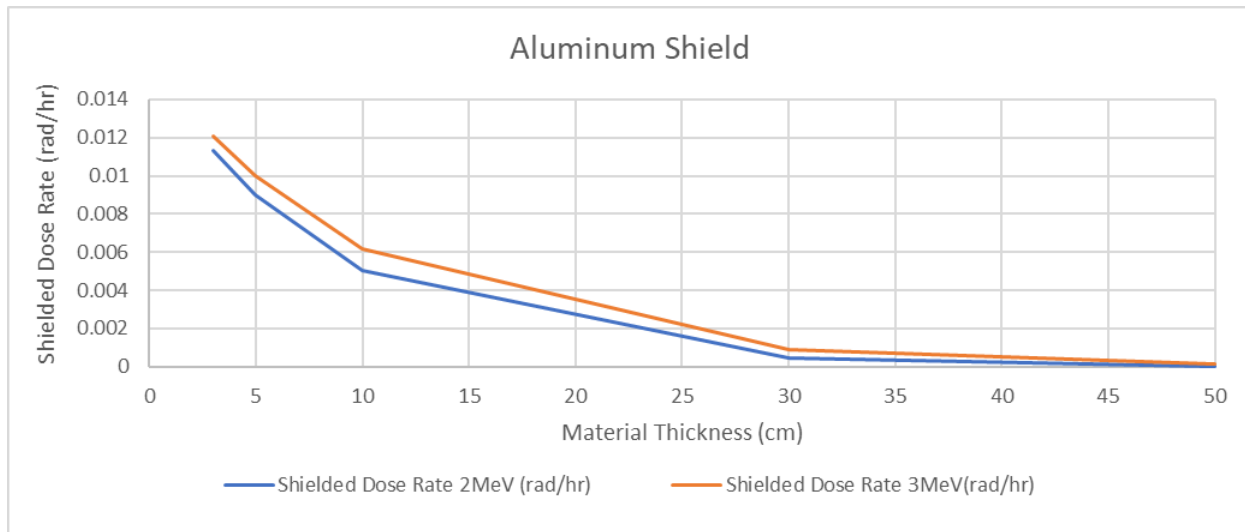


**Figure 42.** Aluminum Shield Attenuation

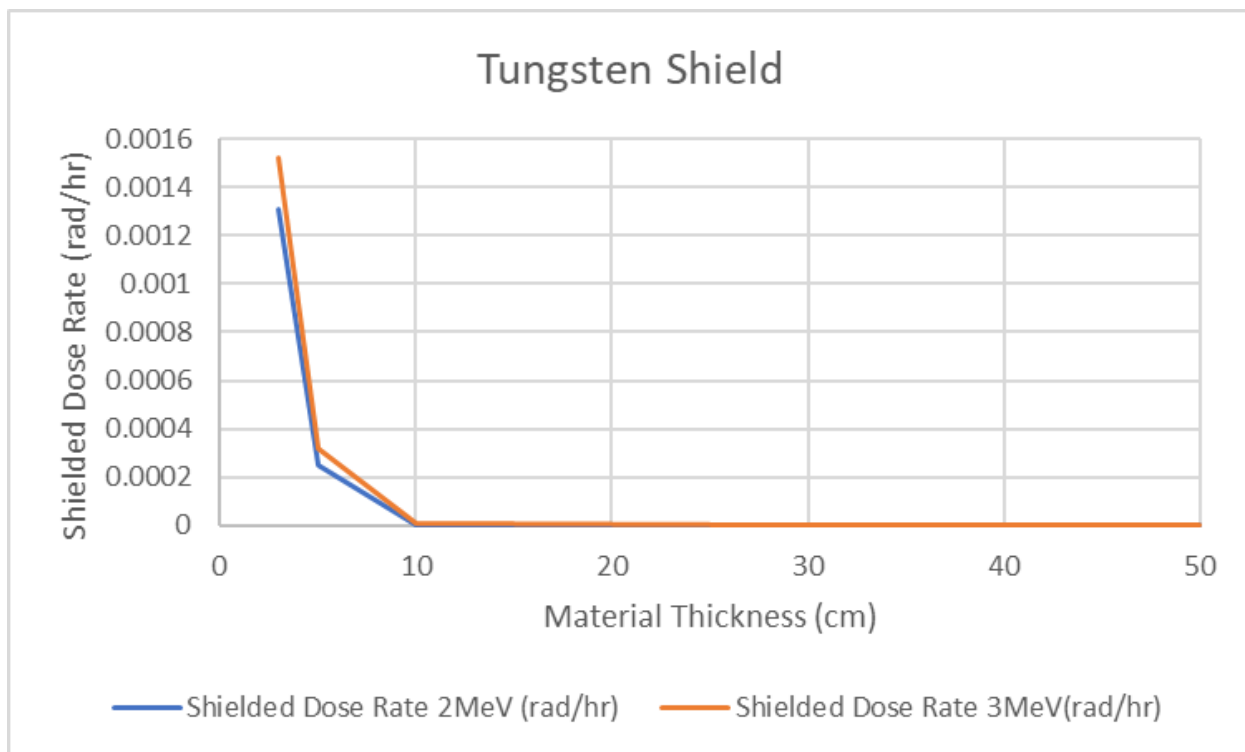


**Figure 43.** Tungsten Shield Attenuation

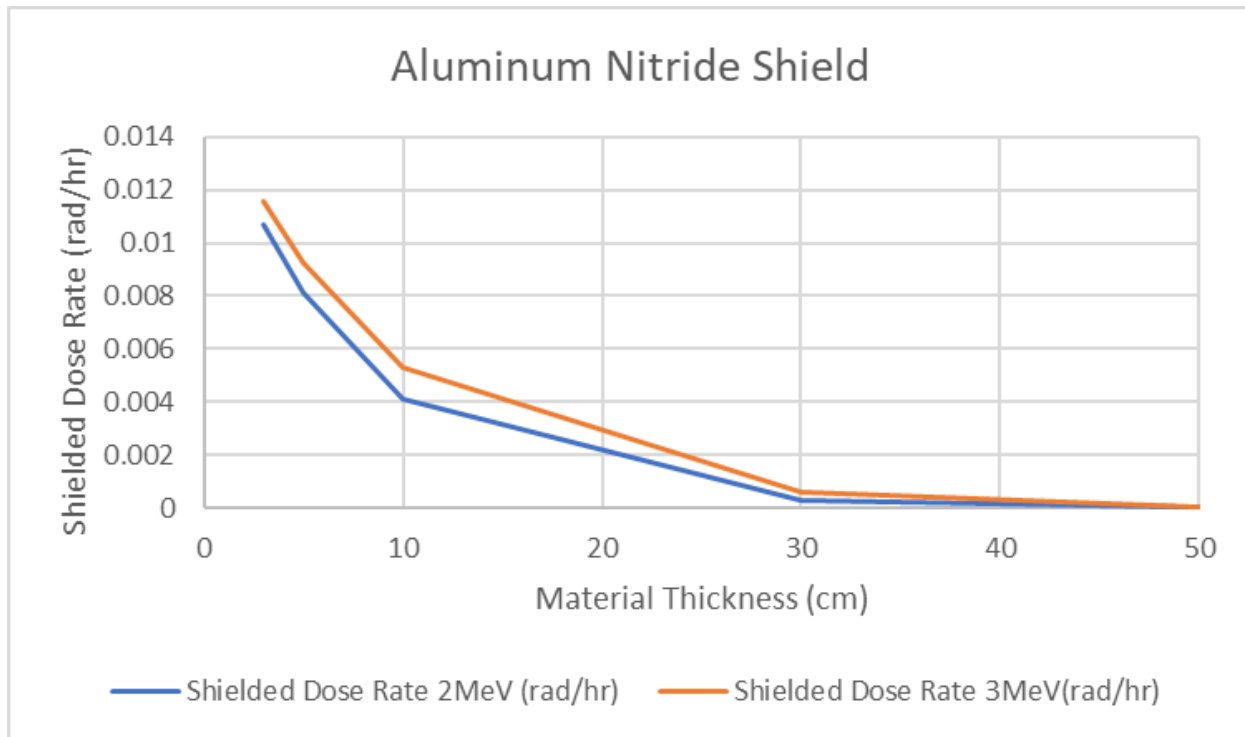


**Figure 44.** Aluminum Shield Attenuation

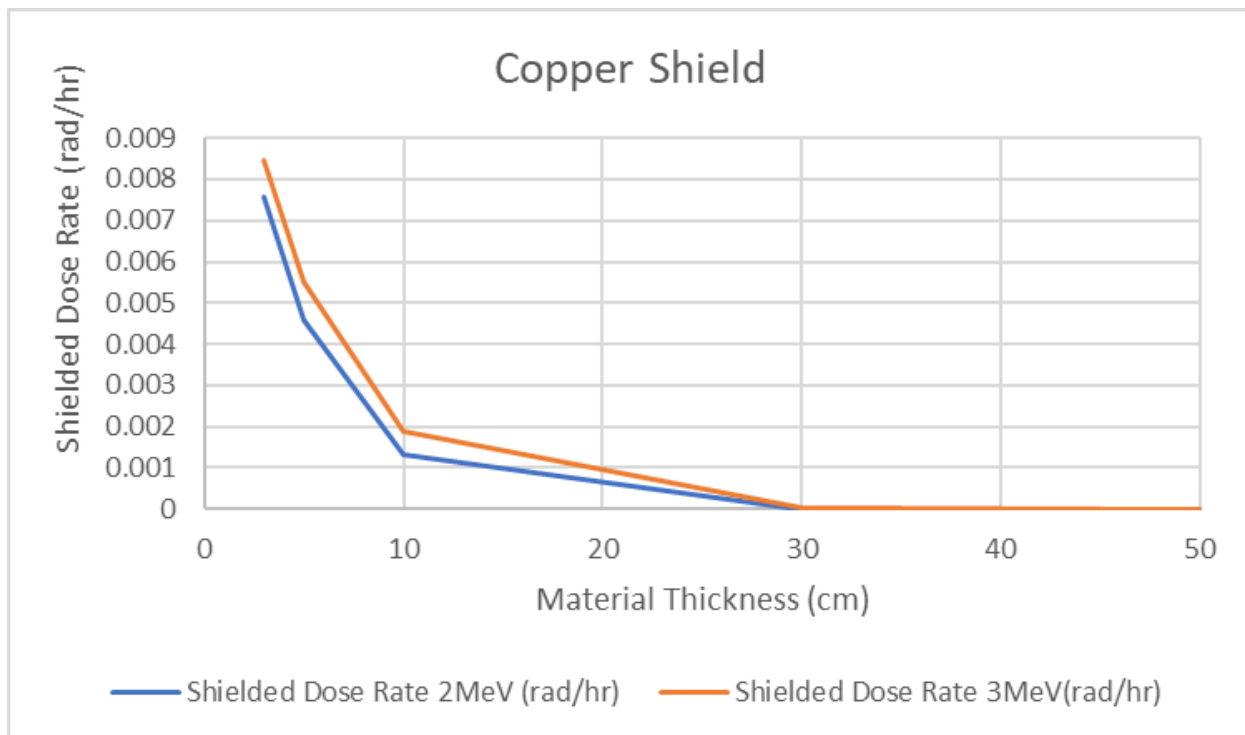


**Figure 45.** Copper Shield Attenuation

## **6.5. Overall Safety Analysis**

After receiving all of the results for the potential radiation exposure, it is safe to say that Tungsten in small quantities is the best shield for when accounting for both beta particles and bremsstrahlung. However, aluminum does also complete the task of keeping the dosage level low and nonexistent with certain amounts. It is important to note that aluminum would be much cheaper and its aluminum oxide counterpart would be more useful because of its higher melting point. Tungsten would be more expensive, but it would severely limit radiation exposure and with enough of it can lower it to non-existent levels. Another thing to note is the device itself could always be improved when regarding shielding. It would be much more costly to have net zero exposure, but for this particular device, it would not be necessary. Another key aspect that makes the RTG safer is where it will inherently be placed. This device would be well kept away from the people or infrastructure benefitting from its power. This would allow more travel distance for the beta particles and gamma rays. Furthermore, only trained personnel with the proper level of PPE and security clearance would be allowed anywhere near the RTG. It would come with the proper level of security in the shape of surveillance and possibly trained personnel. Overall there exist a number of methods that can be further implemented, but in order to make this device cost effective, safety should not go past the point it is no longer useful to the overall structure.

## **7. Economic Analysis**

### **7.1. Overview**

This section will provide an in depth analysis of the economic feasibility for the RTG design. The analysis will focus on comparing the cost to power applications in remote environments with the RTG design as opposed to utilizing diesel fuel. Since diesel fuel will be the design's direct competitor, both the short and long term cost will be evaluated through a variety of metrics.

### **7.2. Total Cost Estimate of Design**

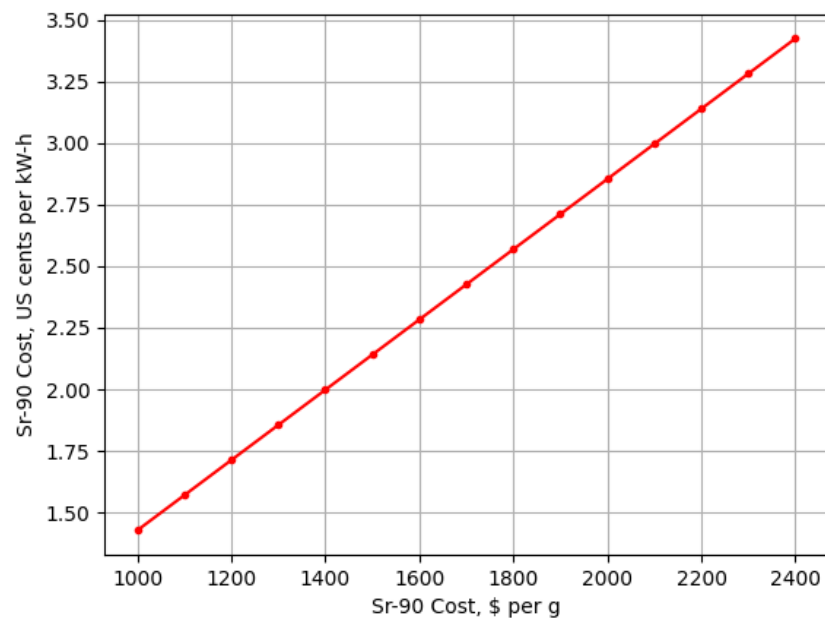
First, the cost to construct the design must be established before performing any type of analysis. With the material market constantly fluctuating and the cost to manufacture unique parts unknown, this task is impossible to complete without many assumptions. Furthermore, there is no terrestrial RTG on the market where the price of the design can be estimated. With this in mind, it was decided that the construction cost of the design would be based on the GPHS-RTG developed by INL for US space missions. This design cost approximately \$120M for both the development

and production [12]. It is important to keep in mind that there are many differences between this RTG design and the GPHS-RTG, which include fuel source and the scale of the electrical output.

### 7.3. Electricity Rates

Despite the immense up front cost to construct this design, the financial upside comes from the non-existent operational cost, and frequency at which the RTG has to be refueled. The fuel cost per kW-h is what ultimately determines how profitable the design is over time. Since the RTG produced around 800 W throughout its operational lifespan, and the cost range of Sr-90 is known, a basic cost analysis can be made. Below in Figure 40 is the fuel cost per kW-h with a varying price range.

**Figure 46.** Cost of Sr-90 per kW-h as a function of Sr-90 market price.



This is slightly higher than the typical 0.5 cents/kW-h that diesel produces which seems that the RTG design would not be feasible to implement. However, there are external factors that were not taken into consideration for this analysis. One being the frequent transportation cost that diesel would require, and the fact that it is not a carbon free energy source. It is hard to quantify how valuable a carbon free energy solution is towards the economics as each individual has their own perspective where many are willing to accept these larger costs in order to produce this clean energy.

#### **7.4. How Can the Design be Improved Economically?**

The biggest difficulty being faced in the fiscal viability of this RTG is the manufacturing of its components. In order to go about attaining the 343 fuel pellets required to build one single RTG of this design, a streamlined manufacturing process must be defined and brought about. As with any large project, the more that you make, the cheaper each unit becomes.

### ***8. Conclusion***

After going through all five technical areas, there is a lot to takeaway from the proposed terrestrial RTG design. Each technical area experienced their own unique successes and hardships which is expected for any design project. In this section, some of the key milestones and failures will be highlighted in addition to the next steps to make this design a reality.

Based upon the design objectives established at the beginning of the design process, the overall RTG design can be considered a success. The proposed RTG was designed in a modular form that can produce power consistently on a 1 kWe scale. Furthermore, the thermoelectric efficiency goal of 8% was exceeded, and the economic feasibility of implementing such a device was confirmed. What sets this design apart from other energy solutions is its inherent ability to be self-reliant and not require any type of operator on site. This is beneficial for our targeted application as we hope to deliver this RTG to remote areas where power is needed for long stretches of time. One aspect of this design that was not touched upon was how Strontium-90 would be obtained to construct the heat source of the RTG. Strontium-90 is a byproduct of nuclear waste from the traditional LWRs that are in operation in the United States. By utilizing

this byproduct of Strontium-90, the amount of nuclear waste required to store is reduced and recycled. This aspect of the design further proves that this system is worth the investment, and will only increase its prospects as a solution due to the need for clean energy devices.

Despite these successes, many approximations were made throughout the design process due to the time frame of the project. Further work will be needed to solidify some of the design and analysis that were performed in the previous sections. For instance, the modular fuel design is currently still a work in progress, and will require more time to fully construct a SolidWorks model. This incomplete model has caused a trickle-down effect for both the thermoelectric and radiation analysis side as both of these areas produced results based on the old design.

Overall, the proposed RTG design addresses a unique problem through a variety of specific features for this application. The energy consumption of the world is only increasing, and for remote areas this is no different. There has been no change in the way these remote areas power their electric grid or specified devices over the years, and with the rapid development in the nuclear and material industry the possibilities for energy solutions are endless. With this design, there is hope that terrestrial RTGs can become apart of revolutionizing the energy industry and enhancing the lives of those who can benefit from this technology.

## ***9. Acknowledgements***

## **10. References**

- [1] Department of Energy. “Advanced Small Modular Reactors (SMRs)”, *DOE*, [Online] Available: <https://www.energy.gov/ne/advanced-small-modular-reactors-smrs>.
- [2] Lovekin, Dave. “Remote communities meet renewable energy solutions”, *Pembina Institute*, [Online] Available: <https://www.pembina.org/blog/remote-energy-challenges>.
- [3] Lovekin, Dave. “The True Cost of Energy in Remote Communities”, *Pembina Institute*, [Online] Available: <https://www.pembina.org/reports/diesel-cost-backgrounder-2019.pdf>
- [4] National Aeronautics and Space Administration. “Radioisotope Thermoelectric Generators”, *NASA*, [Online] Available: <https://solarsystem.nasa.gov/missions/cassini/radioisotope-thermoelectric-generator/>
- [5] United States Nuclear Regulatory Commission. “Backgrounder on Plutonium”, *NRC*, [Online] Available: <https://www.nrc.gov/reading-rm/doc-collections/fact-sheets/plutonium.html>
- [6] Lahwal, Ali. “Thermoelectric Properties of Silicon Germanium”, *Clemson University*, [Online] Available: [https://tigerprints.clemson.edu/cgi/viewcontent.cgi?article=2496&context=all\\_dissertations](https://tigerprints.clemson.edu/cgi/viewcontent.cgi?article=2496&context=all_dissertations)
- [7] Department of Energy. “Thermoelectric Materials, Devices and Systems”, *DOE*, [Online] Available: <https://www.energy.gov/sites/prod/files/2015/02/f19/QTR%20Ch8%20-%20Thermoelectric%20Materials%20TA%20Feb-13-2015.pdf>
- [8] Alimov, Rashid. “Radioisotope Thermoelectric Generators”, *Bellona*, [Online] Available: <https://bellona.org/news/nuclear-issues/radioactive-waste-and-spent-nuclear-fuel/2005-04-radioisotope-thermoelectric-generators-2>
- [9] Azo Materials. “Strontium Titanate - Properties and Applications”, *Azo*, [Online] Available: <https://www.azom.com/article.aspx?ArticleID=2362>
- [10] Thomson, William. “Thermoelectric Generators”, *Western Michigan University*, [Online] Available: <https://homepages.wmich.edu/~leehs/ME539/Chapter%202.pdf>
- [11] Enescu, Diana. “Thermoelectric Energy Harvesting”, *Green Energy Advances*, [Online] Available: <https://www.intechopen.com/chapters/65239>

- [12] Werner, Johnson, Dwight, Lively. “Cost Comparison in 2015 Dollars for Radioisotope Power Systems”, INL, [Online] Available:  
<https://inldigitallibrary.inl.gov/sites/sti/sti/7267852.pdf>
- [13] Accaratus “Alumox”, Accaratus, [Online] Available: <https://accuratus.com/alumox.html>
- [14] Material Property Data “Aluminum, Al”, MPD, [Online] Available:  
<https://www.matweb.com/search/DataSheet.aspx?MatGUID=0cd1edf33ac145ee93a0aa6fc666c0e0&ckck=1>
- [15] Material Property Data “Copper, Cu”, MPD, [Online] Available:  
<https://www.matweb.com/search/DataSheet.aspx?MatGUID=9aebe83845c04c1db5126fada6f76f7e>
- [16] Material Property Data “Silver, Ag”, MPD, [Online] Available:  
<https://www.matweb.com/search/DataSheet.aspx?MatGUID=63cbd043a31f4f739ddb7632c1443d33>
- [17] MI Indication “Aluminum Price”, Business Insider, [Online] Available:  
<https://markets.businessinsider.com/commodities/aluminum-price>
- [18] MI Indication “Copper Price”, Business Insider, [Online] Available:  
<https://markets.businessinsider.com/commodities/copper-price>
- [19] Silver Price Per Kilo “Silver Price per Kilo Today”, GoldPriceOz, [Online] Available:  
<https://www.goldpriceoz.com/silver/silver-price-per-kilo/>
- [20] Thermoelectric Products Engineering, “Silicon Germanium Thermoelectric Materials and Module Development Program (U)”, RCA, 31 Dec 1968, [Online] Available:  
<https://www.osti.gov/servlets/purl/4811638>
- [21] Roberta Shor, Robert Lafferty Jr, P.S. Baker, “Strontium-90 Heat Sources”, Oak Ridge National Laboratory, 24 May 1971, [Online] Available:  
<https://technicalreports.ornl.gov/1971/3445605716035.pdf>
- [22] 17.3: Types of Radioactivity: Alpha, Beta, and Gamma Decay  
<https://chem.libretexts.org>
- [23] RADIONUCLIDE DATA SHEET Yttrium – 90 [Online] Available:  
<https://ehs.missouri.edu/sites/ehs/files/pdf/isotopedata/y-90.pdf>

[24] “Oak Ridge National Laboratory operated by UNION CARBIDE CORPORATION for the U.S. Atomic Energy Commission” S. J. Rimshaw E. E. Ketchen Isotopes Division December 1967 [Online] Available: <https://www.osti.gov/servlets/purl/4503630>

[25] “Nuclide Safety Data Sheet Strontium-90” [www.nchps.org](http://www.hpschapters.org/northcarolina/NSDS/90SrPDF.pdf) [Online] Available: <http://www.hpschapters.org/northcarolina/NSDS/90SrPDF.pdf>

[26] “Bremsstrahlung Radiation” Iowa State University Center for Nondestructive Evaluation [Online] Available :  
<https://www.nde-ed.org/Physics/X-Ray/xrays.xhtml>

[27] “Bremsstrahlung Radiation Dose in Yttrium-90Therapy Applications” Michael G. Stabin, Keith F. Eckerman, Jeffrey C. Ryman and Lawrence E. William August 1994 [Online] Available: [https://www.researchgate.net/publication/15151745\\_Bremsstrahlung\\_radiation\\_dose\\_in\\_yttrium-90\\_therapy\\_applications](https://www.researchgate.net/publication/15151745_Bremsstrahlung_radiation_dose_in_yttrium-90_therapy_applications)

## Appendices

### Appendix A. Time Discretization of Heat Source Decay Python Script

```
1 import numpy as np
2 import scipy.constants
3 import matplotlib.pyplot as plt
4
5 def convert_to_mass(n_atoms,molar_mass):
6     return (n_atoms/scipy.constants.Avogadro)*molar_mass
7
8 def convert_to_power(mass):
9     return mass*0.46
10
11 molar_mass = 89.9 #g/mol of Sr-90
12 dec_con = np.log(2) / 10585 #decay constant of Sr-90
13 #initial values of our heat source
14 initial_mass = 33000 #grams
15 initial_atoms = initial_mass/molar_mass*scipy.constants.Avogadro
16 initial_power = convert_to_power(initial_mass)
17
18 n_points = 3650 #number of discretization points to use
19 mass = np.zeros((n_points))
20 atoms = np.zeros((n_points))
21 power = np.zeros((n_points))
22
23 mass[0] = initial_mass
24 atoms[0] = initial_atoms
25 power[0] = initial_power
26 #loop through each discretization point and solve for respective quantity
27 for i in range(1,n_points):
28     time_int = i
29     atoms[i] = initial_atoms * np.exp(-dec_con*time_int)
30     mass[i] = convert_to_mass(atoms[i],molar_mass)
31     power[i] = convert_to_power(mass[i])
32
33 #Plot desired quantities
34 time = np.arange(0,10,10/n_points)
35 plt.plot(time,power,'-r')
36 plt.grid()
37 plt.show()
```

## Appendix B. Thermoelectric Analysis Python Script

```
1 import numpy as np
2 import matplotlib.pyplot as plt
3
4 #material properties @ 1000K
5 alpha_p = 228e-6
6 alpha_n = -253e-6
7 alpha_pn = (alpha_p-alpha_n)
8 ele_p = 2.68e-5
9 ele_n = 2.11e-5
10
11 #thermal conductivity coefficients
12 k_p = 3.93
13 k_n = 4.07
14
15 s = 4.68e-4 #surface area of thermocouple
16 l = 0.04 #length of thermocouple
17 n = 54 #number of thermocouples in system
18
19 #temperatures for hot and cold side of thermocouple from solid works
20 t_h = 1346
21 t_c = 431
22 delta_t = t_h-t_c
23
24 #dimensionless z parameter for semiconductor materials
25 z = (alpha_pn**2) / ((ele_p+ele_n)*(k_p+k_n))
26 t = (t_c+t_h)/2
27 zt = z*t
28 print("ZT:", zt)
29 #internal resistance and load resistance
30 r = (ele_p*l/s)+(ele_n*l/s)
31 r_ratio = np.arange(0.5, 25, 0.25)
32 rl = r*r_ratio
33 print("Resistance:", r)
34 #material conductance and current calculation
35 k = ((k_p*s/l)+(k_n*s/l))
36 i = alpha_pn*delta_t / (rl+r)
37 i_max = alpha_pn*delta_t/r
38 print("Current:", i)
```

```

39 #voltage calculation
40 v = (n*alpha_pn*delta_t/(r_ratio+1)) * r_ratio
41 v_max = n*alpha_pn*delta_t
42 print("Voltage:" ,v)
43 #Heat absorbed at the hot end
44 q_abs = n*((alpha_pn*t_h*i) - (0.5*(i**2)*r) + (k*delta_t))
45 print("Heat Absorbed: " ,q_abs)
46 #heat released by the system i
47 q_rel = n*((alpha_pn*t_c*i) + (0.5*(i**2)*r) + (k*delta_t))
48 print("Heat liberated: " ,q_rel)
49 print("Total Heat:" ,q_abs-q_rel)
50 #power output calculation
51 p_out = (n*(alpha_pn**2)*(delta_t**2)/r) * (r_ratio/((1+r_ratio)**2))
52 p_max = n*(alpha_pn**2)*(delta_t**2) / (4*r)
53 print("Electrical Power Output for a whole TEG device with 54 thermocouples:" ,p_out)
54 #Efficiency calculation
55 eff = 100*(p_out/q_abs)
56 eff_max = 100*(1 - (t_c/t_h)) * ((np.sqrt(1+zt) -1)/(np.sqrt(1+zt)+(t_c/t_h)))
57 #####
58 #Plotting of all the quantities of interest
59 fig,ax1 = plt.subplots()
60 l1=ax1.plot(r_ratio,eff,-r",label="Efficiency")
61 ax1.set_ylabel("Efficiency (%)")
62 ax1.set_xlabel(r'$\frac{R_L}{R}$',fontsize=15)
63 ax1.grid()
64 #ax1.title(r'Efficiency vs. $\frac{R_L}{R}$')
65
66
67 ax2 = ax1.twinx()
68 ax2.set_ylabel("Power Output (W)")
69 l2=ax2.plot(r_ratio,p_out,-b",label="Power Output")
70 ax1.legend()
71 ax2.legend(loc='upper right')
72 plt.show()
73

```

## Appendix C. Heat Calculator according to Pellet Dimensions

Created on Tue Apr 12 14:41:22 2022

```
@author: eowen
"""

import numpy as np
# Inputs

w = float(input('input pin width(cm), \t')) #width, cm
l = float(input('input pin length(cm), \t')) #length, cm
h = float(input('input pin height(cm), \t')) #height, cm
Qx = float(input('input Target Power(W), \t')) #Target Total Power

# Constants and Relations

PSr = 0.55 # percent Sr in fuel source
AP = 0.0067 # W/Ci
ASr = 139 # Ci/g
DSrT = 4.81 # g/cc
VSrT = l * w * h # cc
ASrT = ASr * PSr # Ci/g
eff = 0.08 #experimental efficiency
# Outputs

Q = Qx / eff
mSrT = VSrT * DSrT # pellet mass
pelA = ASrT * mSrT # pellet activity
pelP = pelA * AP # pellet power
pel = Q / pelP # number of pellets19
# Prints

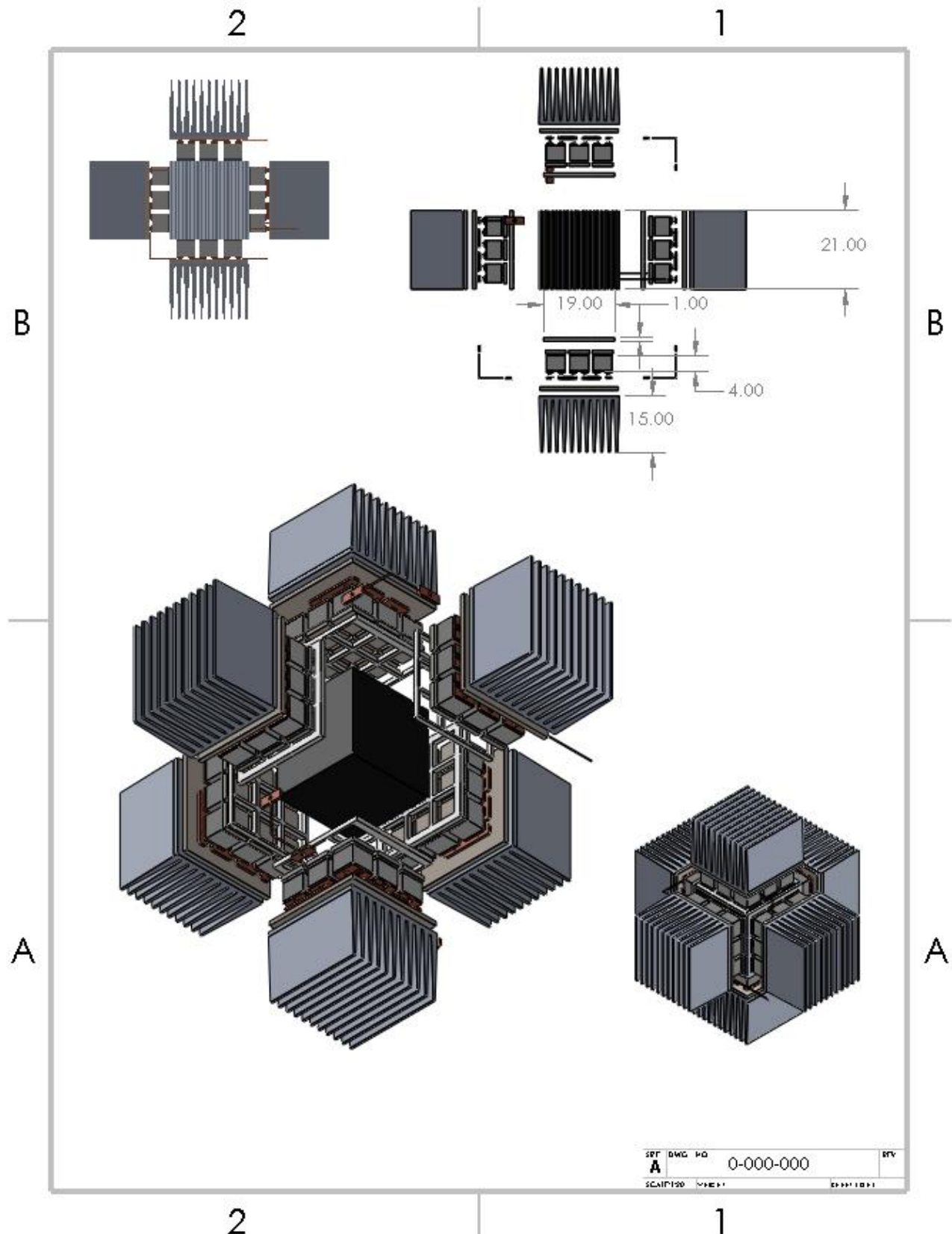
print('\nNumber of Pellets =',pel)

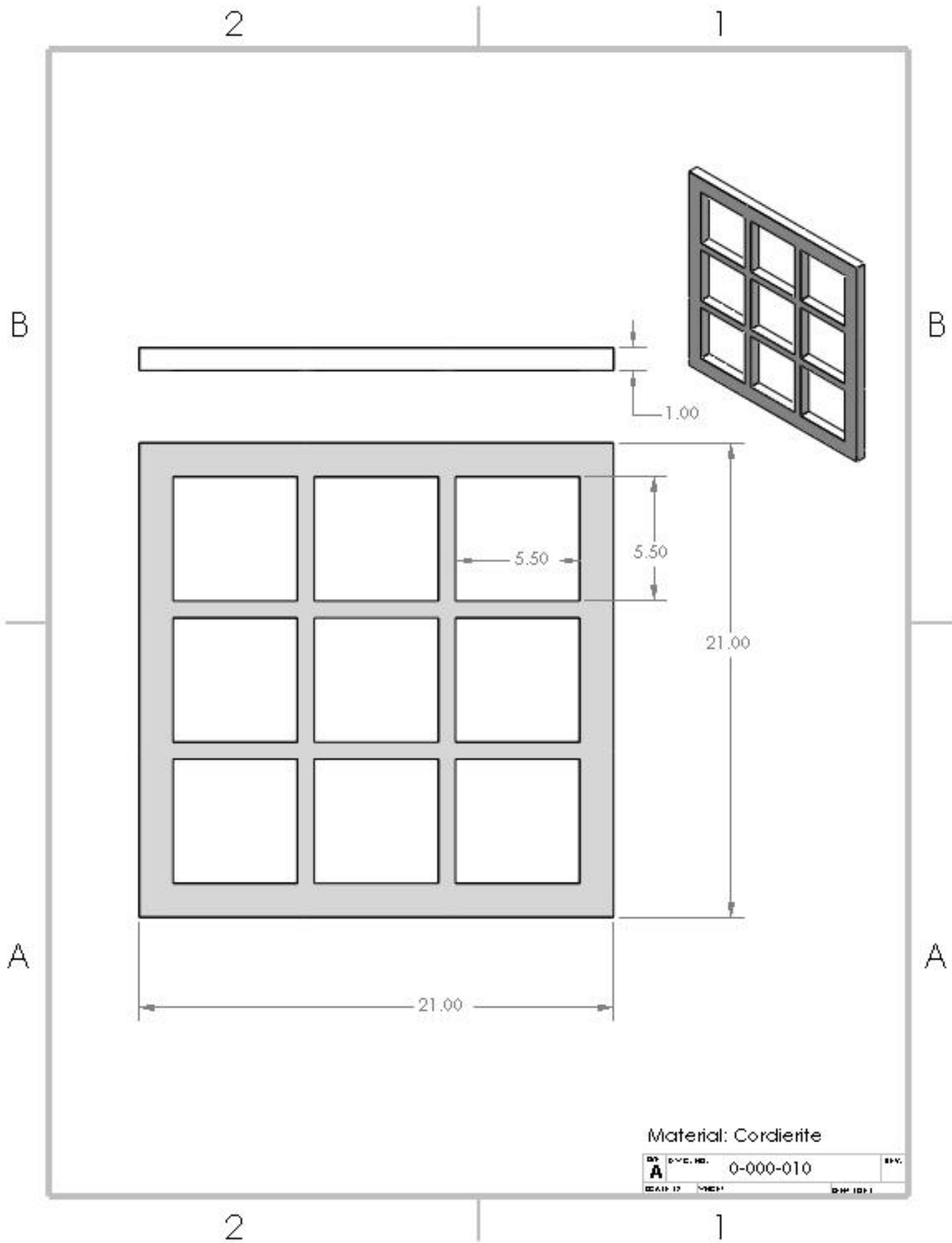
n = 10
t = [1,2,3,4,5,6,7,8,9,10]
M = [32.2206, 31.4596, 30.7166, 29.9911, 29.2828, 28.5912, 27.9159, 27.2566, 26.6128, 25.9860]
PP = np.zeros((n))
PA = ASrT * AP #W/f
print(PP)

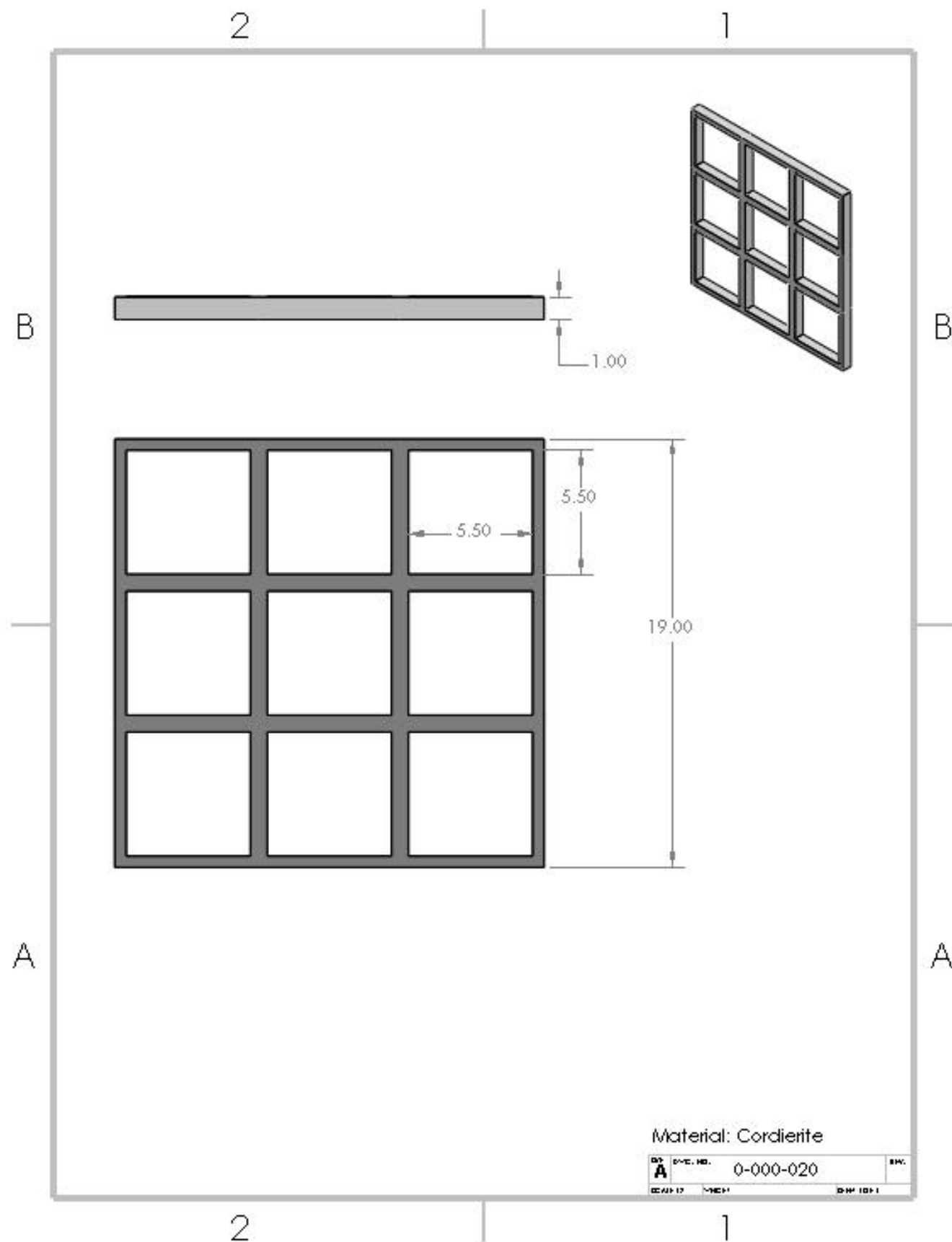
for i in range(0,n):
    PP[i] = PA * (M[i]*1000)

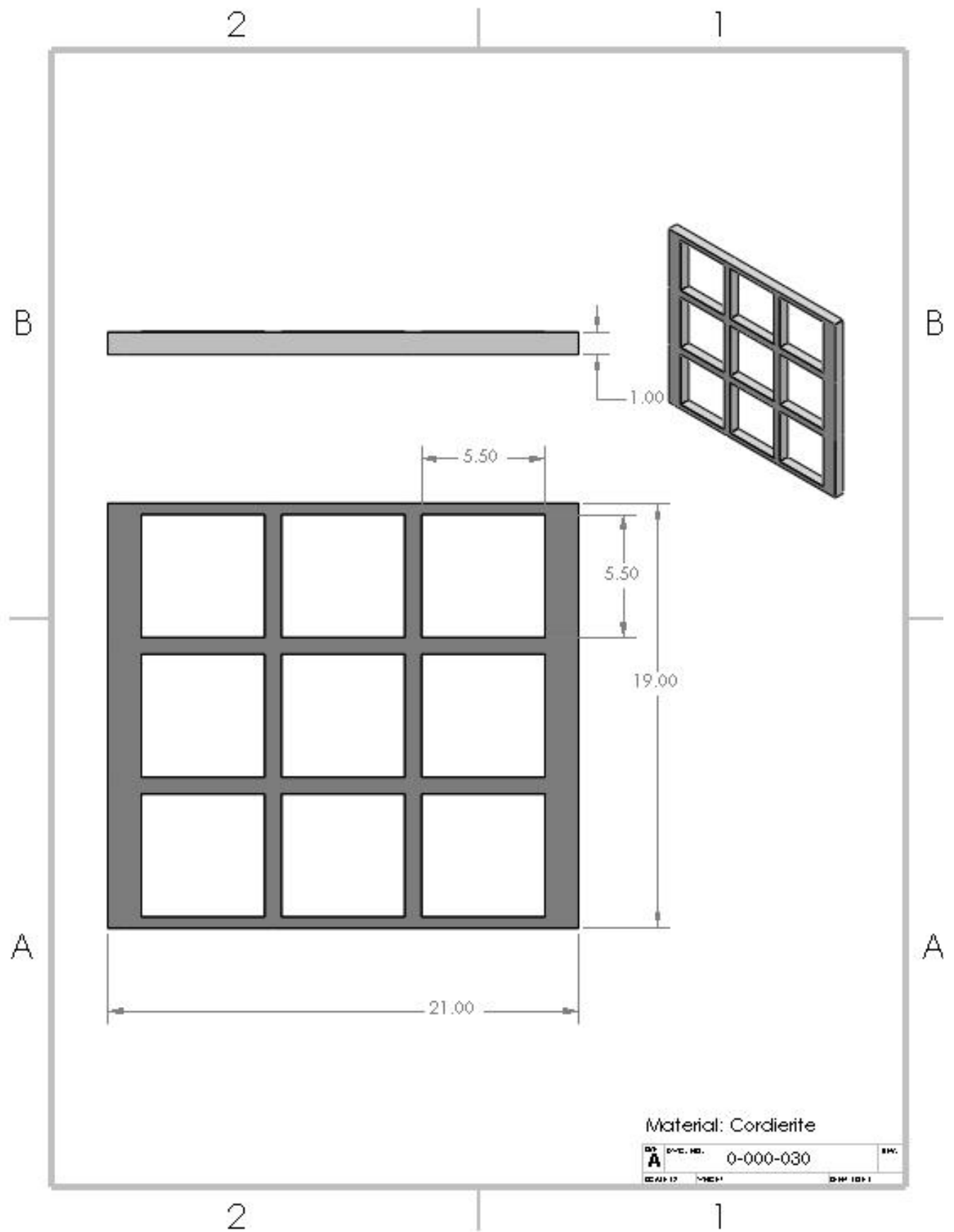
print(PP)
```

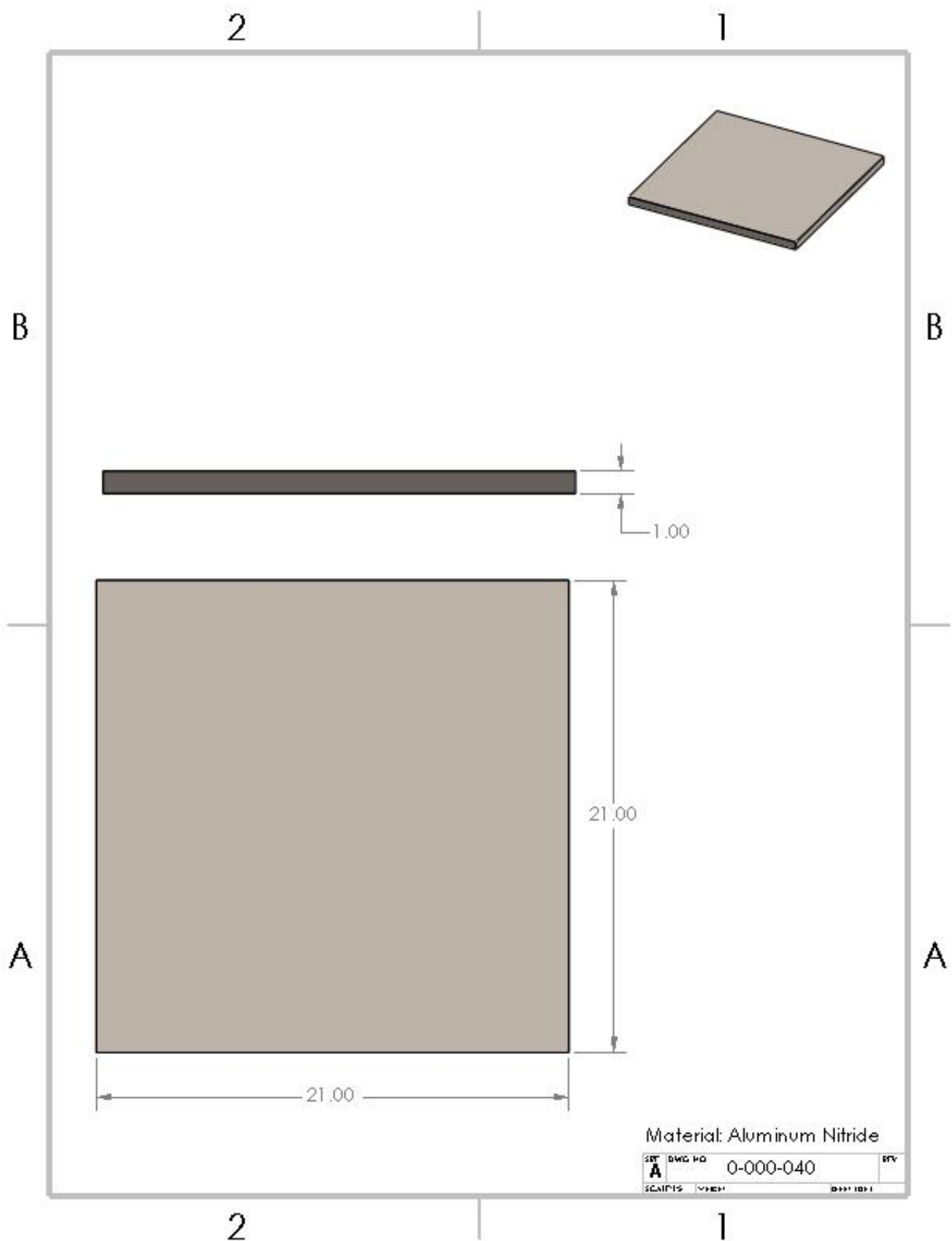
## Appendix D. Solidworks Drawings

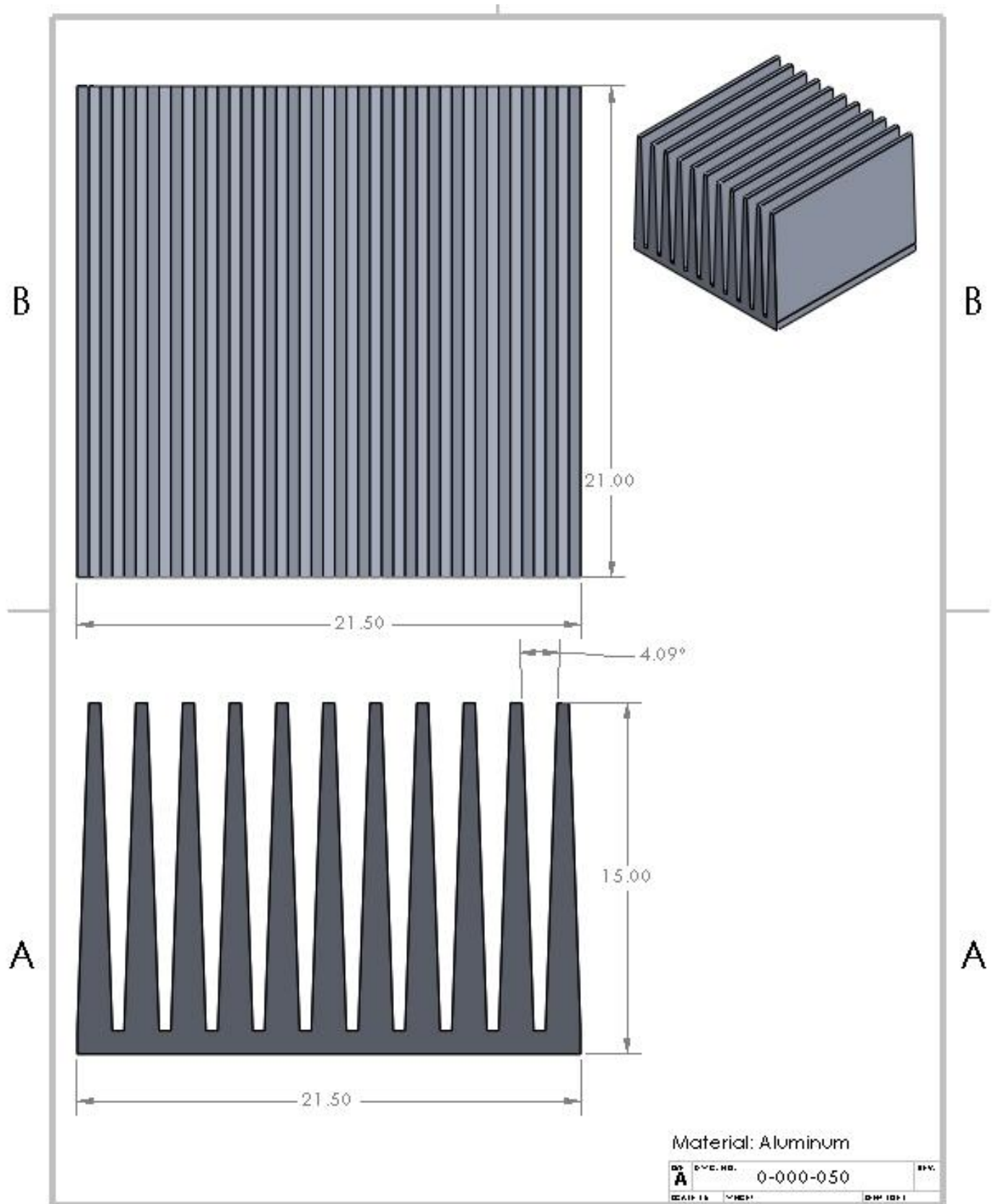






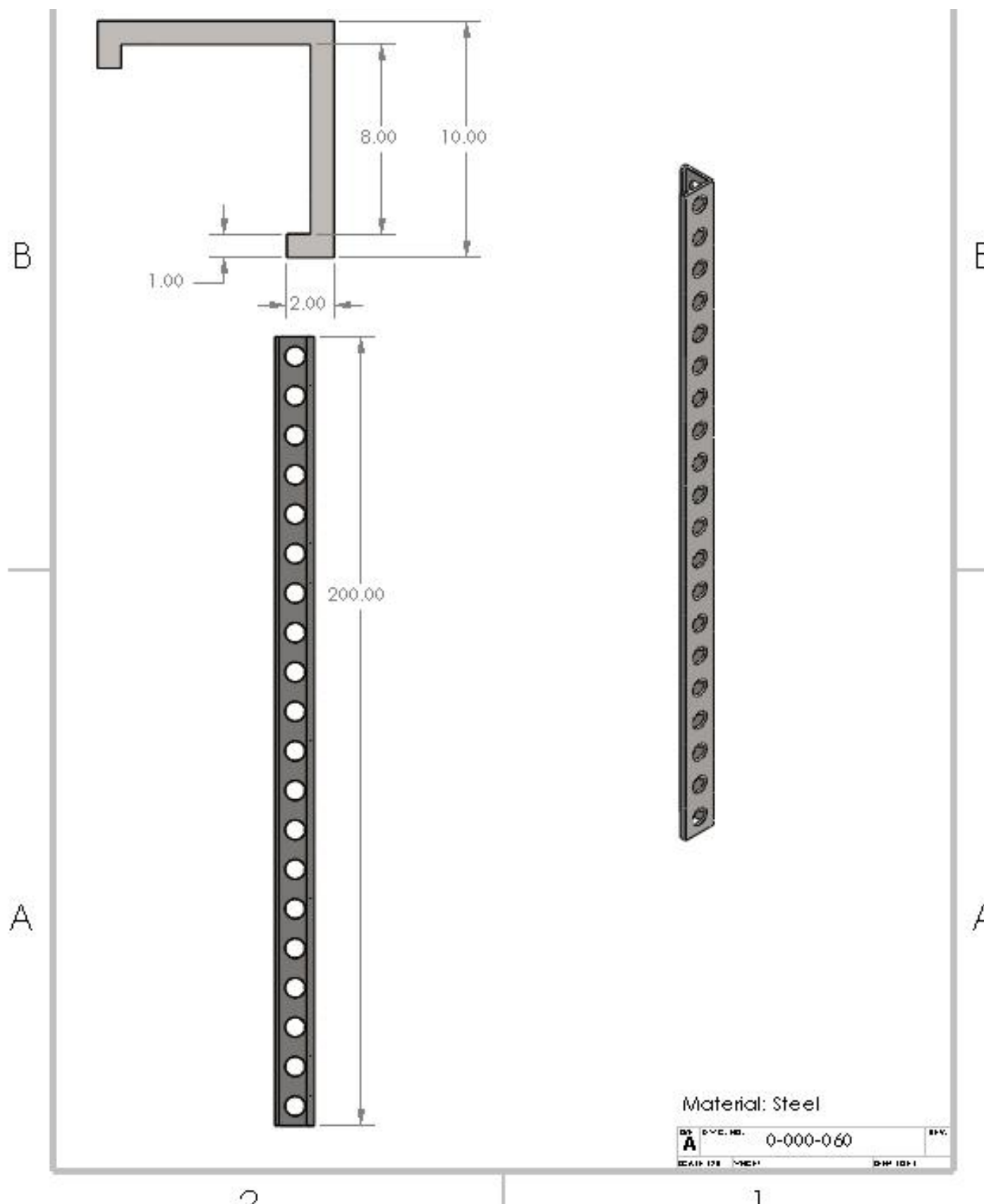


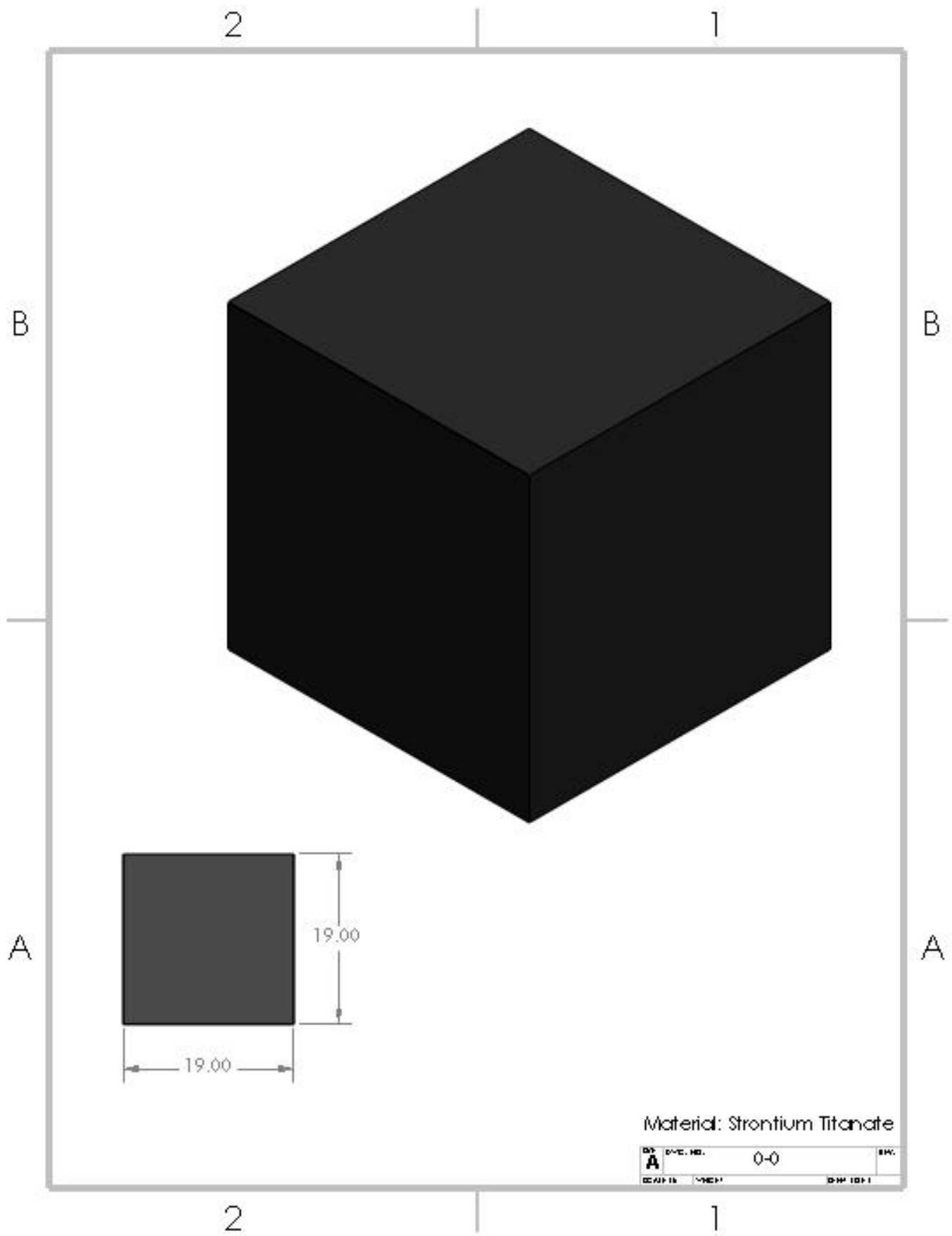


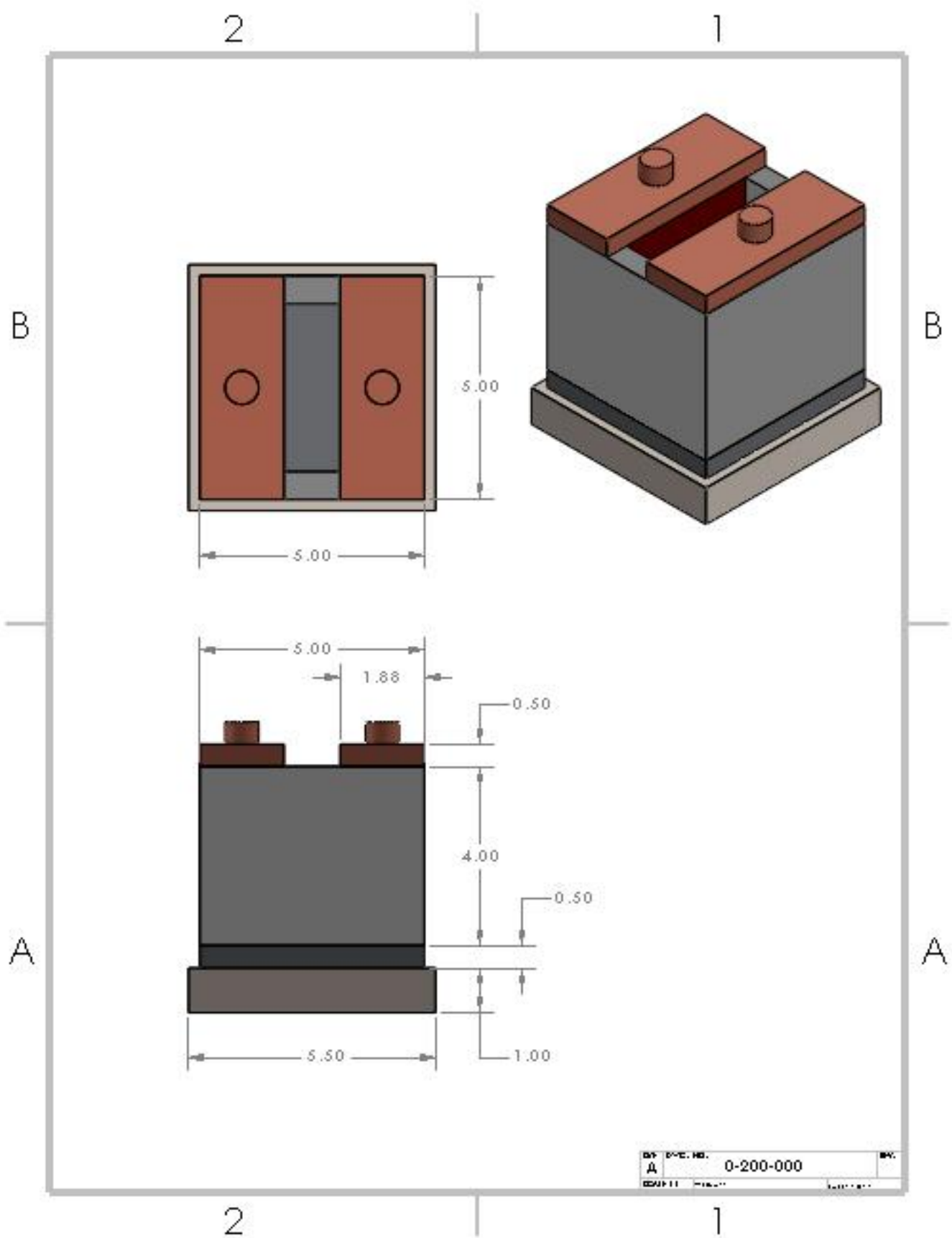


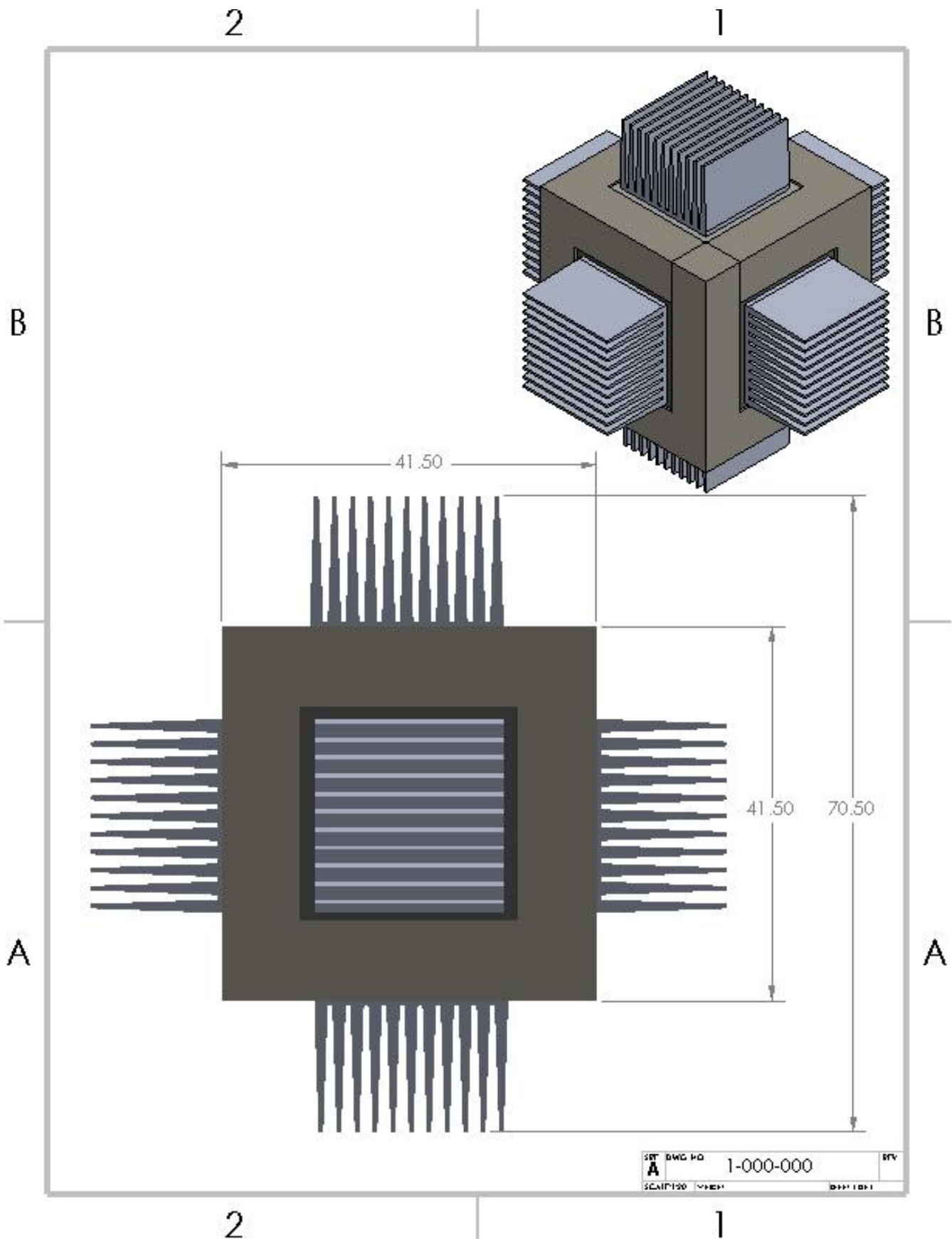
2

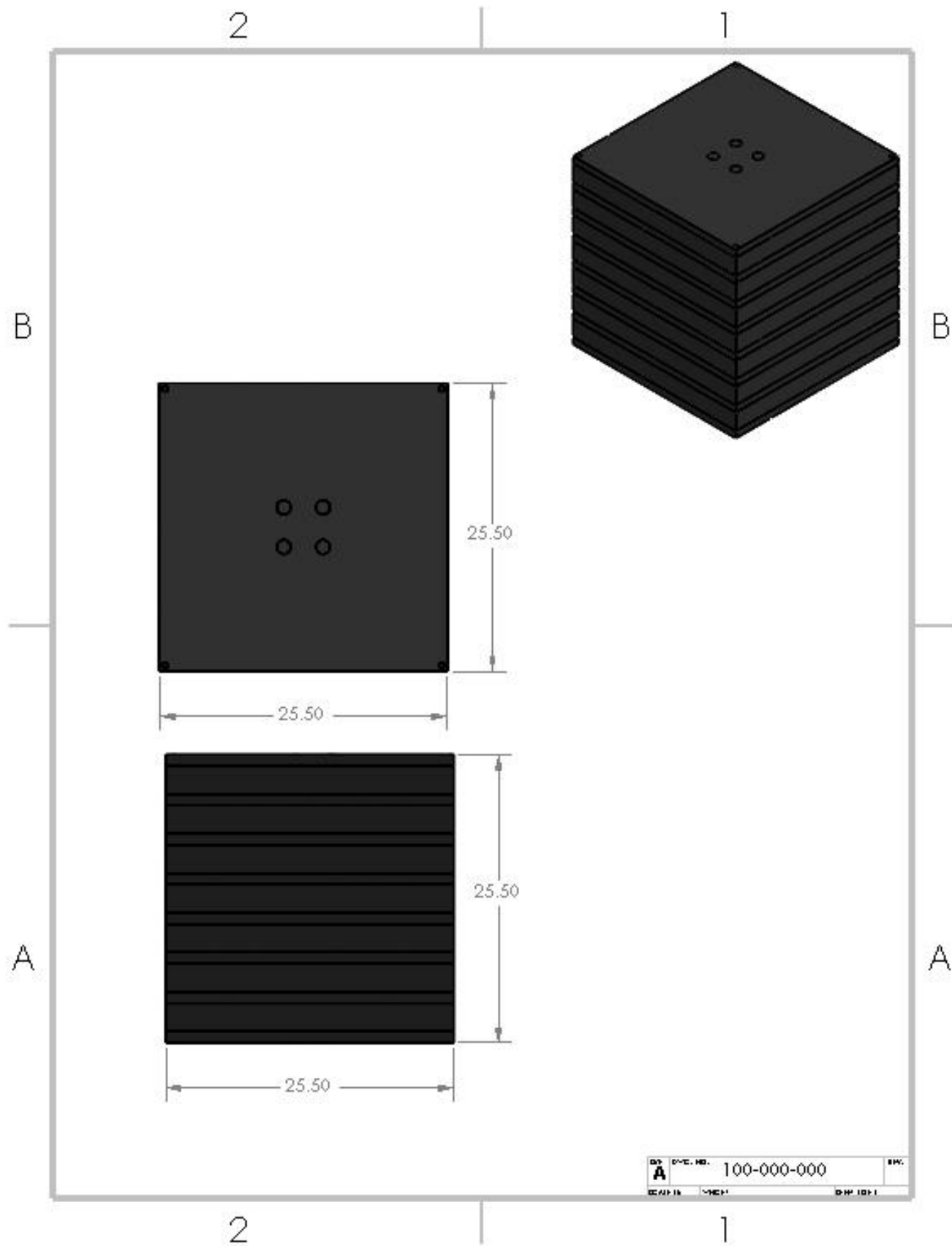
1

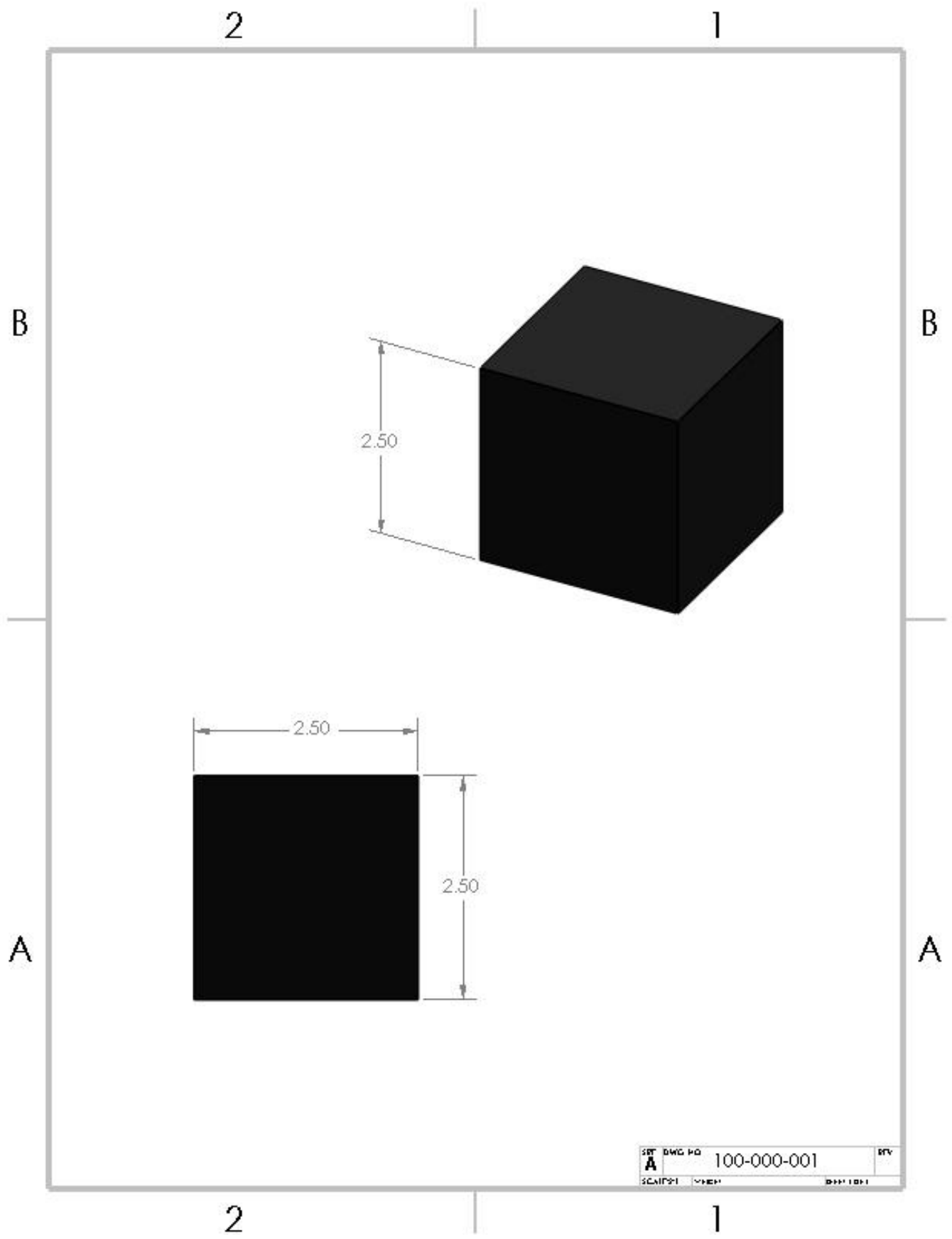


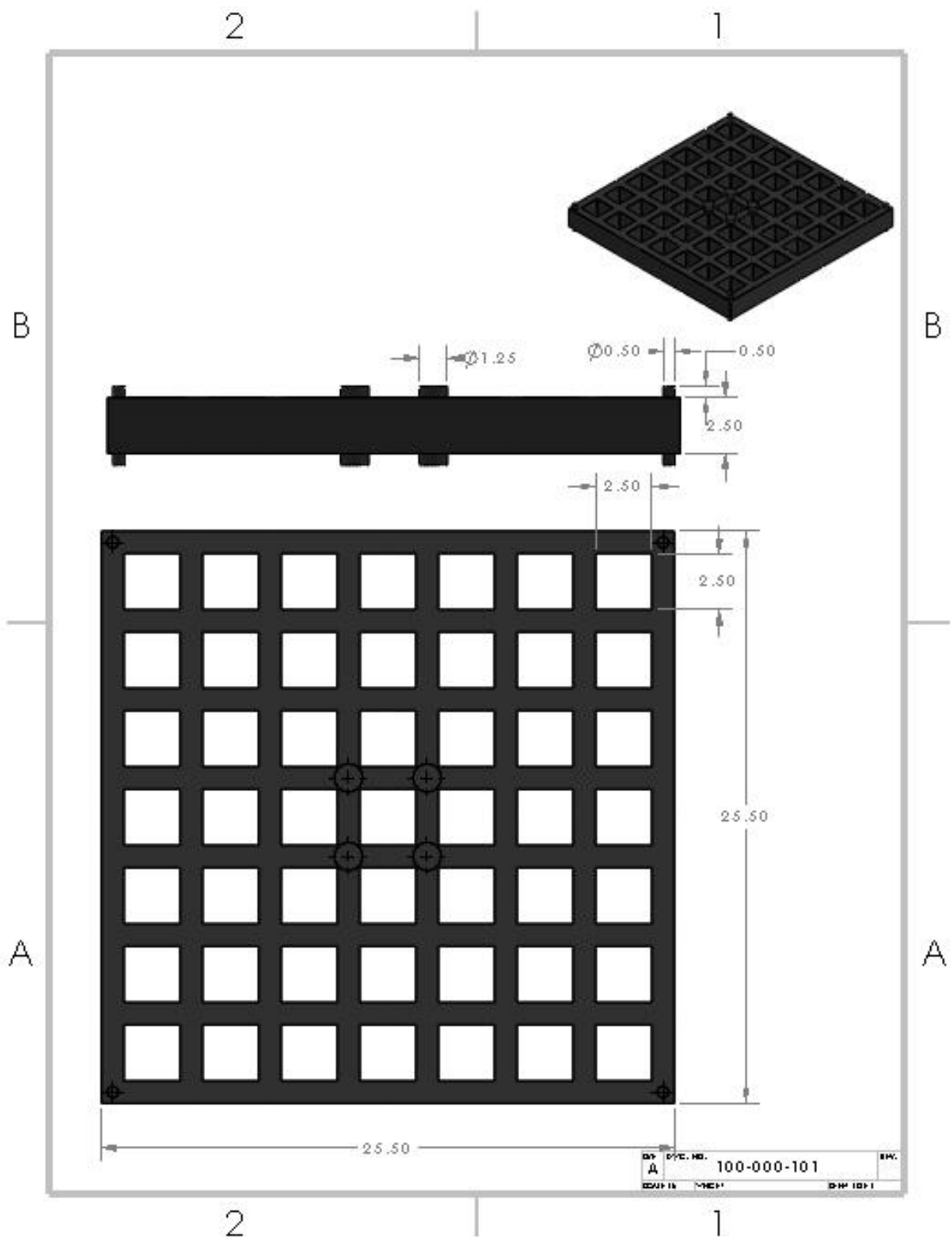


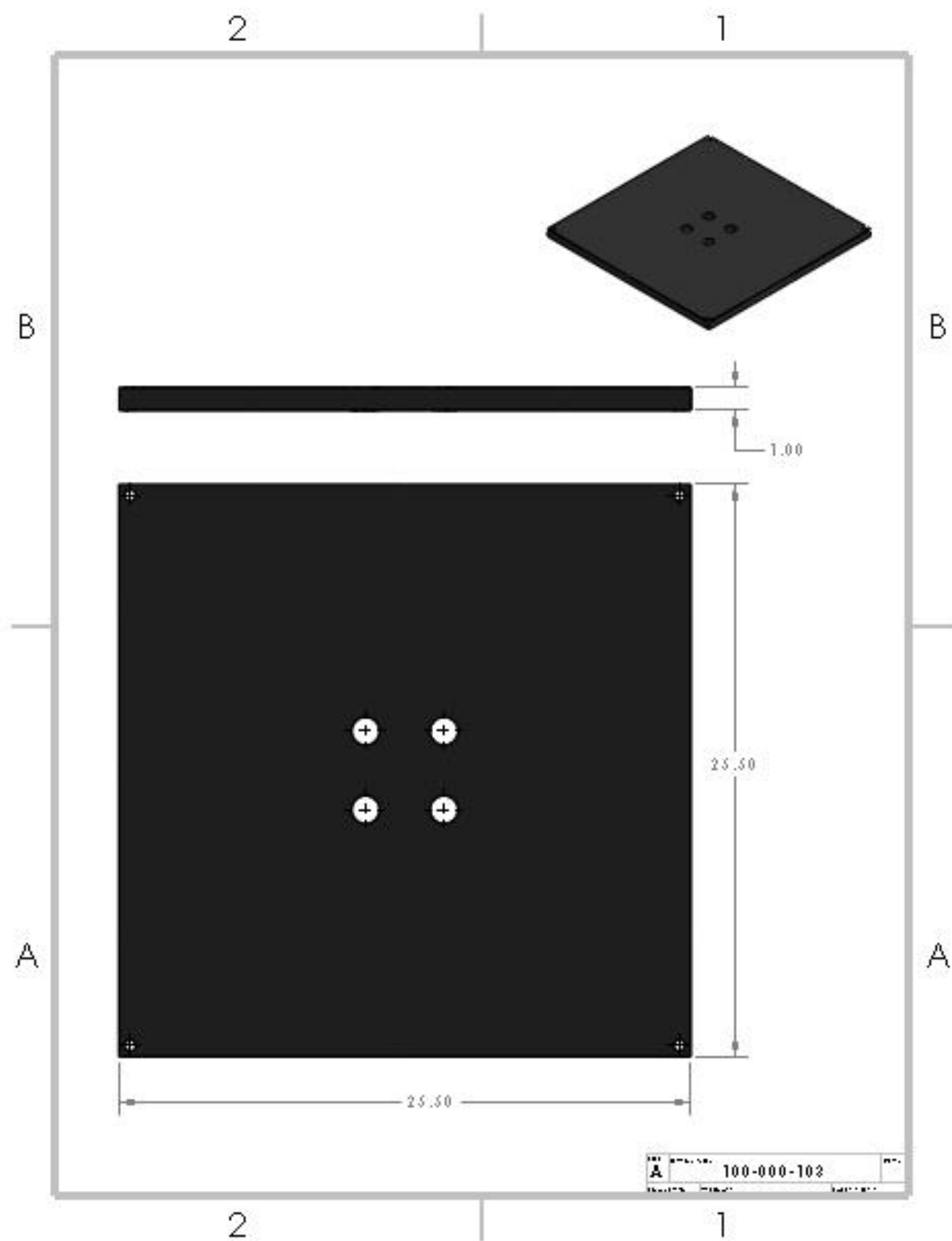












## ***Author Contributions***

Author	Sections Contributed To:
Ian M. Aranda	Thermoelectric Analysis and Appendix A, B
Patricio Bunt	Material Selection and Economic Analysis
Israel Marin	Radiation Safety and Shield Analysis
Ethan Owenby	3, 4, Appendix C, Appendix D